

ISOLATION AND IDENTIFICATION OF SECONDARY METABOLITES FROM
TAXUS MEDIA SUSPENSION CELL CULTURE

by

Sonia Kristin Pawlak

B.Sc., The University of Massachusetts, 1993

A THESIS SUBMITTED IN PARTIAL FUFILMENT OF THE REQUIREMENTS FOR
THE DEGREE

OF

MASTER OF SCIENCE

in

THE FACULTY OF GRADUATE STUDIES

(Department of Chemistry)

We accept this thesis as confirming
to the required standard

THE UNIVERSITY OF BRITISH COLUMBIA

November 1999

© Sonia Kristin Pawlak 1999

In presenting this thesis in partial fulfilment of the requirements for an advanced degree at the University of British Columbia, I agree that the Library shall make it freely available for reference and study. I further agree that permission for extensive copying of this thesis for scholarly purposes may be granted by the head of my department or by his or her representatives. It is understood that copying or publication of this thesis for financial gain shall not be allowed without my written permission.

Department of Chemistry

The University of British Columbia
Vancouver, Canada

Date Sept. 20, 1999

Abstract

The diterpenoid taxol, a compound isolated from the bark of the Pacific Yew tree, *Taxus brevifolia*, has shown remarkable success in the treatment of several types of cancer. Limited supply of taxol, due to low concentrations produced naturally and difficulty in synthesis of the drug, have spurred research attempts to develop alternative methods of producing taxane compounds *in vitro* using suspension cell cultures.

Suspension cell culture propagated from the stems of *Taxus media* were grown in airlift type bioreactors for 28 days using a modified B5 medium. The cells and broth from multiple bioreactor experiments were combined and extracted with ethyl acetate and methanol. The ethyl acetate extracts were roughly separated by partitioning with solvents before high pressure liquid chromatography (HPLC) analysis was performed to determine if taxol, baccatin III, 10 deacetylbaccatin, 14-hydroxy-10-deacetylbaccatin, 14-hydroxybaccatin, cephalomannine, 7-epitaxol or 7-methyltaxol were present. Additionally, the partitioned extract was checked against the taxane standards by thin layer chromatography (TLC). There was no indication that the taxane compounds used as standards were present in the cell extract above the detectable limits for these methods.

To determine what types of compounds the cell culture was producing, the cell extract was separated using column chromatography, preparative TLC and recrystallization. Five compounds were purified and identified as 3- β -O[β -D-glucoside] β -sitosterol, 3B-6B, 23-trihydroxyolean-28-oic acid, cyclo (L-proline-L- valine), by comparing mass spectral (MS) and nuclear magnetic resonance (NMR) spectroscopy with that published in the literature. Two novel compounds 9,10 epoxy, 11-hydroxy

12,13 linoleic acid and 4,6- dihydroxy,-2-methoxy, 8-methyl xanthone were found in the cell culture. They were identified using NMR and MS data and by comparison with compounds of like structure in the literature.

Table of Contents

Abstract	ii
List of Figures	vii
List of Tables	x
List of Abbreviations	xi
Chapter I. History and Development of Taxol (Paclitaxel)	1
1.0 Introduction	1
1.1 Early Screenings of <i>Taxus brevifolia</i> Extract	1
1.2 Structure Elucidation of Active Principle	2
1.3 Antitumor Activity	8
1.4 Mechanism of Biological Activity	12
1.5 Formulation Studies	14
1.6 Supply for Continued Testing	14
1.7 Toxicology Studies	15
1.8 Phase I Trials	16
1.9 Phase II Trials	17
1.10 Phase III Trials and Approval by FDA	19
1.11 Future Prospects of Taxane Drugs	20
Chapter II. Supply Issues: Solutions via Synthesis	22
2.0 Natural Abundance and Projected Demand	22
2.1 Environmental Problems Associated with Large Scale Harvest	22
2.2 Challenge of Total Synthesis	23
2.2A Selected Synthetic Routes: Holton and Wender	23
2.2B Selected Synthetic Routes: Nicolaou and Danishefsky	25
2.2C Commercial Taxol from Total Synthesis?	27
2.3 Semisynthesis, a Solution to Supply Issues	28
2.3A Portier's Semisynthesis	28
2.3B Manufacturing via Holton's Synthesis	30
2.3C Benefits of Semisynthesis	31
2.4 Benefits of Synthetic Research: Structure Activity Relationships (SAR)	32

Chapter III. Plant Cell Culture	34
3.0 Advantages of Plant Cell Culture	34
3.1 Impediments in Development	34
3.2 Issues of Scale Up	35
3.3 History of <i>Taxus</i> Cell Culture	36
3.4 Development of Plant Cell Culture Systems	37
3.5 Choice of Explant Material	38
3.6 Variability in Taxol Production	38
3.7 Kinetics of Cell Growth and Taxol Production	39
3.8 Optimization of Media for Maximum Taxane Production	40
3.8A Effect of Growth Hormones	41
3.8B Carbohydrate Manipulations	42
3.8C Use of Amino Acids	44
3.9 Gas Composition	45
3.10 Effect of Light	46
3.11 Use of Elicitors	47
3.11A Biotic Elicitors	48
3.11B Jasmonic Acid Derivatives as Elicitors	48
3.12 Commercial Production of Taxol from Cell Culture	50
Chapter IV. Biosynthesis of Taxol	51
4.0 Introduction	51
4.1 Isoprene Formation	51
4.2 Cyclization of GGDP	55
4.3 Oxygenation	58
4.4 Formation of the Oxirane Ring	59
4.5 Later Oxidative Steps	61
4.6 Formation of the N-benzoyl Phenylisoserine Side Chain	62
4.7 Attachment of the Side Chain	66
4.8 Conclusion	68

Chapter V. Results and Discussion	69
5.0 Previous Work at UBC	69
5.0A Initiation of callus	69
5.0B Media Composition	69
5.0C Maintenance of Callus	71
5.0D Establishment of Suspension Cultures	71
5.0E Screening of Cell Culture	73
5.1 Partial Characterization of <i>Taxus x media</i> Cell line	75
5.1A Extraction	76
5.1B Crude Separations: Solvent Washing and Partitioning	79
5.1C Separation and Purification	83
5.2 Isolates from Fraction IIID	88
5.2A IIID-4A	88
5.2B IIID-3B4	97
5.2C Remaining material	101
5.3 Isolates from Fraction IIIA	101
5.3A IIIA5A	102
5.3B IIIA-4G3	105
5.3C Remaining Fractions of IIIA	105
5.4 Fraction IIIB	106
5.4A IIIB-3B5	107
5.4B Remaining Fractions of IIIB and Fraction IIIC	114
5.5 Bioreactors F88-107	114
5.5A IIB11B1	116
5.5B Remaining Fractions	125
Chapter VI. Conclusion	126
Chapter VII. Experimental Details	129
Bibliography	141

List of Figures

Fig. 1. Structure and Numbering of Baccatin V	3
Fig. 2. Mild Base Hydrolysis Reaction of Structure 1	4
Fig. 3. Structures of 4 and 5 Determined by X-ray Crystallography	4
Fig. 4. Structure of Taxinine (6)	5
Fig. 5. Oxidation of Diol 3	6
Fig. 6. Basic oxidation of 1	6
Fig. 7. Structure of Taxol (11)	7
Fig. 8. Microtubule Polymerization: Normal and in Presence of Taxol	13
Fig. 9. Holton's Total Synthesis of Taxol	24
Fig. 10. Wender's Total Synthesis of Taxol	25
Fig. 11. Nicolaou's Total Synthesis of Taxol	26
Fig. 12. Danishefsky's Total Synthesis of Taxol	27
Fig. 13. Potier's Semisynthesis of Taxol	29
Fig. 14. Commercial Method of Producing Taxol	30
Fig. 15. SAR Nomenclature for Taxol	32
Fig. 16. Typical Cell Growth and Taxol Production by Cell Culture	39
Fig. 17. Phenylalanine (13) as Precursor to Phenylisoserine (14) Side Chain of Taxol	44
Fig. 18. Shikimic Acid Pathway to Phenylalanine (13)	45
Fig. 19. SAR of Jasmonic Acid and Derivatives on Taxol Production by Cultured Cells	39
Fig. 20. Mevalonic Acid Pathway to IPP	52
Fig. 21. Labeling pattern of Taxuyunnine (15) from [U- ¹³ C] Glucose Experiments	53
Fig. 22. Rohmer's Pathway to IPP	54
Fig. 23. ¹³ C Enrichments of IPP Deduced from Taxuyunnine C from [1- ¹³ C] Glucose	53
Fig. 24. Cyclization of GGDP (16) to Taxa-4(20), 11(12)-diene (18)	56
Fig. 25. Cyclization of GGDP to Taxa-4(5), 11(12)-diene	57
Fig. 26. Taxol Content with Respect to Taxadiene Synthase Activity	58
Fig. 27. Effect of Taxadiene Hydroxylase on Taxa-4(20), 11(12)-diene	59

Fig. 28. Direct Intramolecular Mechanism of Oxetane Ring Formation	60
Fig. 29. Proposed Alternative Mechanisms of Oxetane Formation	61
Fig. 30. Cinnamic Acid Pathway to Phenylisoserine Side Chain	62
Fig. 31. Formation of Benzoyl Moiety	63
Fig. 32. Biosynthetic Pathway to Phenylisoserine (14)	64
Fig. 33. Mass Spectra Fragmentation of Side Chain	65
Fig. 34. Nitrogen Migration via Aminomutase Enzyme Isolated from <i>Taxus sp.</i>	66
Fig. 35. Sequence of Phenylisoserine Side Chain Attachment to Baccatin III	66
Fig. 36. Method of Creating Suspension Cell Culture	72
Fig. 37. Method of Processing <i>Taxus x media</i> Cell Culture	77
Fig. 38. Method of Solvent Partitioning Cell Culture Extracts	80
Fig. 39. Separation Scheme for Hexanes:CH ₂ Cl ₂ Subextract	84
Fig. 40. Separation Scheme for CH ₂ Cl ₂ Subextract	85
Fig. 41. Separation Scheme for Fraction IIID	86
Fig. 42. EI Mass Fragmentation Pattern of β -Sitosterol (21)	90
Fig. 43. Structure and Numbering of β -Sitosterol	91
Fig. 44. Labeling of Glucoside Portion of IIID-4A	94
Fig. 45. Structure and Numbering of 3- β -O[β -D-glucoside] β -sitosterol (22 IIID-4A)	95
Fig. 46. Mass Spectrum Fragmentation Pattern of Trihydroxy Triterpene Acid	98
Fig. 47. Structure and Numbering of 3 β ,6 β -23 trihydroxy olean-28-oic acid (23 IIID-B4)	98
Fig. 48. Separation Scheme of Fraction IIIA	102
Fig. 49. Possible Structure of IIIA-5A (24)	104
Fig. 50. Separation Scheme for Fraction IIIB	106
Fig. 51. Structure of Linoleic Acid (25)	108
Fig. 52. Possible Products from Oxidation of Linoleic Acid	108
Fig. 53. Structure and numbering of Methyl 11(R), 12(R)-epoxy-13(S)-hydroxy-(9Z)- octadecenoate (26)	109
Fig. 54. Structure and Numbering of Compounds 27 and 28	
Fig. 55. Mass Spectrum Fragmentation of Hydroxy, Epoxy Linoleic Acid	112

Fig. 56. Proposed Assignment of Compound IIIB-3B5 (29)	113
Fig. 57. Separation Scheme of Hexanes:Methylene Chloride Subextract	115
Fig. 58. Mass Spectrum Fragmentation Pattern of Xanthones	118
Fig. 59. Proposed Numbered Structure of IIB11B1	119
Fig. 60. Possible Structures of IIB11B1	122
Fig. 61. Expected vs. Observed HMBC Correlations	124

List of Tables

Table 1. ¹ H NMR Data of Baccatin V and Compound 1	3
Table 2. Early Biological Evaluation of Taxol	9
Table 3. Phase II Trial Results: Taxol vs. 18 Cancer Types	17
Table 4. Major Fragments of Labeled Taxol from Various Feeding Studies	67
Table 5. Modified Gambourg B5 Media	70
Table 6. HPLC Solvent Systems for Taxane Analysis	73
Table 7. Dried Biomass, EtOAc and MeOH Extract Masses from F66-107	78
Table 8. Subextract Masses after Partitioning with Solvents	81
Table 9. HPLC Retention Times of Taxane Standards	82
Table 10. HPLC Retention Times of <i>Taxus x media</i> Cell Subextracts	83
Table 11. NMR and EI Mass Spec. Data for IIID-4A	88
Table 12. Comparison of ¹³ C Data between IIID-4A and β-Sitosterol in Pyridine	91
Table 13. NMR Data of Glucoside Residue of IIID-4A	93
Table 14. IIID-4A Glucoside Residue ¹³ C NMR Assignments	95
Table 15. Published Spectra of 3-β-O[β-D-glucoside]β-sitosterol	96
Table 16. NMR and EI Mass Spec. Data of IIID-3B4 Compared with Published Data	99
Table 17. NMR and EI Data for IIIA-5A	103
Table 18. Published Spectra of Cyclo-(L-pro-L-val)	104
Table 19. NMR and EI Mass Spec. Data of IIIB-35B	107
Table 20. Comparison of NMR Data Between IIIB-3B5 and 26	110
Table 21. Comparison of NMR Data of IIIB-3B5 with 27 and 28	111
Table 22. Results of 2D NMR Experiments of IIIB-3B5	113
Table 23. NMR and EI Mass Spectrum Data of IIB11B1	117
Table 24. Results of 2D NMR Experiments of IIB11B1	118
Table 25. Published NMR Data of Meta Coupled C ₁₅ H ₁₂ O ₅ Xanthones	120

List of Symbols and Abbreviations

Listed in order of appearance

Chapter I.

NCI : National Cancer Institute

USDA : United States Department of Agriculture

sp. : species

NMR : nuclear magnetic resonance

^1H NMR : proton NMR

δ : NMR units in parts per million

J : NMR coupling constant

Hz : hertz

s : singlet

d : doublet

t : triplet

m : multiplet

br : broad

Fig. : figure

lb. : pounds

MnO_2 : manganese dioxide

[O] : oxidation

AcO : Acetyl

OBz : benzoyl

nm : nanometers

λ_{max} : wavelength (nm) at which a local maximum in absorption is observed

MeOH : methanol

ϵ : extinction coefficient

ν_{max} : wavenumber in units of cm^{-1}

CHCl_3 : chloroform

FDA : Food and Drug Administration

ILS : increase in life span

T/C : tumor weight of treated/control animals * 100

i.p. : interperitoneal

Ca²⁺ : calcium ion carrying a +2 charge

Cremophor EL : polyoxyethylated castor oil

CH₂Cl₂ : methylene chloride

CRADA : Cooperative Research and Development Agreement

BMS : Bristol Myers-Squibb

kg : kilogram

Taxol[®] : refers to BMS marketed formulation of taxol

Taxotere[®] : refers to Rhone-Poulenc Rorer marketed formulation of docetaxel

Chapter II.

USA : United States of America

C₃ bridge : 3 carbon bridge

10 DAB : 10 deacetyl- baccatin III

Troc : trichloroethyl carbonyl (Cl₃CH₂OC(O)-)

DCC : dicyclohexylcarbodiimide

TMSi : trimethylsilane

AcOH : acetic acid

TES : triethylsilane

DMAP : dimethylaminopyridine

C₅H₅N : pyridine

SAR : Structure Activity Relationship

mg : milligram

l : liter

Chapter III.

USD : United States Dollars

CO₂ : carbon dioxide

T. : *Taxus*

MS : Murashige-Skoog

SH : Scenk and Hildebrandt

WPM : Woody plant Medium

TM5-TM10 : optimized mediums developed specifically for *Taxus sp.*

GA₃ : gibberellins

ABA : abscisic acid

IAA : indole-3-acetic acid

2,4 D : 2,4 dichlorophenoxyacetic acid

NAA : naphthalenacetic acid

IBA : indole-3-butyric acid

P : 4-amino-3,5,6-trichloropicolinic acid

K : kinetin

BA : benzyladenine

2iP : 6-(γ , γ - dimethylallylamino)purine

Z : zeatin

dZ : dihydrozeatin

Th : thiadiazuron

Chapter IV.

GGDP : geranylgeranyl diphosphate

Acetyl-CoA : acetyl-Coenzyme A

IPP : isopentyl diphosphate

¹³C INADEQUATE : incredible natural abundance double quantum transfer

NMR spectroscopy

Mg⁺² : magnesium ion carrying +2 charge

kDA : kilodaltons

μg : micrograms

nmol : nanomoles

Chapter V.

PVP : polyvinylpyrrolidone

cm : centimeters

rpm : rotations per minute

HPLC : high pressure liquid chromatography

MeOH : methanol

UV : ultraviolet

CH₃CN : acetonitrile
THF : tetrahydrofuran
TLC : thin layer chromatography
g : gram
RI : refractory index
EtOAc : ethyl acetate
EI : electron impact mass spectroscopy
ppm : parts per million
CDCl₃: deuterated chloroform
q : quartet
¹H COSY : proton correlated spectroscopy
HMQC : Heteronuclear Multiple Quantum Coherence
¹³C APT : Attached Proton Test
MHz : megahertz
R_f: ratio to front
H₂SO₄ : sulfuric acid
DCI : desorption chemical ionization
NaOMe : sodium methoxide
AlCl₃ : aluminum chloride
HCl : hydrochloric acid
NaOAc : sodium acetate
D₂O : deuterated water
IR : infrared spectroscopy
HMBC : Heteronuclear Multiple Bond Connectivity
2D : two dimensional

History and Development of Taxol (Paclitaxel)

1.0 Introduction

The first reports of significant use of chemotherapeutic agents to treat human cancer occurred in 1946 when Goodman found nitrogen mustards to be effective against leukemia. Soon after Ferber found aminoterin effective against childhood leukemia and Burchenal discovered 6-mercaptopurine was active against a variety of leukemias (Suffness 1995). Thus the foundation for the "War on Cancer" was set. This program, initiated in 1960 by the US National Cancer Institute (NCI) was a systematic screening project of plant materials for anticancer agents.

Random plant samples, with an emphasis placed on those used for folkloric medicine, were collected by the US Department of Agriculture (USDA) and tested for cytotoxicity. Extracts from the yew tree (*Taxus sp.*) have been most notably used as poisons throughout history by the Romans, Greeks and Celts. However, numerous accounts of the medical uses of the plant have also been made by other cultures. Yew extracts have been used for abortions by the Japanese, for tuberculosis by the Germans, for rheumatism, scurvy, numbness, pain, cold, fever, arthritis and as a diuretic by the Canadian First Nations (Hartzel 1995). Other cultures have used extracts and teas from *Taxus* species to treat heart ailments, rheumatism, malaria and epilepsy (Wickremesinha 1998). Perhaps most significantly, Indians have used a preparation of yew extract mixed with butter to treat skin cancer (Hartzel 1995). The many documented cases of the medicinal properties of yew extracts led Arthur Barclay of the USDA to collect two

samples, stems and fruit and stem and bark, from *Taxus brevifolia*, the Pacific yew (Wall 1998).

1.1 Early Screenings of *Taxus Brevifolia* Extract

The initial evaluation of the extract of *Taxus brevifolia* was not very promising. Screening results on the extract from the bark showed activity against KB cancer cells, however, they did not show antitumor action *in vivo* using the Dunning leukemia model or the P-1798 lymphosarcoma system. Additionally, the bark extract was found to be toxic at 500/mg/kg/day and non active at 250 mg/kg/day in the L1210 leukemia model (mouse assay, then considered to be the most important animal test by the NCI). At this point interest in the plant extract waned but a sample was sent to M.E. Wall's laboratory at the Research Triangle Institute, North Carolina, for characterization of the active principal on the basis of its 9KB (human epidermal carcinoma of the nasopharynx) cytotoxicity. Wall had previously noted correlation between 9KB cytotoxicity and *in vivo* activity, in camphothecin studies (Wall 1995). Fractionation studies began on a 30 lb. shipment of bark in 1964 in which certain fractions were found to be moderately active against P-1534 leukemia, Walker 256 carcinoma and P-388 leukemia (Suffness 1995).

1.2 Structure Elucidation of Active Principle

Due to the complexity of the structure and the primitive state of Nuclear Magnetic Resonance spectroscopy (NMR), it wasn't until 1971 that structure elucidation of the active principal was completed by Monroe Wall and Mankush Wani using X-ray

crystallography. The ^1H NMR data (Table 1) of the isolated active component was in close correlation with the published spectrum of baccatin V (Fig. 1).

Fig. 1. Structure and Numbering of Baccatin V

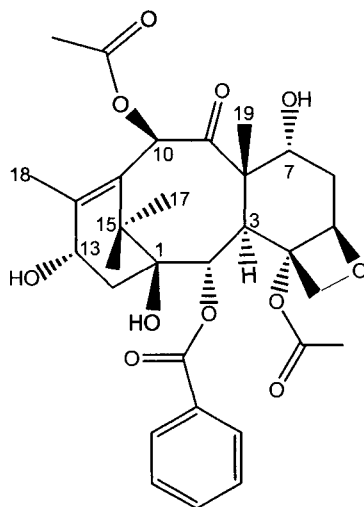


Table 1. ^1H NMR Data of Baccatin V and Compound 1

Position	Compound 1	Baccatin V
C-17 CH_3	1.14 (s)	1.04 (s)
C-16 CH_3	1.22 (s)	1.10 (s)
C-19 CH_3	1.67 (s)	1.62 (s)
C-10 OAc	2.20 (s)	1.99 (s)
C-18 (C-13 α in Baccatin V)	1.80 (s)	
C-4 OAc	2.36 (s)	
C-3 H	3.80 (d, $J=6$)	4.02 (d, $J=6$)
C-20 2H	4.20 (d, $J=8$), 4.30 (d, $J=8$)	4.38 (s)
C-5 H	4.92 (d, $J=10$)	4.99 (m)
C-2 H	5.68 (d, $J=6$)	5.74 (d, $J=6$)
C-13 H	6.20 (br t, $J=8$)	6.18 (br t, $J=8$)
C-10 H	6.28(s)	6.83(s)

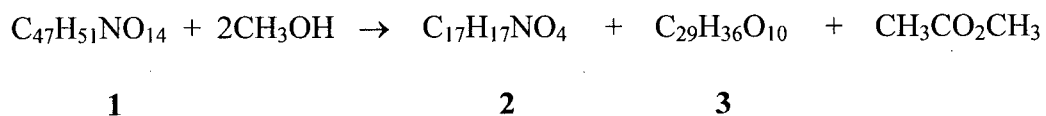
chemical shifts in units of δ

s,d,t,m : indicates multiplicity (singlet, doublet, triplet or multiplet)

J : coupling constants in units of Hz

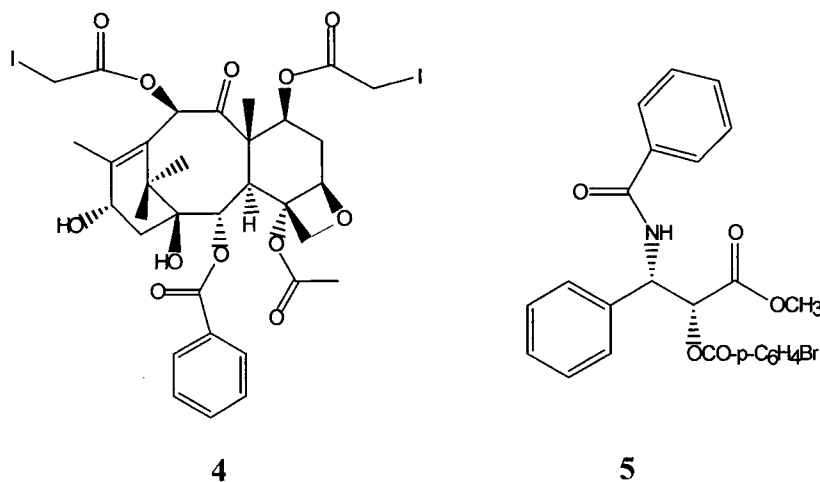
Mass spectrometry (M^+ at 853 m/z corresponding to $C_{47}H_{51}NO_{14}$ versus M^+ at 526 m/z corresponding to $C_{31}H_{38}O_{11}$) indicated that $C_{16}H_{13}NO_3$ needed to be accounted for. Halogenated derivatives of **1** for X-ray analysis were attempted but no successful preparations achieved. Mild base hydrolysis at 0° yielded a nitrogen containing α -hydroxyl ester **2** ($C_{17}H_{17}NO_4$), tetraol **3** ($C_{29}H_{36}O_{10}$) and methyl acetate.

Fig. 2. Mild Base Hydrolysis Reaction of Structure **1**



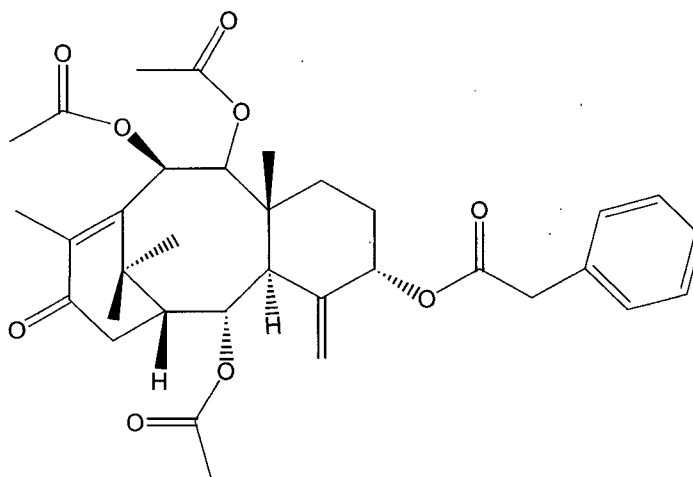
The two products of interest were converted to **4** and **5**, iodo and bromo halogenated derivatives, and characterized by X-ray analysis to have the structures indicated in Fig. 3.

Fig. 3. Structures of **4** and **5** Determined by X-ray Crystallography



The assumption that no rearrangement of tetrol **2** occurred under mild methanolysis conditions was made since taxinine (**6**) can be converted to diacetyltaxinine under the same conditions then converted back to taxinine upon deacetylation.

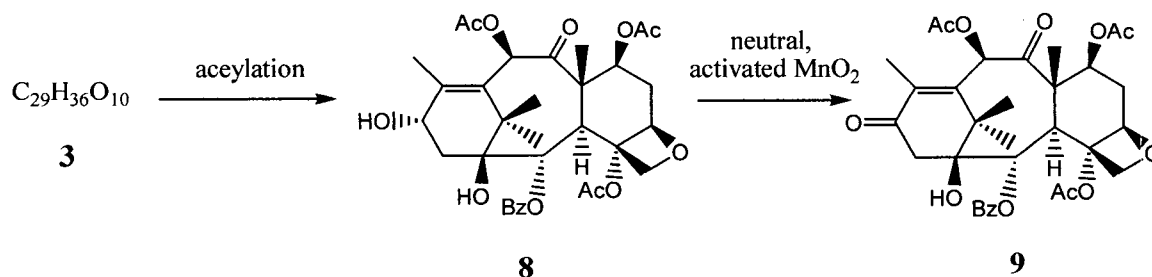
Fig. 4. Structure of Taxinine (**6**)



6

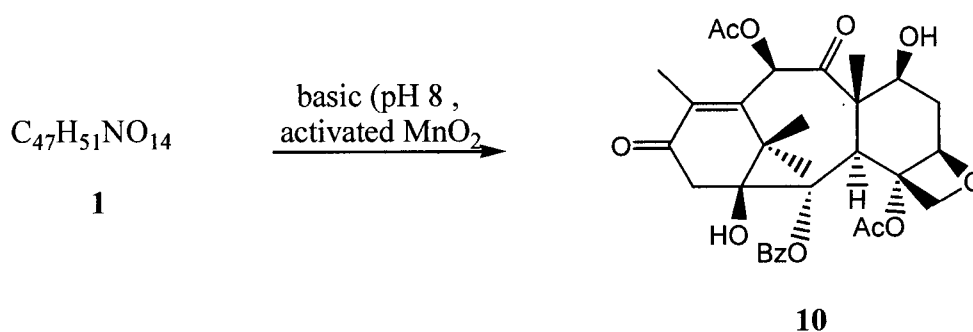
As NMR techniques were primitive compared to today's standards, the two ester functional groups were placed using a combination of chemical tests along with the available NMR, ultraviolet and infrared spectroscopy. As compound **1** could not be oxidized by neutral, activated manganese, the two esters were presumed to be located at allylic positions 10 and 13. The 7,10-diacetate **8** obtained from tetrol **3** was easily oxidized to the corresponding conjugated ketone **9**.

Fig. 5. Oxidation of Diol 3



When **1** was oxidized under basic conditions (activated manganese dioxide in acetone) the 7 β -hydroxyl conjugated ketone **10** was formed. High resolution mass spectrometry of **10** was in accordance with the formula $C_{31}H_{36}O_{11}$, which indicated that **10** was formed due to loss of the nitrogen containing α -hydroxyl ester and oxidation of the liberated allylic α -hydroxyl group.

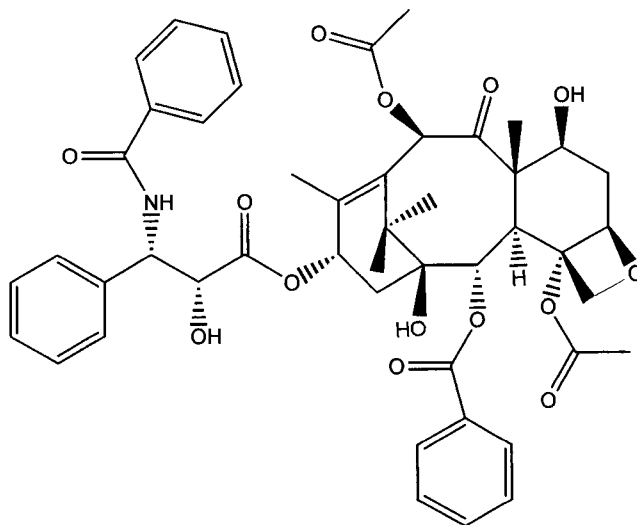
Fig. 6. Basic oxidation of **1**



It was concluded that the nitrogen containing ester portion was attached to C-13 based on a number of different observations. The alternative Δ^{11} -9,10-dioxo formation

was ruled out based on the ultraviolet (λ_{max} MeOH, 272nm, ϵ 4800) and infrared (ν_{max} CHCl_3 1680 cm^{-1}) spectra. Additionally, a singlet was observed in the ^1H NMR spectrum of **10** due to the C-10 (δ = 6.46) proton (Wall 1995). In 1971, 7 years after its biological activity was determined, the highly functionalized tetracyclic diterpenoid, 5 β , 20-epoxy-1,2 α ,7 β ,10 β ,13 α -hexahydroxytax-11-en-9-one-4,10-diacetate-2-benzoate 13-ester with (2R,3S)-N-benzoyl-3-phenylisoserin, named paclitaxel was assigned the following structure (Kapoor 1997). Later, the compound's name changed and it is most commonly known as taxol (**11**).

Fig. 7. Structure of Taxol (**11**)



11

1.3 Antitumor Activity

Much work had gone into isolating, identifying and evaluating the compound at this point. However, taxol was not considered a promising candidate for development by NCI for a number of reasons. Its relatively poor activity in the tumor models used at the time translated into high expense, given the large dose that was required for activity. Additionally, adding to its expense, was the extremely low natural abundance which made obtaining enough of the drug difficult even for completing the predevelopmental tests required by the Food and Drug Administration (FDA). Furthermore, its low aqueous solubility indicated that formulation would be a challenge.

During this period the two most important tumor models were the L1210 and P388 leukemia systems. In both taxol's optimal percent increase in life span (ILS) fell way below the development criterion. The P1534 system experiments showed some promising results but, at the time of evaluation, this system was being phased out of use since it was insensitive to the accepted chemotherapy drugs and therefore not shown to be predictive of clinical activity. Taxol met the development criterion in three of the Walker 256 experiments, however two trials showed inactivity and two only marginal activity. Although minimal activity criteria was met, developmental activity criteria was not reproducibly met (Suffness 1995).

Table 2. Early Biological Evaluation of Taxol

Tumor System	Lab and experiment ^a	Dose Range ^b	Optimal Dose ^b	Duration (days)	Optimal ILS or (T/C) ^c	Activity Criterion ^d	Develop. Criterion ^e
P1534 Leukemia	B00153	1.9-15	3.75	10	200	35	not estab.
	B00150	25-50	50	5	50	35	
L1210 Leukemia	A02297	20-40	20	daily to death	29	25	50
	A02511	10-20	10	15	22		
	A2718	10-35	20	15	31		
	A2781	15-25	15	15	39		
	A2853	4.4-10	10	15	19		
P388 Leukemia	B00106	25-50	50	10	40	25	75
	A00768	5-40	40	10	20		
	B00093	10-25	25	10	40		
Walker 256 Carcinosarcom ^a	C00554	2.9-15	4.4	4	(78)	(42)	(10)
	C00696	20-50	50	4	(81)		
	A00500	2-9	4	4	(43)		
	A00532	4-10	10	4	(16)		
	A00548	5-14	14	4	(37)		
	B004570	7-20	20	4	(0)		
	A00382	2-10	10	4	(69)		

^a Laboratory with five digit experiment # A = Hazelton Labs, B = A.D Little, C = Wisconsin Research Foundation

^b Dose in mg/kg/injection

^c Optimal percent increase in life span (ILS) or tumor weight of treated/control animals * 100 (T/C)

^d Criterion for minimal acceptable activity as ILS% or T/C %

^e Criterion for selection for pre-clinical development

The NCI lost interest in pursuing development until 1974 when taxol was screened against the new B16 melanoma tumor system, which was more clinically predictive against solid tumors than previous models. At the time there was a great demand for clinical agents that would be effective against slower growing tumors than the currently used compounds which were mainly effective against only leukemias, lymphomas and childhood cancers. Taxol had a reproducible ILS up to 126% at 10 mg/kg/injection on a daily administration over 9 days, well above the developmental criterion of 50% in the B16 model (Suffness 1995).

However, the NCI was still reluctant to pursue development since taxol was; not highly active against the leukemias, was markedly less potent than the other antitumor natural products in use clinically, and faced serious formulation problems due to the relatively high dose and low solubility in water (~6mg/ml) (Straubinger 1995). Additionally, the high expense of developing a drug which required a high dose, had low abundance (0.02% dry wt.) and required long difficult purifications meant that investment in the procedure was a costly and risky endeavor (Croom 1995).

Despite the hurdles to overcome, the NCI Decision Network Committee approved taxol for development based on the B16 activity. Initial results were discouraging, since in the B16, L1210, P388 and P1534 systems, no substantial activity was observed when the drug was administered either orally or intravenously against implanted tumors, and only marginal activity when administered interperitoneal (i.p.) against subcutaneously implanted tumors. It seemed as though the only effective combination was that of i.p tumors and i.p administrated drugs. As the i.p / i.p system does not take the pharmacological considerations of drug adsorption, transport, distribution, metabolism

and clearance into account, development of taxol was again in jeopardy. Routinely, the NCI dropped potential drugs in which the site of the tumor implant and route of drug dosing were not separated.

In 1976, a new development in tumor modeling rescued taxol from being shelved, when NCI began using human xenografts in nude mice. The 1968 discovery that hairless or "nude" mice had an essentially non-working immune system due to the lack of a thymus gland, was very encouraging to the field of tumor modeling. The production of the animals was high enough by 1976 for the NCI to introduce xenographic tumor modeling into their screening program (Suffness 1995). Previously, many of the drugs shown to have antitumor activity in mice and rats were found ineffective when brought to clinical trials on humans. Attempts at developing human tumor models were unsuccessful since human tumor implants in rodents generally failed as the immunosuppressive techniques used greatly compromised the health of the rodents.

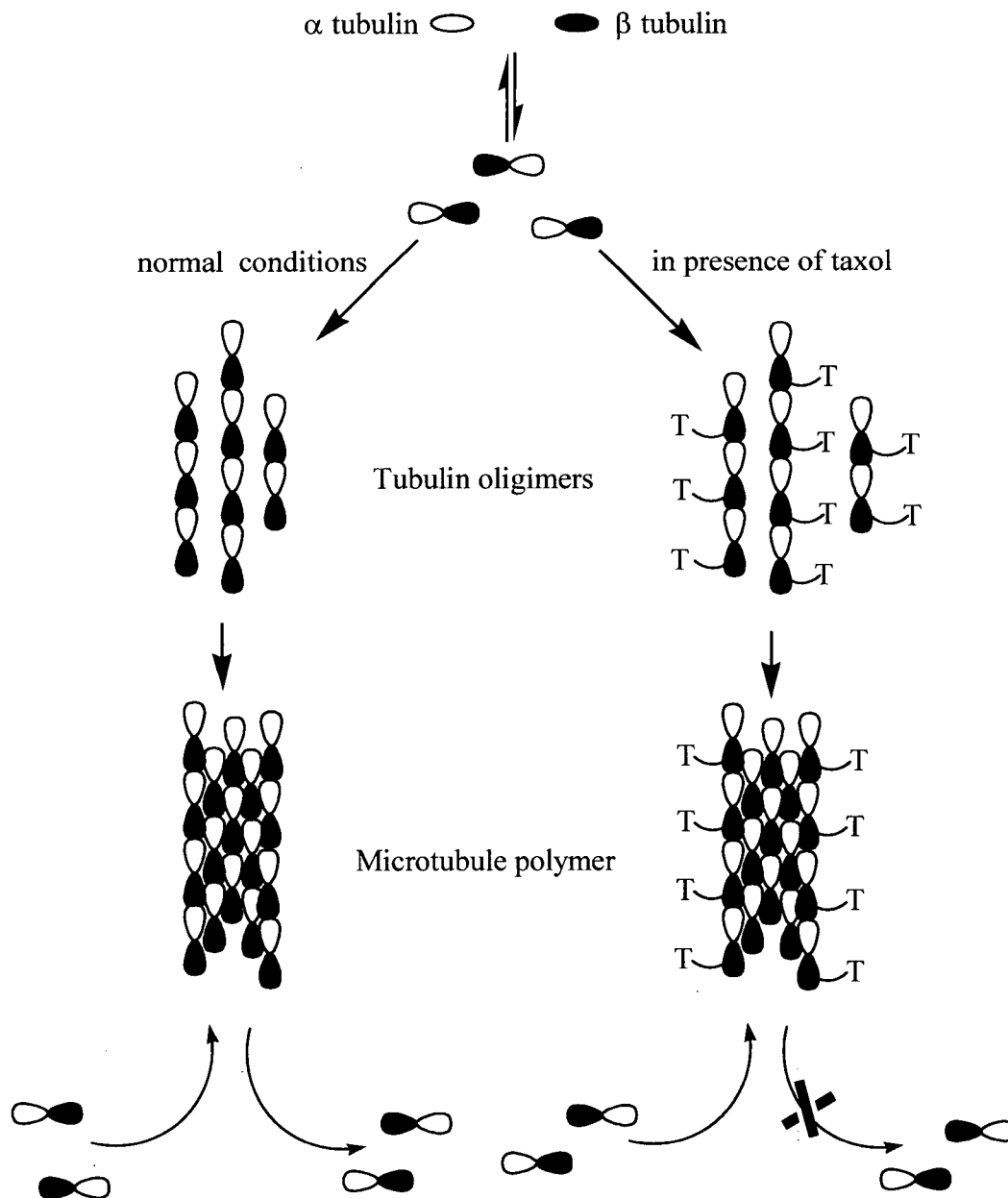
Taxol was approved for phase 2A development by the NCI Decision Network Committee in April of 1977, when its activity in the new potentially more clinically relevant tumor systems was evaluated. Three models the LX-1 lung, MX-1 breast and CX-1 colon xenografts, were developed to simulate the major solid tumor types against which current chemotherapy agents were only marginally effective. Taxol inhibited 80 to 90% tumor growth in the LX-1 and CX-1 models and caused regression of the implanted MX-1 tumor. Additionally, in all three cases the tumor was implanted under the kidney and the drug administered subcutaneously, thus the developmental criterion that the tumor implant and drug administration site must be separate was met (Suffness 1995).

1.4 Mechanism of Biological Activity

Interest in the compound increased in 1979 when biologist Susan Horowitz determined that taxol employed an unique mode of action against cancer cells. Many of the important chemotherapy agents such as the vinca alkaloids, operate by destabilizing microtubules while taxol appeared to work by microtubule stabilization. Cells treated with taxol were visualized using indirect immunofluorescence microscopy. After 22 hours the morphology of the cells consisted of three zones: microtubules, microtubule bundles and microtubule free. These microtubules were stable even under conditions which normally cause microtubule disintegration such as the presence Ca^{2+} or low temperatures (Nicolaou 1994 ; National Cancer Institute 1983).

Microtubules are involved in many areas of cell physiology, but are essential in the cell division process. During cell division they are the major structural components of the mitotic and meiotic spindle (the area of the cell where the two sets of chromosomes align for separation) (Phillips 1997). Taxol is believed to act as a mitotic spindle poison by binding to polymeric tubulin forming a highly stabilized microtubule. Inhibiting the release of monomeric tubulin from the ends of the microtubule polymer causes the inherently unstable assembly disassembly process to be hampered and therefore cell division is suppressed (National Cancer Institute 1983 ; Simpkins 1997).

Fig. 8. Microtubule Polymerization: Normal and in Presence of Taxol



1.5 Formulation Studies

About the same time as the Horowitz discovery, the main requirements for entering NCI phase 2B development (toxicology studies) were met. In order to proceed to this level of testing, requirements were; acceptable formulation, demonstrated antitumor activity of the formulated drug in an appropriate model, completion of route and schedule dependency studies, and assurance of supply for animal toxicology and Phase I clinical studies.

Finding appropriate formulation for taxol was not an easy task. It has very low solubility in water and other aqueous based solvents, and is 3 to 10 fold less potent than other natural product derived chemotherapy agents. The problem of administering a high dose of a compound with low aqueous solubility was initially tackled using mixed solvents, emulsions, liposomes as well as pro-drug approaches. After much trial and error, the delivery vehicle chosen for toxicology studies was polyoxyethylated castor oil (Cremophor EL) and ethanol (Arbuck 380). This formulation had been used previously with other drugs, however taxol required the highest Cremophor EL concentration per dose attempted and problems in the animal toxicology studies were expected. Using this formulation, route and schedule dependency studies were done against P388 leukemia. Optimal ILS was found to be 78% with around the clock 6.0 mg/kg injections every three hours over one day (Suffness 1995).

1.6 Supply for Continued Testing

The last criteria to be met before 2B approval, was that of supply. Polysciences Inc. was subcontracted by the NCI to provide taxol for the toxicology studies. Using a

modified version of the method originally used by Wall, *Taxus brevifolia* bark was extracted with methanol and the resulting extract partitioned between methylene chloride (CH_2Cl_2) and water. The organic phase was then treated with acetone – hexanes to remove the tars. Next, the taxol rich fraction was obtained using Florisil then purified with multiple silica gel chromatographies and recrystallization (Suffness 1995). This work resulted in 145 g of taxol isolated at 0.025% yield, which presented to the NCI in November of 1979, enabled entry of taxol into Stage 2B development by October of 1980.

1.7 Toxicology Studies

The toxicology studies performed on mice, Sprague-Dawley rats, and beagle dogs were quite problematic. This was as expected, due to the high concentration of Cremaphor EL required. In large single doses, the formulation was in itself toxic to the point of death when administered to beagle dogs, but tolerable on repeated smaller doses. Tests on rats and mice had to be performed i.p since the animals could not tolerate the large volumes of the vehicle which need to be administered by vein. The major toxicities assigned to taxol were myelosuppression, lymphoid depletion, emesis, diarrhea, mucosal ulcerations and toxicity to the male reproductive organs. These toxicities were cumulative over a five day period which indicated a single injection schedule may be preferred. However, as a single injection schedule would require problematically large vehicle volumes, the clinical plan was to try a variety of administration schedules in the clinical trials. The toxicology studies were completed in 1982 and presented to the NCI

Decision Network Committee. An Investigational New Drug Application was filed with the FDA in 1983 and approval was granted for Phase I clinical trials (Suffness 1995).

1.8 Phase I Trials

In the spring of 1984, patients began to be enrolled in Phase I trials in order to determine optimal doses and clinical toxicities for the Phase II efficacy trials. The most significant toxicities observed in the early trials, possibly due mainly to the Cremophor EL, were hypersensitivity reactions (anaphylaxis, dyspnea, hypotension, flushing, urticaria, rash and pruritis). These reactions were so severe (resulting in one death) and prevalent that taxol's clinical development was nearly terminated. Similar adverse effects were previously observed in the use of iodinated radiological contrast dyes. Fortunately, the premedication treatment which had been developed to prevent hypersensitivity to the dyes was effective for taxol and thus adopted as part of the drug regime for Phase I trials from 1985 on. Additionally, increasing the infusion time from 1-3 to 24 hours decreased the incidence of the above mentioned adverse reactions (Arbuck 1995).

The major dose limiting toxicities were found to be leukopenia and neurotoxicity. Doses of 135 to 250 mg/m² caused grade II and IV neutropenia in most patients 8 to 11 days after initial exposure to taxol. After 15 to 21 days the patients recovered, thus retreatment was possible every three weeks. The 24 hr infusion schedule caused neutropenia in more patients than the 3 hr schedule indicating that the neutropenia was both schedule and dose dependent. In efforts to increase the allowable dose an additional premedication was added to the regime to counteract the neutropenia (Arbuck 1995).

At doses higher than 250 mg/m² on a three week interval, peripheral neuropathy became dose limiting. Symptoms such as paresthesias and stocking glove numbness appeared between 24 to 72 hours after treatment. Neuropathy is reversible and recovery is usually complete but since effect was found to be cumulative with taxol, it sometimes took months. Once the patients neuropathic symptoms subsided or lessened pretreatment was possible at a lower dose. The other significant but manageable toxicities associated with the drug were found to be alopecia, fatigue, arthralgia, myalgia, muscositis, nausea, vomiting and diarrhea (Arbuck 1995).

1.9 Phase II Trials

Phase II trials were begun in April 1985 using doses from 135 to 250 mg/m² on a 24 hr infusion schedule on 18 varieties of cancer. Although there were positive responses in all tumor types except renal, pancreatic, and colon the most notable results were found for ovarian, breast, lung (small and non small cell) and head and neck (Arbuck 1995).

Table 3. Phase II Trial Results: Taxol vs. 18 Cancer Types

Cancer Type	# Evaluable Patients	Dose (mg/m ²)	Complete Response	Partial Response	% Objective Response (95% CI) ^a
Ovarian	40	135-250	1	11	30(17-47)
	41	175	5	10	37(22-53)
	44	250	6	15	48(32-63)
	652	135	23	118	22(19-25)
	25	200	1	5	24(9-45)
	30	200	0	1	21(6-46)

^a CI = Confidence Intervals

* One sided CI

Table 3. cont.

Cancer Type	# Evaluable Patients	Dose (mg/m ²)	Complete Response	Partial Response	% Objective Response (95% CI) ^a
Breast	25	250	3	11	56(35-76)
	18	150	0	6	33(13-59)
	156	175	3	33	23(17-31)
	135	34	2	4	18(7-35)
	175	15	1	6	46(21-73)
	135	229	12	53	28(23-35)
	175	225	5	46	23(17-35)
Non-Small cell Lung	25	200	1	5	24(9-45)
Small cell lung	24	250	0	11	34(19-53)
Head and neck	19	250	2	5	37(16-62)
Lymphoma	19	140	0	4	21(6-46)
Melanoma	28	250	3	1	14(4-33)
	25	200,250	0	3	12(3-31)
Renal	18	250	0	0	0(0-15) [*]
Prostate	22	135,170	0	1	5(0-23)
Colon	19	250	0	0	0(0-15) [*]
Cervix	30	135,170	0	3	10(2-27)
Gastric	20	250	0	1	5(0-25)
Pancreas	20	250	0	0	0(0-14) [*]
Bladder	26	250	5	6	42(23-63)
Multiple myeloma	22	125,150	0	5	23(8-45)
Germ cell	25	250	2	4	24(9-45)
Kaposi's sarcoma (HIV assoc.)	6	135	0	1	N.R
Esophagus	42	250	0	13	31(17-45)

^a CI = Confidence Intervals

* One sided CI

The promising results of the phase II trials and the limited supply of taxol for continued testing led the NCI to request applications for a Cooperative Research and Development Agreement (CRADA) in 1989. Bristol-Myers Squibb (BMS) was chosen as

the CRADA partner and began large scale production of taxol under the trade name Taxol® in cooperation with Hauser Corp (Suffness 1995).

1.10 Phase III Trials and Approval by FDA

The phase II trials of ovarian cancer, in which taxol consistently gave complete as well as partial responses, initiated the Gynecological Oncology Group to begin phase III trials in 1991. A combination of taxol and cisplatin was compared with the routine treatment, cyclophosphamide and cisplatin, in women with previously untreated suboptimally debulked ovarian cancer. The results of the taxol and cisplatin arm of the study were promising and had an increased clinical response rate (79% vs. 63%, an improved surgical response rate (26% vs. 19%) and a longer median progression free survival rate (17.9 vs. 13.8 months) (Arbuck 1995). Upon completion of these studies a New Drug Application was filed with the FDA in July of 1992. Twenty eight years after cytotoxicity was first noted in extracts from *Taxus brevifolia* and after development was nearly abandoned numerous times, taxol was approved for treatment of refractory ovarian cancer in December 1992 (Suffness 1995).

Two years later in April of 1994, taxol was FDA approved for treatment of breast cancer. Phase III trials of taxol alone, and in combination with doxorubicin or vinblastine, were sponsored by the NCI and BMS. Response rates in the phase II trials had been between 22 and 66% however, exceptionally high response rates were observed in trials of taxol in combination with doxorubicin. Using this drug combination an overall response rate of 96%, including a 40% complete response rate in women with previously untreated metastatic breast cancer, has been recorded (Rowinsky 1997). Taxol

alone had achieved 23-28% response rates in the phase III trials with only about 5% of the patients showing complete response. However, what was significant about these trials was the fact that similar overall responses were achieved by patients with multi-drug resistant cancer (Arbuck 1995).

1.11 Future Prospects of Taxane Drugs

Taxol[®], and an analogue discovered during synthetic research, Taxotere[®], as solo agents have been proven to be more effective than many routinely used chemotherapy agents. Improved results are seen when used in combination with other agents. Taxol[®] with cisplatin is now the routine primary treatment for advanced ovarian cancer with ongoing trials evaluating its efficacy for early ovarian cancer (McGuire 1998; Young 1998). Recent studies have shown that Taxotere[®] is more active against metastatic breast cancer than the routinely used doxorubicin and may in fact be the most active single agent developed to date (Aapro 1998). Taxol[®] has also been proven to be effective in treating anthracycline-resistant liver metastases and current opinion is that its role in cancer treatment should be moved from “last resort” to adjunctive and neoadjuvant therapy (Hortobagyi 1998).

Besides the two cancers against which the taxane drugs are approved for use, clinical activity has been confirmed in lung (small and non -small cell), head and neck (squamous and nasopharyngeal), esophageal, bladder, testicular, lymphoma, endometrial and Kaposi's sarcoma. Thus within the next few years it is likely that the list of cancers for which these drugs are the front line for treatment will continue to grow. As

prototypes for a new class of anticancer agents, the taxanes have been lauded as the most important discovery in the field of chemotherapy of the decade.

Supply Issues: Solutions via Synthesis

2.0 Natural Abundance and Projected Demand

Continued harvest of the bark *Taxus brevifolia* as a source of taxol is problematic for a number of reasons. The most efficient procedures up to date required 5000 to 6000 kg of bark to produce 1 kg of taxol (Wickremesinhe 1998). Given that a mature (100 year old) tree yields about 5 kg of bark, 1000 mature trees need to be harvested for every kilogram of taxol produced (Croom 1995). Estimates were projected that 350,000 kg of dried bark would be needed yearly to satisfy demand for the drug (Campbell 1994).

2.1 Environmental Problems Associated with Large Scale Harvest

Given that the Pacific Yew is too small and irregular in shape to be used for lumber and the fact that the bark constituted less than 5% of the plants weight, the process of bark harvest is extremely wasteful (Suffness 1995). Additionally, as species rarely grows in groves and prefers limited light under the canopy of taller trees, it is a difficult species to harvest efficiently (Campbell 1994). Environmental concerns for the yew tree itself and the effect of large scale harvesting on the habitat of many animals, including the Northern Spotted Owl, created a set of guidelines for harvest in the USA. Seven separate harvesting plans were constructed which attempted to provide as much taxol as possible for cancer treatment while protecting the yew tree and its ecosystem. The plans which hypothetically would meet supply demands did so at the expense of the ecosystem and its wildlife, while those which preserved the environment provided taxol

for only approximately half of the projected cancer patients who could benefit from treatment (Croom 1995 ; Campbell 1994).

2.2 Challenge of Total Synthesis

It was clear that an alternative method of production was necessary and also potentially very lucrative so research groups around the world began work on the total synthesis of taxol. It took researchers twenty years to construct this complicated molecule which; a) contained an eight membered carbocycle, notoriously difficult to synthesize due to entropic and enthalpic factors, and had geminal methyl groups projecting into the interior of the ring increasing transannular strain, b) had a bridgehead alkene formally forbidden in six membered rings by Bredt's rule, c) imposed the challenging task of inserting a 1,3 C₃ bridge to *trans* fuse the angular methyl group containing C ring with the A ring, d) due to the high degree of oxygenation, required differential protection of five alkoxy groups, and e) required careful considerations of the reaction environments as certain functionalities such as the oxetane ring and 7-hydroxyl groups were quite sensitive (Nicolaou 1994).

2.2A Selected Synthetic Routes: Holton and Wender

The race ended in a tie as total synthesis of taxol was achieved in 1994 by Holton and Nicolaou independently. Since 1994 other groups have successfully synthesized the molecule and the following represents only a selection of the total synthesis of taxol to date (Phillips 1997). The methods of Holton and Wender begin with readily available

optically active chemicals and are based on fragmentation of a tricyclic systems to give the A/B ring system with following attachment of the C and D rings.

Fig. 9. Holton's Total Synthesis of Taxol

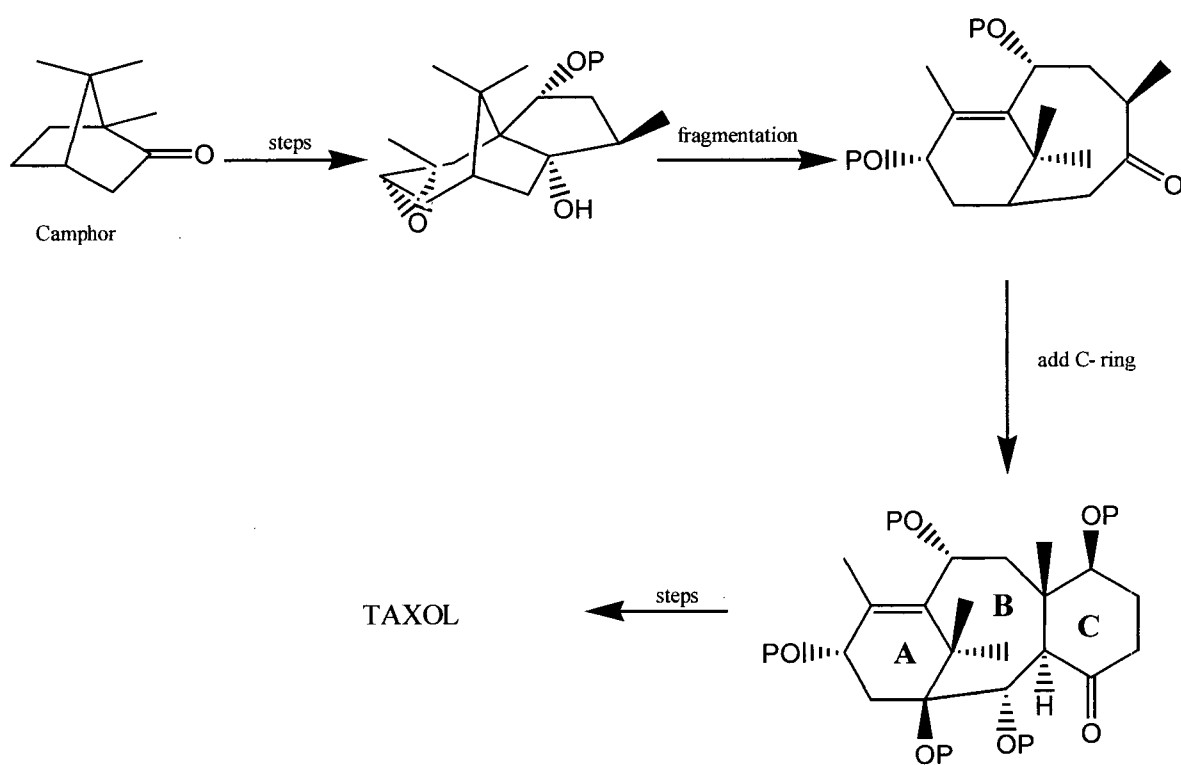
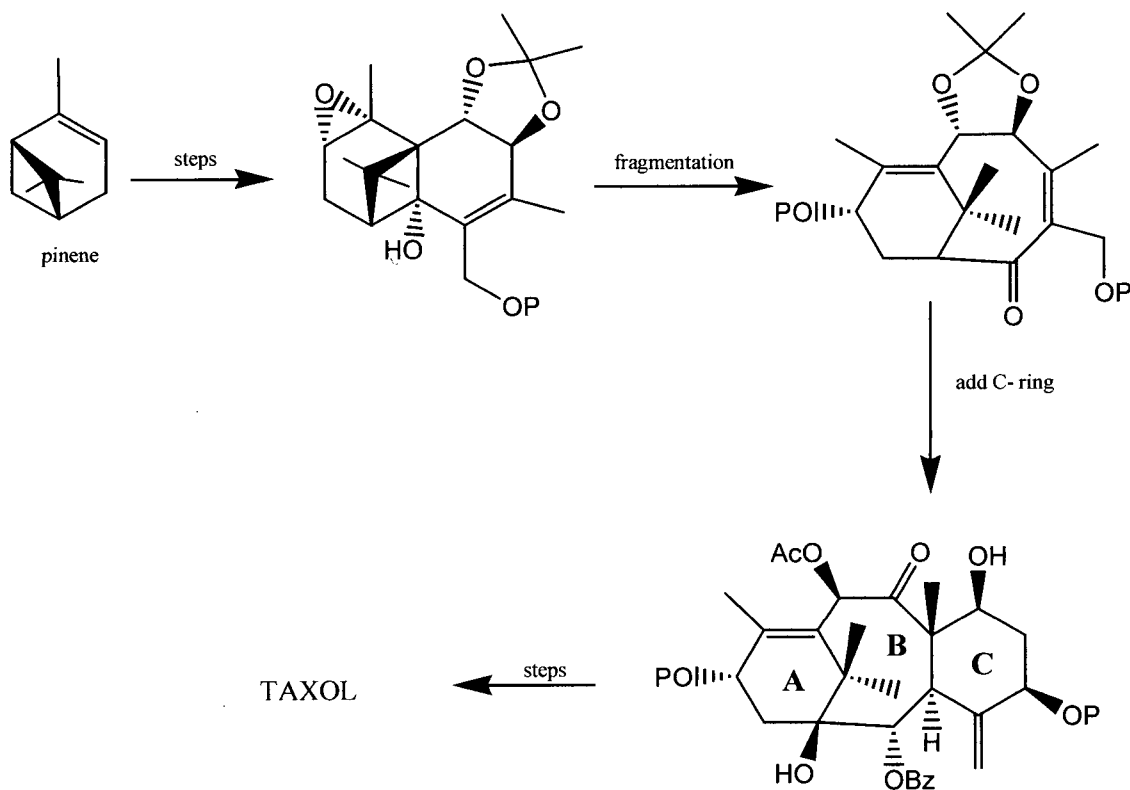


Fig. 10. Wender's Total Synthesis of Taxol



2.2B Selected Synthetic Routes: Nicolaou and Danishefsky

Danishefsky and Nicolaou's methods join the A and C rings using six membered ring starting materials and construct the B ring via reactions between the functionalities of the two starting compounds. The synthesis of Nicolaou differs in that none of the starting materials are optically active.

Fig. 11. Nicolaou's Total Synthesis of Taxol

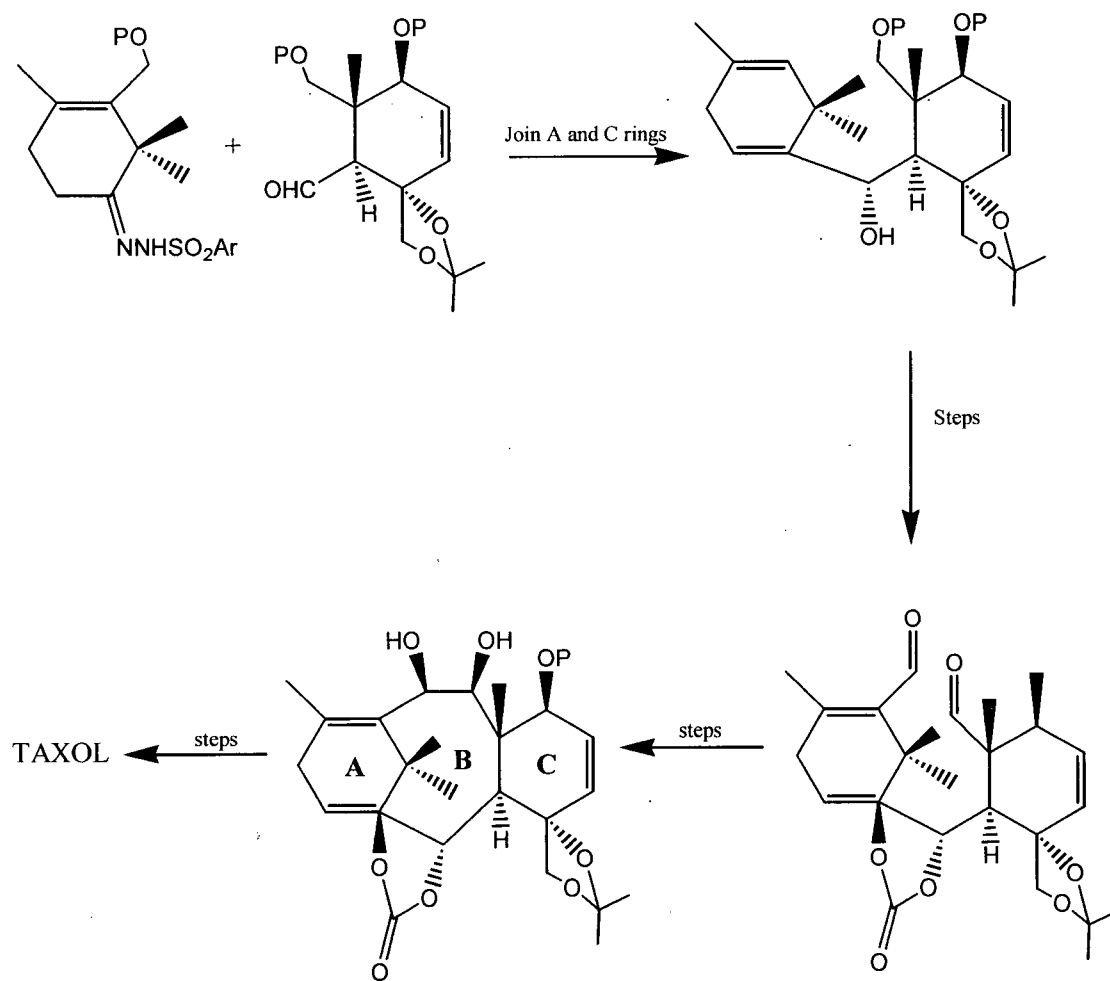
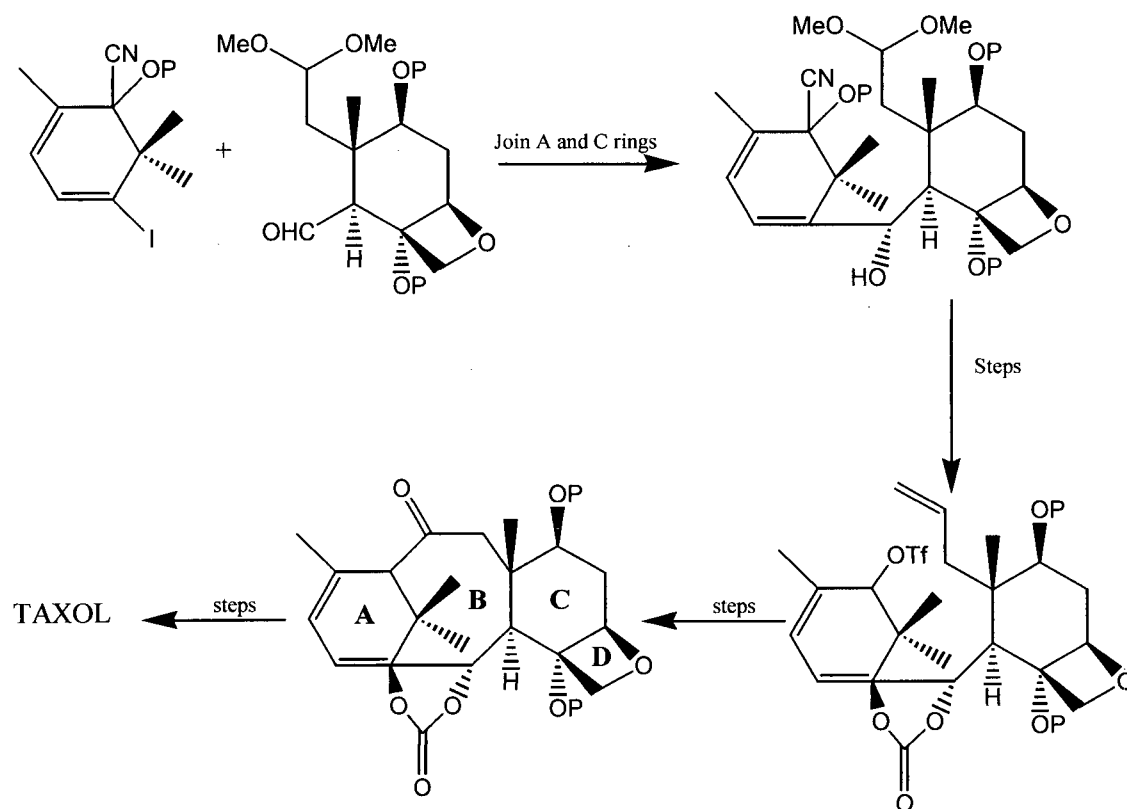


Fig. 12. Danishefsky's Total Synthesis of Taxol



2.2C Commercial Taxol from Total Synthesis?

More recent synthetic routes to taxol have used different starting materials and strategies to elegantly construct this complex compound (Kuwajima 1998 ; Mukaiyama 1998). However, it is unlikely that total synthesis will ever be competitive with the established semisynthetic methods, as a route of no more than 25 steps would need to be established and yields greatly increased (Phillips 1997). As perhaps one of the most challenging natural products ever to be "built" on the bench top, the efforts of these

researchers to construct taxol contributed a great deal to the field of asymmetric synthetic chemistry.

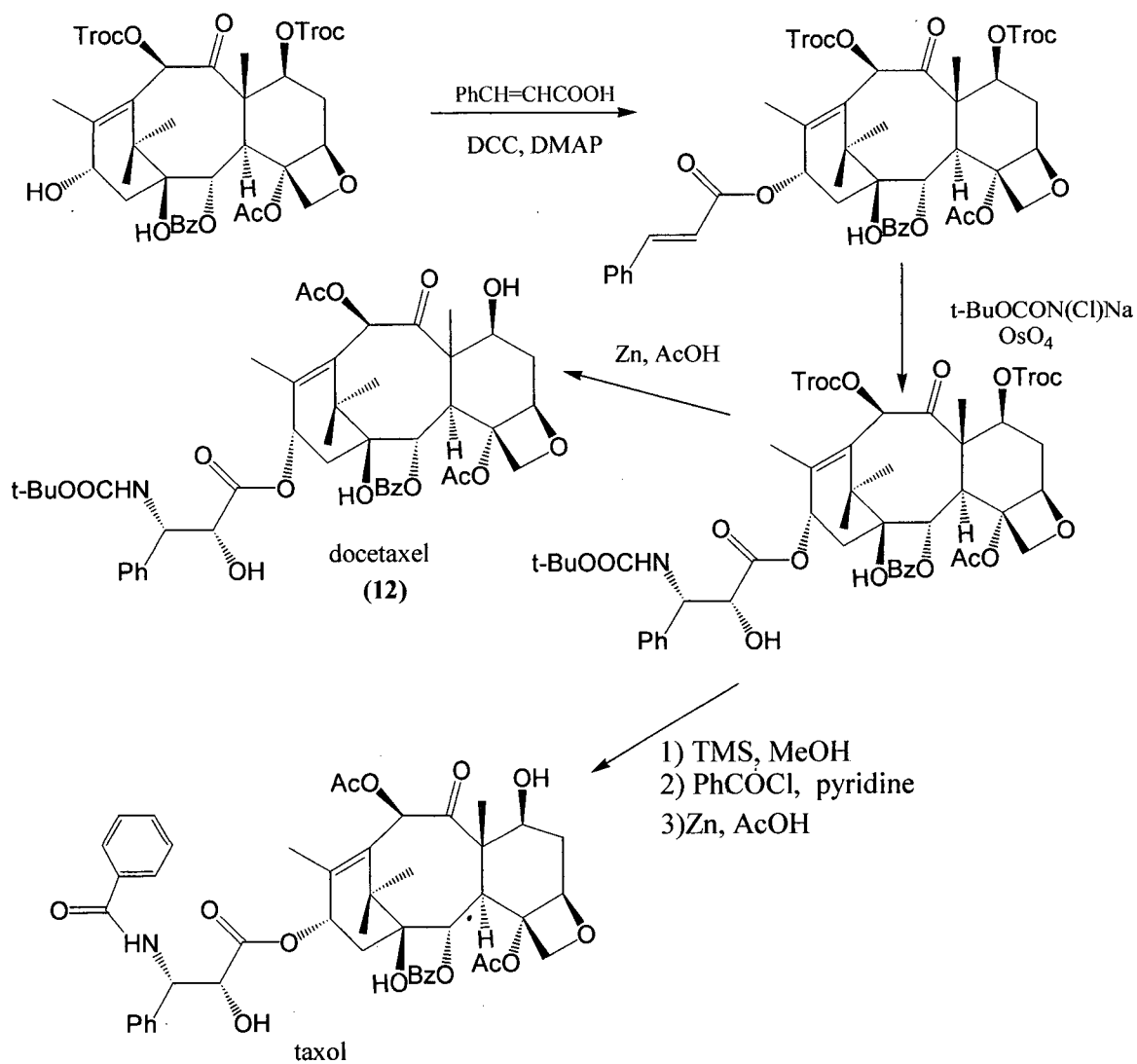
2.3 Semisynthesis, a Solution to Supply Issues

As total synthesis was not a practical solution to supply issues, semisynthetic routes from 10 deacetyl- baccatin (10 DAB) were explored. Concentrations of 10-DAB in the needles of *Taxus baccata* have been reported at 0.1% and higher and it is significantly simpler, thus more economical, to isolate and purify than taxol. Confident that sufficiently efficient semisynthetic methods would be developed the NCI and BMS supported Weyerhaeuser Company in the establishment of a commercial scale nursery plantation of *Taxus* in 1989 (Croom 1995). In August of 1994 the original contract naming Hauser as the supplier of *Taxus* bark for Taxol[®] production by BMS expired and was not renewed as the FDA approved use of semisynthetically derived Taxol[®] in October of the same year (Suffness 1995).

2.3A Potier's Semisynthesis

Pioneering studies of semisynthesis of Taxol from 10-DAB were led in France by Potier in which the reactivity of the four hydroxyl groups was ranked. The C-7 hydroxyl was found to be the most reactive, followed by the C-10, C-13 and C-1. Potier successfully synthesized taxol from 10-DAB via the following route, however the time involved coupled with the overall yield made the process inappropriate for commercial development (Holton 1995).

Fig. 13 Potier's Semisynthesis of Taxol



Although not a commercially viable route to taxol, Potier's studies provided numerous taxane compounds which were tested for biological activity. One compound,

docetaxel (**12**), was found to be more active than taxol and has since been FDA approved for the treatment of breast and non-small cell lung cancers. It is currently marketed under the trade name Taxotere[®] by Rhone -Poulenc Rorer (Rhone-Poulenc Rorer 1995).

2.3B Manufacturing via Holton's Synthesis

Currently Taxol[®] and Taxotere[®] are manufactured using a semisynthetic method in which 10- DAB harvested from the needles of *Taxus baccata* is converted to the desired compound. Numerous reaction schemes have been developed, however production of the compounds by BMS and Rhone -Poulenc -Rorer in multi-kilogram quantities is via a method developed by Holton (Phillips 1997 ; Wall 1998). The starting material, 10- DAB is selectively acetylated and protected with triethylsilane (TES). The hydroxyl group at C-13 of this compound reacts with the selected β -lactam to give either taxol (**11**) or docetaxel (**12**) (Wall 1998).

Fig. 14. Commercial Method of Producing Taxol

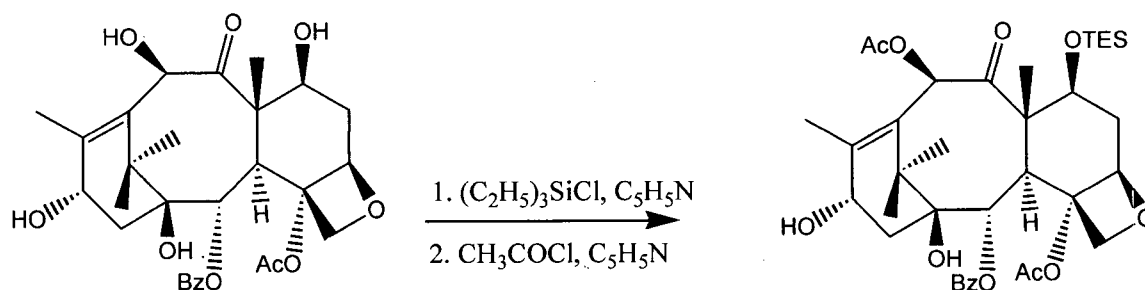
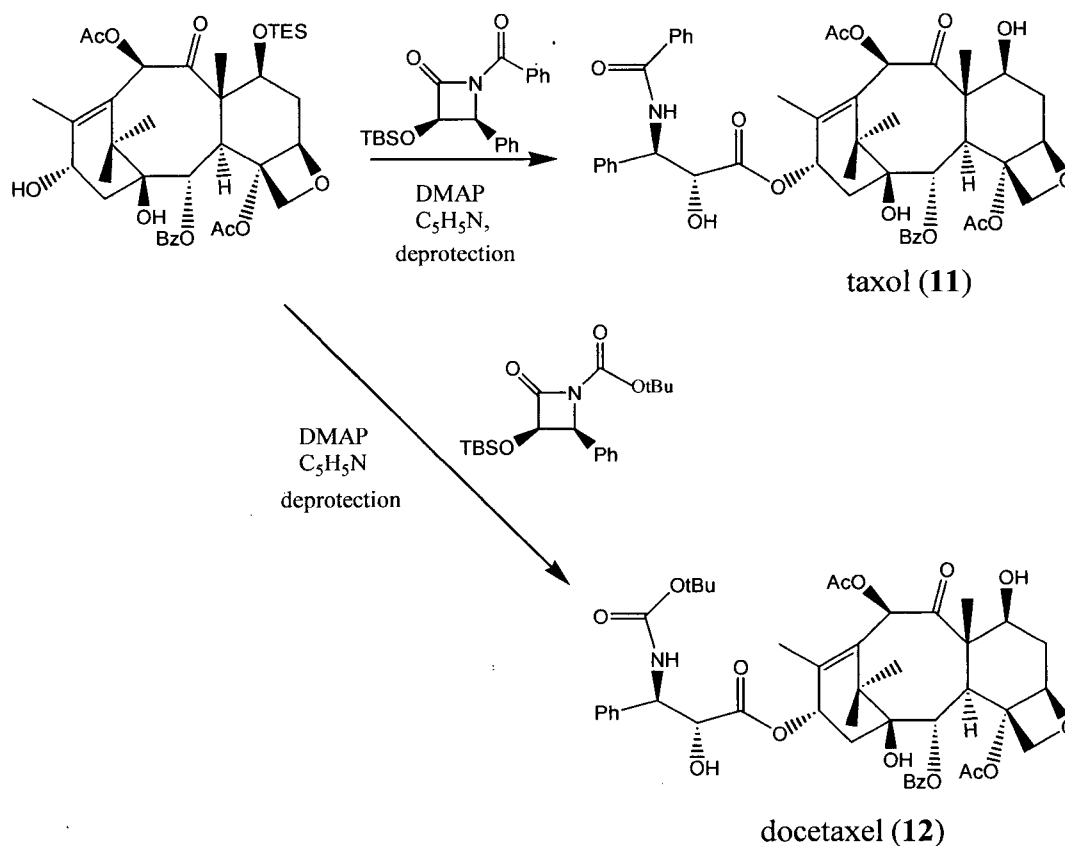


Fig. 14. cont.



2.3C Benefits of Semisynthesis

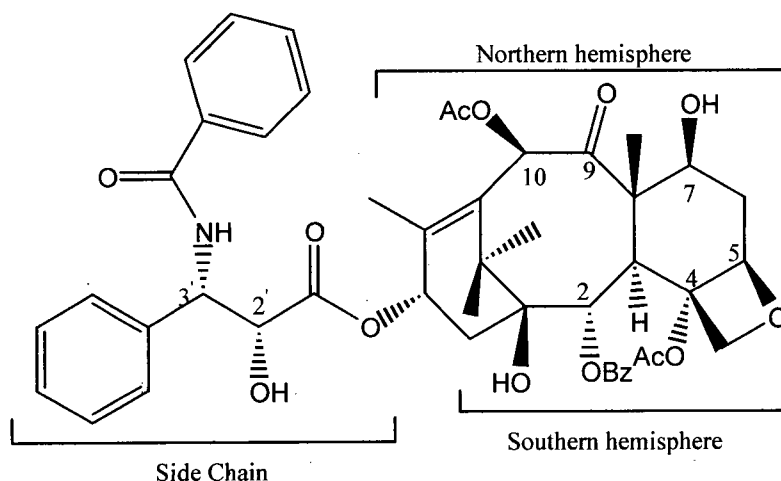
Semisynthesis solves and simplifies a number of the problems associated with the original source, isolation from the bark of *Taxus brevifolia*. Needles as the source of the starting material are a renewable resource and can be grown on plantations alleviating problems associated with the environmental impact of bark harvest. Concentrations of 10-DAB in the needles of *Taxus baccata* are high compared to the 0.0001 to 0.069% range of taxol found in the bark (Croom 1995). Also, 10 DAB need be only pure enough

to use as starting material while the taxol isolated had to be pure enough to pass FDA standards for direct drug formulation, therefore the semisynthetic isolation is less costly (Holton 1995). Additionally, availability of a starting material with the complex taxane skeleton facilitates synthesis of novel compounds which may be found to be even more effective anticancer agents than taxol, as in the case of docetaxel.

2.4 Benefits of Synthetic Research: Structure Activity Relationships (SAR)

Synthetic research has provided a number of compounds which through biological screening have mapped out a great deal of the structure activity relationship. The molecule can be roughly broken down into three portions, side chain, northern and southern hemispheres, using the nomenclature of Kingston.

Fig. 15. SAR Nomenclature for Taxol



Briefly, the side chain is considered critical for bioactivity, while the structural integrity of the southern hemisphere is less critical than the side chain, but less open to modification than the northern hemisphere (Nicolaou 1994). Key sites in the more sensitive portions of the molecule have been identified as:

Side chain: free 2' - hydroxyl group or hydrolyzable ester thereof, C-3' phenyl group or close analog, a N-acyl group

Southern hemisphere: 2-benzoyl group, 4,5 oxetane ring, 4-acetate group (may be essential, however removal is difficult without effecting 4,5 oxetane)

The northern hemisphere can undergo considerable modification without loss of activity. The carbonyl group at C-9 is unessential as reduction leads to no loss of activity. Esterification, epimerization and removal of the 7- β -hydroxyl group is possible with only slight loss of activity. Additionally the C-10 acetate can be hydrolyzed or replaced with another ester and still exhibit activity (Wall 1998).

Plant Cell Culture

3.0 Advantages of Plant Cell Culture

Potentially the most viable alternative industrial source of taxol or taxane compounds as starting materials for semisynthesis are plant cell culture systems. Currently two compounds shikonin (a red dye and anti-inflammatory) and ginsenoside (a tonic in Asian medicine) are produced in Japan by plant cell culture with other cultures which produce vanillin, berberine and rosmarinic acid very close to commercialization (Yeoman 1990 ; Gibsons 1995).

Plant cell culture offers many advantages over field grown materials. Climate does not effect *in vitro* systems thus production is possible anywhere in the world. Furthermore, as cell culture systems are not effected by disease, weather and season, they are potentially a much more reliable renewable source. Optimization of nutrient or gas composition, and addition of elicitors produce higher yields enabling supply to be consistent with demand. For example, the production of shikonin by cultured cells is 23% shikonin per gram of dry weight compared to 1.5% gram per dry weight found in the plant's roots (Lambie 1990). Additionally, once defined conditions are set, cell culture produces more consistent product quality within a less complicated mixture, thus making the process of isolation and purification more economical.

3.1 Impediments in Development

The question arises: why are cell cultures not currently being used to produce taxanes? Three companies Phyton Catalytic Inc., ESCAgenetics, and Mitsui

Petrochemical Industries have patented processes and report being on the brink of commercial production of taxol by plant cell culture (Wickremesinhe 1998 ; Yukimune. 1997). To date, the difficulties preventing commercial use of *Taxus sp.* cell cultures have been achieving acceptable reproducible product levels in a reasonable amount of time. The economic feasibility of a developed system is evaluated on the basis of volumetric productivity or amount made per liter per day. Required productivity to make taxol via cell culture economically viable has been estimated at 1-2/mg/l/day (Jaziri 1996). Only recently have these titers been exceeded and only in one liter shake flasks, not industrial size bioreactors. In the latest patent application by Phyton Inc. reports of 13 mg/l/day, 18 mg/l/day and 14 mg/l/day for batch production of taxol, baccatin III and 10- DAB respectively made in an 11 day process (Bringi 1997). *Echinacea purpurea* has been successfully cultured in 75,000 liter tanks thus, if this technology can be transferred to a high producing *Taxus sp.* cell line, the potential to produce great profits exists from operation of just one bioreactor, as bulk wholesale value for taxol is approximately 200 USD per gram (Signh 1994 ; Gibsom 1995).

3.2 Issues of Scale Up

The process of moving from one liter shake flasks to industrial size bioreactors is more than a matter of increased vessel size, and the problems associated with upscaling must be addressed before taxol from cell culture becomes a reality. Although there have been successful large scale fermentations of plant cell culture, each type of bioreactor has limitations which may be difficult to overcome for any one particular plant species. For example, if the cells are particularly shear sensitive, the

culture may not be able to be grown in a stirred tank reactor. Airlift reactors typically have low density per unit volume making them inefficient, and require large amounts of sterile air. Additionally, the air must be enriched with carbon dioxide (CO₂) or the cells may be over oxygenated (Lambie 1990). Currently, much research into immobilized cell systems is being undertaken. The advantages being that the cells secrete the product into the medium thus they can be used over a prolonged period of time and the product recovered simply by exchanging the medium. Costs are cut since labor is reduced and medium can be recycled (Pierik 1997). However, these systems must compete with successful modifications in the conventional reactor designs preceded in the microbial fermentation industry and used in the albeit small but existing plant cell fermentation industry (Singh 1994).

3.3 History of *Taxus sp.* Cell Culture

Research into the development of *Taxus sp.* cell cultures began prior to the discovery of taxol. Cultures of *Taxus* gametophyte and pollen were established as early as 1953 by Larue and 1959 by Tuleke. These early studies investigating the organogenetic potential of *Taxus sp.* pollen, were followed up by Lepage and Degivry who published several papers in 1970 on the germination of *Taxus sp.* embryos. At this time interest was focused on the role of abscisic acid in breaking seed dormancy. A few years later *Taxus sp.* callus culture was grown by Rohr which spurred research by David who improved proliferation of callus cultures initiated from mature stem explants. The mineral and phytohormone composition was manipulated to improve growth and tobacco callus

was used as a nurse culture. It was determined through these studies that the slow growth of *Taxus sp.* callus was due to the accumulation of tannins (Jaziri 1996).

After the discovery of the unique mechanism of taxol in 1979, and given the supply issues at the time, research was initiated in the development of a taxol producing cell culture. Christen et al. first reported the production of taxol by *Taxus sp.* callus culture in 1989. Their work led to the first patent granted for production of taxanes by cell culture to the USDA in 1991 (Christen 1991). Since then, many groups have been working on the development of a high producing cell line. Between 1991 and 1996 approximately 75 papers including 18 patents were published on *Taxus sp.* cell and tissue culture (Jaziri 1996).

3.4 Development of Plant Cell Culture Systems

Interest remains high in developing a commercially viable system since the wholesale bulk market value of taxol was 941 million USD in 1997 alone (Jacobs 1998). However, development of a producing culture can be described as trial and error research on a two week to one month per experiment time scale. Contamination problems are common as over 300 endophytic fungi have been isolated from the bark and needles of *T. brevifolia* (Jazirii 1996). Fungi contaminations are frequently observed after incubation of the tissue culture and often lead to termination of experiments. It is important also to note that although growing in a controlled environment, cell culture is a biological system and thus the element of unpredictability demands that results be confirmed many times before deemed “reproducible”.

3.5 Choice of Explant Material

The process of developing a taxane producing cell culture system begins with the choice of a high metabolite producing cell line. However, finding a high producing explant is not necessarily an elementary task. Numerous studies have shown that there is great variety in the taxol content in the different varieties of *Taxus sp.* found throughout the world. On examining the taxol content found in the stem, amounts reported range between 0.0006 % to 0.021% dry weight for the different species. Incidentally, the highest and lowest values are obtained from the same species reported by different research groups. This probably reflects not the accuracy of the technique used in quantifying taxol but the great variety observed within populations of the same species. A study of 25,000 plants generated from 700 parents found the range of 10-DAB to be 0.008 to 0.172 % and baccatin to vary between 0.005 and 0.12% dry weight (Croom 1995).

However, even if a high producing explant is chosen the resulting cell culture may not produce desirable results. Studies on *Taxus canadensis*, *Taxus cuspidata*, *Taxus baccata*, *Taxus Brevifolia*, and *Taxus x media* have shown growth of the cell culture and taxane content to be variable for cell lines taken from similar explant material and incubated under the same conditions (Ketchum 1993 ; Wickremesinhe 1993).

3.6 Variability in Taxol Production

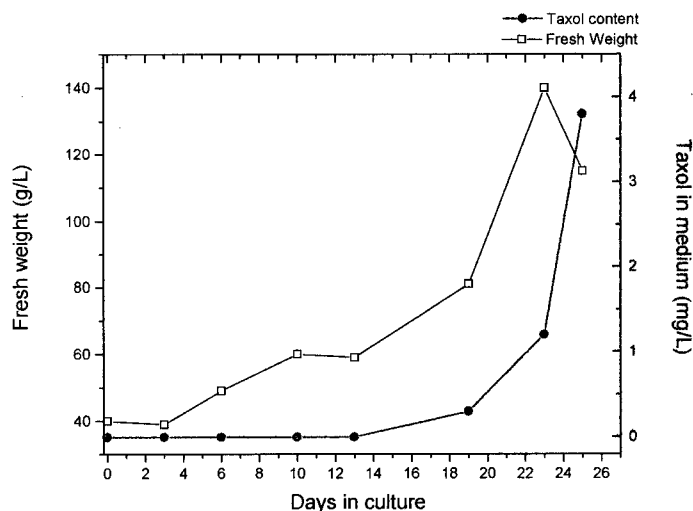
Variability in the production of taxanes within an individual cell line is also observed with respect to time (Shuler 1995). Ketchum observed one cell line produce 25 mg/l of taxol in January 1994, decline to undetectable levels between July and December

1994, increase to 10 mg/l in February 1995, fall to less than 1 mg/l from March to June 1995, climb to 5 mg/l in July 1995, and fall back to 1- 3 mg/l in August 1995 (Ketchum 1996). In these experiments, variation in taxol production was independent of the growth rates of the cell culture.

3.7 Kinetics of Cell Growth and Taxol Production

The kinetics of taxol production in plant cell culture has been extensively studied by numerous groups with varying results. Generally, the growth curve of cells grown without elicitors is biphasic in shape with taxane production reaching a maximum at the end of the growth cycle (Shuler 1995 ; Gibsom 1995).

Fig. 16. Typical Cell Growth and Taxol Production by Cell Culture



Optimization of the culture conditions has led to systems which will produce maximum concentrations of taxanes in about half the time (Bringi 1996 ; Yukimune 1996).

3.8 Optimization of Media for Maximum Taxane Production

Cell culture media is a complex mixture containing major inorganic nutrients, trace elements, an iron source, vitamins, carbohydrates, and phytohormones. Given the great number of variables optimization is a lengthy process. Additionally, optimal conditions are unique for *every cell line*, thus development of plant cell culture systems is somewhat more of an art than a science.

Much investigation into the optimal growth medium for cell cultures of *Taxus sp.* has been done. Up to date, modified versions of the B5 media developed by Gambourg remain the most common nutrient mixture used for growing *Taxus sp.* cell culture, however others such as Murashige-Skoog (MS), Scenk and Hildebrandt (SH), Woody plant Medium (WPM) and optimized mediums developed specifically for *Taxus* (TM5-TM10) by Ketchum and Gibson have also been used (Zhong 1995).

Studies by DiCosmo indicated increased growth of callus culture did not correspond to increased taxane content in studies done comparing B5, SH, and MS media (DiCosmo 1993). Likewise, in the latest patent application by Phyton Inc. results indicated that cell culture growth and taxane production were independent of one and another in suspension cultures of *Taxus sp.* in sixteen different media compositions (Bringi 1996). This phenomenon could be the result of any number or combination of factors such as; repression of regulatory genes in non-specialized cells, diversion of

substrates from secondary metabolism, non-operational end product transport mechanisms, lack of proper storage sites or unregulated catabolism of synthesized products (DiCosmo 1994). However, optimizing growth conditions is desirable in the hopes that future research may lead to shorter doubling times and the discovery of an elicitor that would induce the cells to produce high levels of taxol during the growth phase. Indeed, a fast growing cell culture system producing a high concentration of taxanes is the most desirable commercially viable system.

3.8A Effect of Growth Hormones

Most cell culture media contain either or both an auxin (cell elongation and division inducer) and a cytokin (cell division inducer). However, gibberellins (GA_3) and abscisic acid (ABA), hormones which play a role in dormancy and senescence, have also been used. Both naturally occurring auxins (indole-3-acetic acid (IAA)) and synthetic (2,4 dichlorophenoxyacetic acid (2,4 D), naphthalenacetic acid (NAA), indole-3-butyric acid (IBA), picloram (4-amino-3,5,6-trichloropicolinic acid (P)) have been used in growing *Taxus sp.* cell culture. Cytokins, such as kinetin (K), benzyladenine (BA), 2iP (6-(γ , γ -dimethylallylamino)purine) zeatin (Z), dihydrozeatin (dZ) and Thiadiazuron (Th), used in combination with an auxin are also common (Ketchum 1996).

The effect of phytohormone optimization on taxane production was exemplified by Ketchum. In multiple flask experiments of a single cell line, manipulations of auxin and cytokin type produced taxol in concentrations between $< 1\text{mg/l}$ and 14mg/l . However, the results were not transposable between species, as it was also found that IAA/BA combination was superior for lines of *T.cuspidata* but NAA/Th best for

T.canadensis (Ketchum 1996). Other researchers have noted similar results, for example the most recent patent application Phyton INC. reports the P/BA combination best for *T. globosa*, *T.floridana*, *T.baccata*, *T.cuspidata*, *T. media* and *T.wallichiana* but, cite P/2iP as additional preferred conditions for *T.brevifolia*, P/K for *T.canadensis*, and N/BA for *T.chinensis* (Bringi 1997).

3.8B Carbohydrate Manipulations

As the carbon source is important not only to cell growth, but also in the production of secondary metabolites, manipulations of the carbohydrate type and concentration used in the nutrient mixture have also been investigated to achieve enhancements in taxane production. Most secondary metabolites are synthesized later in the culture cycle after division has stopped and are affiliated with the processes of cell differentiation. Often an inverse relationship between growth and accumulation of secondary metabolites is observed.

The kinetics of carbohydrate uptake were studied in suspension cultures of *T. cuspidata* and *T. x media*. Sucrose was hydrolyzed in the first week of culture indicating the *Taxus sp.* cells possess an excess amount of invertase. After one week there was an apparent preference for glucose over fructose until carbohydrate sources were depleted or the experiment terminated on week three (DiCosmo 1994 ; Wickremesinhe 1994).

When added during the stationary phase of the culture carbohydrates can provide a carbon source for secondary metabolite production. For example, a doubling effect on the amount of taxol has been noted when fructose is added on day 11 (Linden 1995). To maximize product accumulation another approach has been to slow down or restrict

growth by limiting the available sugar or other nutrients (Yeoman 1990). Conversely, high concentrations of sugar (7 to 10%) can also be used to increase osmotic pressure which is believed to stimulate stress induced secondary metabolite production (Kim 1995 ; Gibsom 1995).

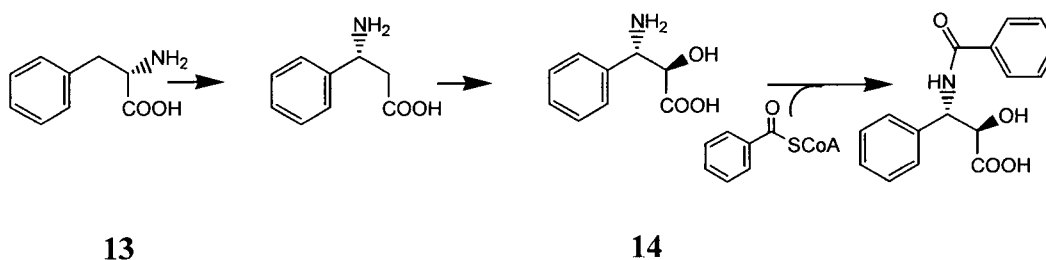
Many studies comparing the effects of carbohydrate source on taxane production indicate that use of fructose and sucrose enhance taxane production while glucose is inhibitory, however individual cell lines respond differently to each tested carbohydrate regime. Ketchum found that sucrose produced superior results to sucrose/fructose combinations and to fructose alone in cultures of *T. canadensis* and *T. cuspidata* (Ketchum. 1996). However, fructose was found to be the superior source in cultures of *T. brevifolia* by Kim, *T. x media* by Wickremesinhe and *T. baccata* by Shuler (Kim 1995 ; Wickremesinhe 1993 ; Shuler 1995). It is not to be inferred that each *Taxus* species shows a carbohydrate preference. In cultures of *T. Baccata*, Shuler observed that low (<0.1 mg/l) and moderate (4 mg/l) producing cell lines produced 703% and 165% increases in taxol and baccatin III respectfully when 10 g/l fructose was used in the media. Yet high (13 mg/l) producing cell lines showed a decrease of 23% with fructose (Shuler 1995).

Use of other sugars including lactose, maltose, galactose, raffinose, mannose, cellobiose, arabinose and xylose have been mentioned in the literature. Besides glucose, sucrose and fructose, only maltose and lactose have been named among preferred carbohydrate sources in patents assigned to Phyton Inc. and Mitsui Petrochemicals Ltd. respectfully (Bringi 1997 ; Yukimune 1997).

3.8C Use of Amino Acids

Although cell cultures are normally capable of synthesizing all the required amino acids required for growth and metabolite production from the nitrate and ammonium in the media, supplementation has resulted in positive effects. (Wickremesinhe 1993). Functioning as a nitrogen source or biosynthetic precursor, amino acids such as glutamine, casamino acid, alanine, phenyl alanine, serine, glycine, N-benzoylglycine, asparic acid, arginine, proline and mixtures of amino acids such as casein hydrolysate have been used to enhance growth and taxane production. DiCosmo significantly increased taxol production using serine (~280% increase), glycine (~280%) phenylalanine(~400%) and N-benzoylglycine (~500%) (DiCosmo 1994). The promotion of taxol production by these compounds is likely due to their role as precursors in the biosynthesis of the C13 side chain. Feeding studies indicate that the phenylisoserine (**14**) side chain is formed via an aminoase reaction of phenylalanine (**13**). Addition of Benzoyl CoA completes the side chain structure (Floss 1995).

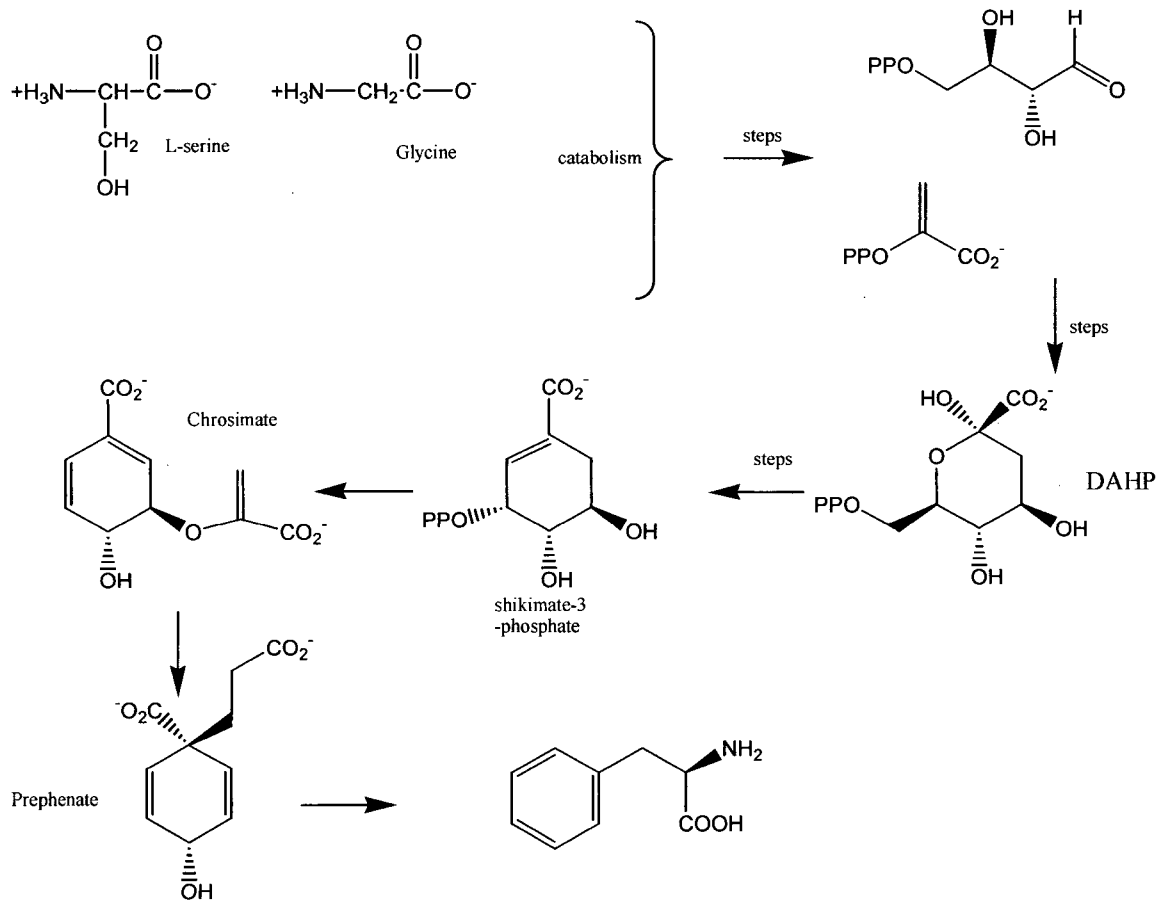
Fig. 17. Phenylalanine (**13**) as Precursor to Phenylisoserine (**14**) Side Chain of Taxol



Once metabolized, serine and glycine could enter the shikimic acid pathway leading to phenylalanine to provide precursor moieties. Increase in taxol production due to addition

of N-benzoylglycine could be explained by a hydrolysis reaction producing benzoic acid and glycine (DiCosmo 1994).

Fig. 18. Shikimic Acid Pathway to Phenylalanine (13)



13

3.9 Gas Composition

Correlations between gas transfer and culture performance have been noted in numerous plant culture systems. Ethylene, oxygen and carbon dioxide are the three gases

which are essential to growth and production of secondary metabolites. Oxygen is important not only in respiration and other aspects of cell metabolism, but also facilitates oxidative steps in the biosynthesis of secondary metabolites (Linden 1995 ; Hall 1974). Carbon dioxide, also important in respiration, is reduced and incorporated into compounds involved in primary and secondary metabolism. Ethylene, frequently produced when plants undergo stress, can stimulate production of secondary metabolites. Linden found the ideal gas ratio to be 10% (v/v) oxygen, 0.5% (v/v) CO₂ and 5 ppm ethylene at which cell cultures of *Taxus cuspidata* nearly doubled their productivity from 6.5 mg/l to 12.2 mg/l. However, patents by Phyton Inc. and Mitsui Petrochemicals found either that ethylene was detrimental to taxane production or use of an anti-ethylene agent such as silver ion promoted taxane production (Bringi 1997 ; Yukimune 1997).

In the latest patent application by Phyton Inc., the inventors indicated that optimal gas concentrations differed with growth and kinetics of the culture. They report 25%-95% oxygen (v/v) and 0.3% - 8% (v/v) CO₂ as preferable conditions for their cell cultures with higher oxygen lower carbon dioxide concentrations being preferable in the growth phase (Bringi 1997).

3.10 Effect of Light

Taxus cuspidata cell culture grown in the presence of white light was found to produce lower concentrations of taxol and baccatin III (DiCosmo 1995). Light is known to stimulate biosynthesis of phenolics by stimulating the activity of the phenylalanine ammonia lyase. In the presence of the enzyme, phenylalanine deaminates to cinnamic acid, a precursor to other phenolic compounds having a two fold effect on inhibiting taxol

and baccatin III production. Phenolic compounds are detrimental to growth of the culture. Additionally, as phenylalanine is needed for the biosynthesis of the phenylisoserine side chain and production of benzoic acid is needed to functionalize both taxol and baccatin III, decreases in availability of these building blocks deter formation of the desired compounds. The effect of white light on cell culture mirrors previous reports which found that the concentrations of taxol and cephalomannine in sun exposed bark of *Taxus brevifolia* was significantly less than that found in shade grown trees (DiCosmo 1995).

In their latest patent application, Phyton Inc. reports two positive effects of a Standard Gro-Lux light (increased wattage in the 600-700 nm range) on their cell culture. Although, the total taxane content was not affected by the light treatment the taxol content was increased by 2.8 fold. Furthermore, 20% more of the compound was excreted into the media which is desirable since extracellular material is easier to extract and isolate (Bringi 1997).

3.11 Use of Elicitors

Many of the phytochemicals of interest for pharmaceutical purposes are not essential for development or growth of the plant but have an auxiliary purpose such as protection from pathogens, or have anti-feedant or insect attractant properties (Wink 1990). Addition of pathogens or compounds which elicit the cells to respond as if they have been wounded has been shown to induce production of secondary metabolites.

3.11A Biotic Elicitors

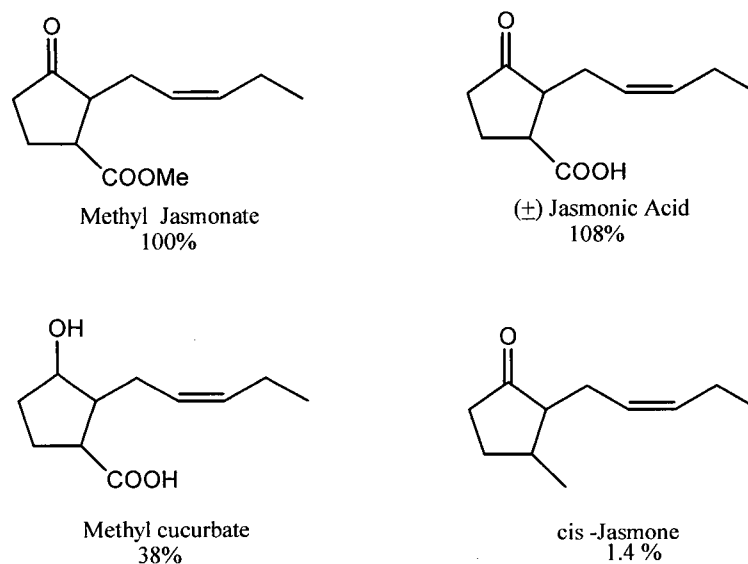
Elicitors of biological origin such as cell extracts and filtrates from *Penicillium minioluteum*, *Botrytis cinerea*, *V. dahliae*, and *Gilocladium deliquescens* bacteria were found to increase taxane production. More specifically it was found that chitosan glutamate and lichenan, complex polysaccharides derived from microbial cell walls and ferulic, arachidonic and benzoic acids stimulated taxane synthesis (Bringi 1997 ; Shuler 1996). The exact role taxol plays for the yew tree is not well understood, given its toxicity one might propose it be of an antipathogen nature. However, a large number of taxanes are present at high concentrations in parts of the plant which are not toxic. Furthermore, the taxanes mechanisms of action involve interaction with tubulin and therefore are nontoxic to prokaryotic organisms, indicating that perhaps this molecule has a more specialized purpose (Suffness 1994).

3.11B Jasmonic Acid Derivatives as Elicitors

Currently, the elicitors which have produced the most dramatic effects in enhancement of taxol production are jasmonic acid and its esters. Jasmonates are believed to be the key signal transducers regulating defense genes in plants leading to the biosynthesis of secondary metabolites. A study comparing the elicitation effect of methyl jasmonate, (\pm) jasmonic acid, methyl curcubate, and cis jasmone revealed that the structural components of the molecule responsible for the enhancement in taxol production were the acetic acid (or ester) functionality and the keto group at C- 3 (Yukimune 1996). These results were in agreement with other experiments which

reflected a similar structure activity relationship in tuber inducing activity for potatoes and senescence promotion in oat leaves.

Fig. 19. SAR of Jasmonic Acid and Derivatives on Taxol Production by Cultured Cells



$$\% \text{ Promoting activity} = (T-C)/(J-C) * 100$$

T = Taxol production

C = Taxol production in control

J = Taxol Production in methyl jasmonate treated cultures

Use of methyl jasmonate as an elicitor has been shown to increase taxol and baccatin III production in cell lines by twenty fold (Linden 1996 ; Yukimune 1996). Additionally, a secondary beneficial effect is observed in that production of cephalomannine seems to be suppressed. Cephalomannine is problematic in the purification of taxol as it is very structurally similar to taxol, differing only in that the phenyl amide of the side chain is replaced by 2-butenyl amide. In one study, the production of taxol rose by 68%, and baccatin III by 28% , while cephalomannine only

increased by 4% (Yukimune 1996). As purification is timely and therefore expensive, progress in making the process more efficient is key in developing an economically viable cell culture system.

3.12 Commercial Production of Taxol from Cell Culture

Two companies, Phyton Inc. and Mitsui Petrochemicals have manipulated *Taxus* *sp.* cell cultures to produce 100 times more taxol and baccatins than the titers reported in early systems and report being on the verge of moving into commercial production. Bristol -Myers Squibb, who held exclusive marketing rights of taxol in North America until 1997, has invested 25 million USD in the past five years in Phyton Inc. to commercialize Phyton's existing plant cell fermentation technology (Jacobs 1998). Mitsui Petrochemicals has been successfully producing shikonin from fermentation of *lithospermum erthrohizon* in large scale bioreactors for years (Lambie 1990). As much progress has been made in maximizing the yield of taxol and other taxanes while minimizing time and costs, and since the great potential profits motivate industry to fund research, it is likely that taxol from cell culture will be marketed within the next few years.

Biosynthesis of Taxol

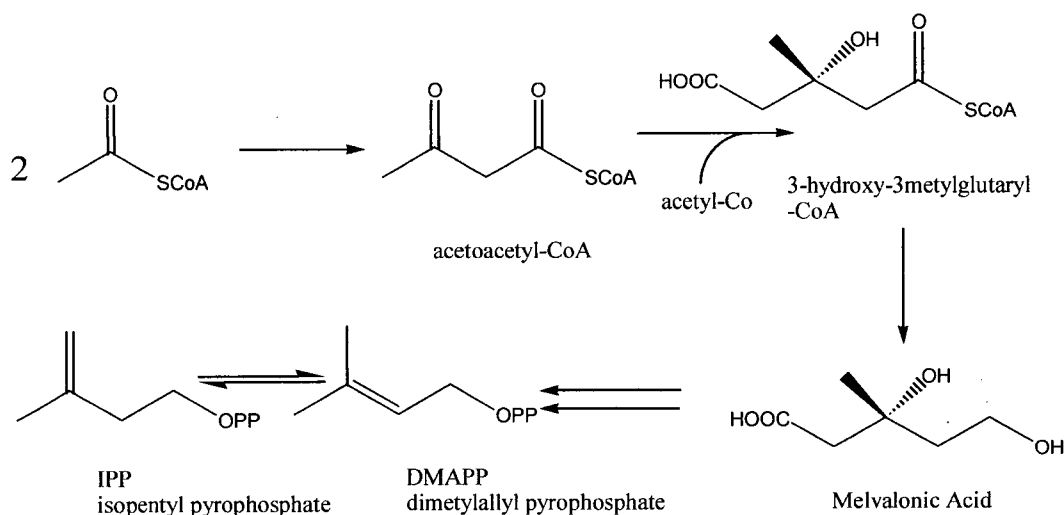
4.0 Introduction

In order to optimize taxane production in cell culture it is important to understand the biosynthetic pathway so that appropriate precursors can be used and the rates of slow steps in the process increased. However, deciphering the origin of taxol proves to be quite a challenging problem as the structure contains; the complex taxane diterpene skeleton, eight oxofunctional groups including an oxetane ring, a novel N-benzoyl phenylisoserine side chain, and eleven stereocenters. In order to facilitate discussion of the biosynthesis it is convenient to break the process into three parts; formation and functionallization of the diterpene moiety, formation of the phenylisoserine side chain, and assembly of the taxol from these components.

4.1 Isoprene Formation

Geranylgeranyl diphosphate (GGDP), the diphosphate ester of five connected isoprene units, is the universal precursor to diterpenes. Although not fully resolved for higher plants, the synthesis of isoprene is generally believed to follow what is known as the mevalonic acid pathway. This pathway begins with condensation of three units of acetyl-Coenzyme A (Acetyl-CoA), followed by reduction to mevalonate, two successive phosphorylations at C-5 of mevalonate, then decarboxilation and elimination to form isopentyl diphosphate (IPP) (Rohr 1997).

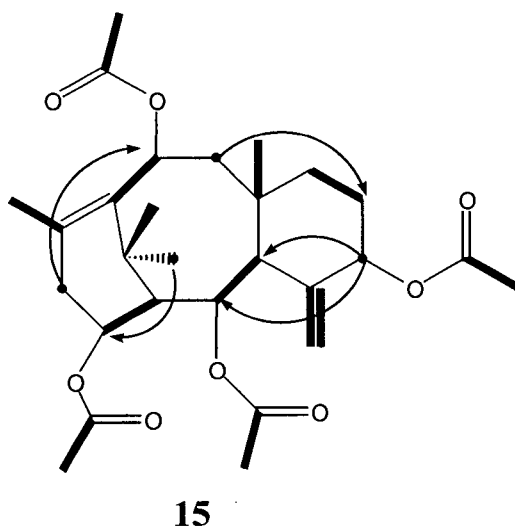
Fig. 20. Mevalonic Acid Pathway to IPP



Until recently the mevalonic acid pathway was believed to be responsible for forming the building blocks of taxol. Labeling studies using $[1,2-^{13}\text{C}]$ labeled acetate and $[\text{U}-^{13}\text{C}_6]$ labeled glucose showed that this was not the case. Eisenreich used ^{13}C INADEQUATE spectroscopy to determine the labeling patterns of taxuyunnanine C (**15**) produced by feeding $[1,2-^{13}\text{C}]$ labeled acetate and $[\text{U}-^{13}\text{C}_6]$ labeled glucose to suspension cultures of *T.chenisis*. Incorporation of ^{13}C was noted in the acetyl functionalities but not in diterpene skeleton when the labeled acetate was fed to the cultures. Furthermore, twelve pairs of adjacent ^{13}C pairs were observed when $[\text{U}-^{13}\text{C}_6]$ labeled glucose was fed to the culture. Closer analysis revealed that in four of these pairs, a long range coupling

was observed to a different ^{13}C labeled atom indicating that it was diverted to the diterpene together with the two adjacent ^{13}C atoms (Eisenreich 1996).

Fig. 21. Labeling pattern of Taxuyunnanine C (**15**) from $[\text{U-}^{13}\text{C}]$ Glucose Experiments

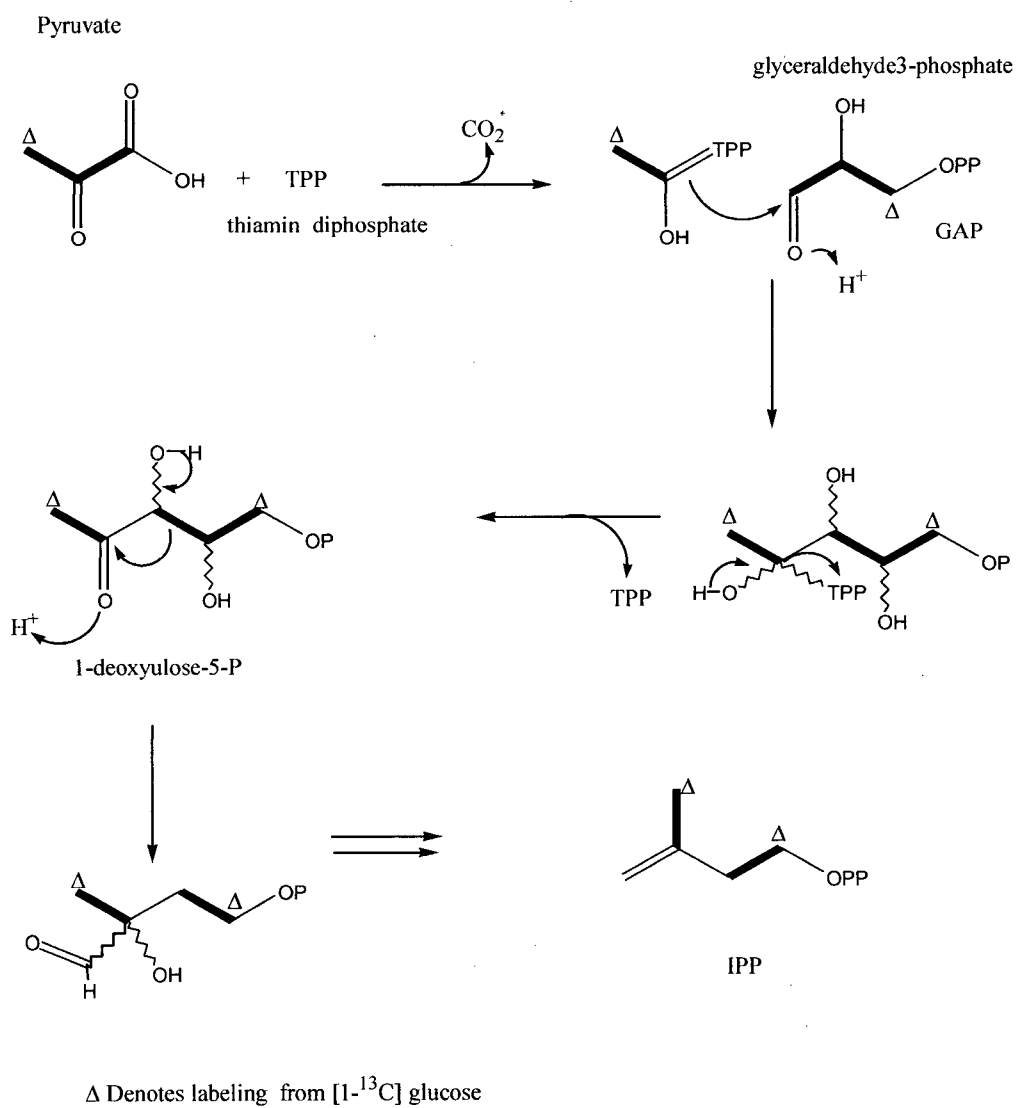


Pairs of adjacent ^{13}C atoms shown in bold, multiple bond couplings indicated by arrows

Since the mevalonic acid pathway starts with the two carbon precursor acetate, it is impossible for a three carbon intermediate to be inserted into the structure via IPP by this route.

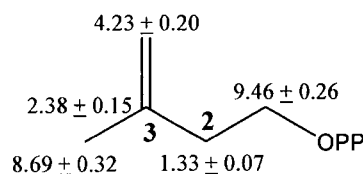
An alternative pathway of IPP synthesis has been proposed by Rohmer based on feeding studies with eubacteria and green algae. This mechanism involves the incorporation of a 3- carbon and a 2-carbon precursor with subsequent rearrangement which disrupts the connectivity of the 3-carbon precursor (Rohmer 1996).

Fig. 22. Rohmer's Pathway to IPP



Eisenreich could not confirm that this was indeed the pathway to the IPP which made up Taxyunnine C with $[1-^{13}\text{C}]$ labeled glucose experiments.

Fig. 23. ^{13}C Enrichments of IPP Deduced from Taxyunnine C from $[1-^{13}\text{C}]$ Glucose

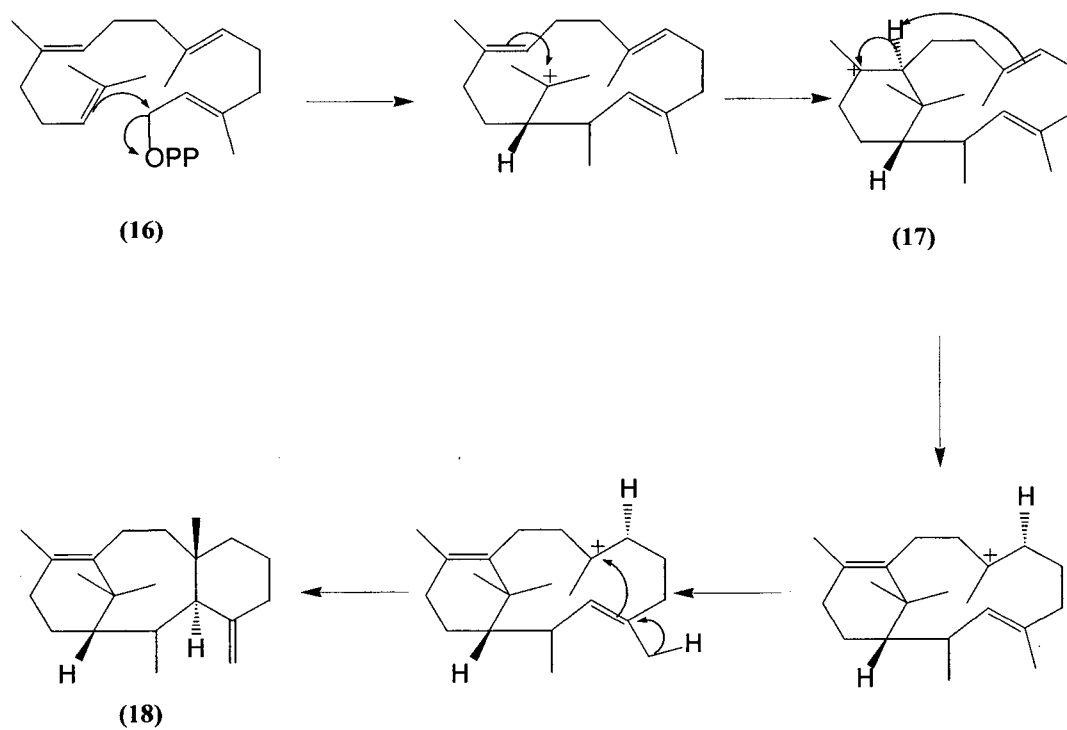


In Rohmer's pathway C-2 and C-3 are expected to be equally enriched by such labeled glucose. However, the results do reflect a non mevalonic acid pathway in which a 2-carbon and a 3-carbon precursors play a role (Eisenreich 1996).

4.2 Cyclization of GGDP

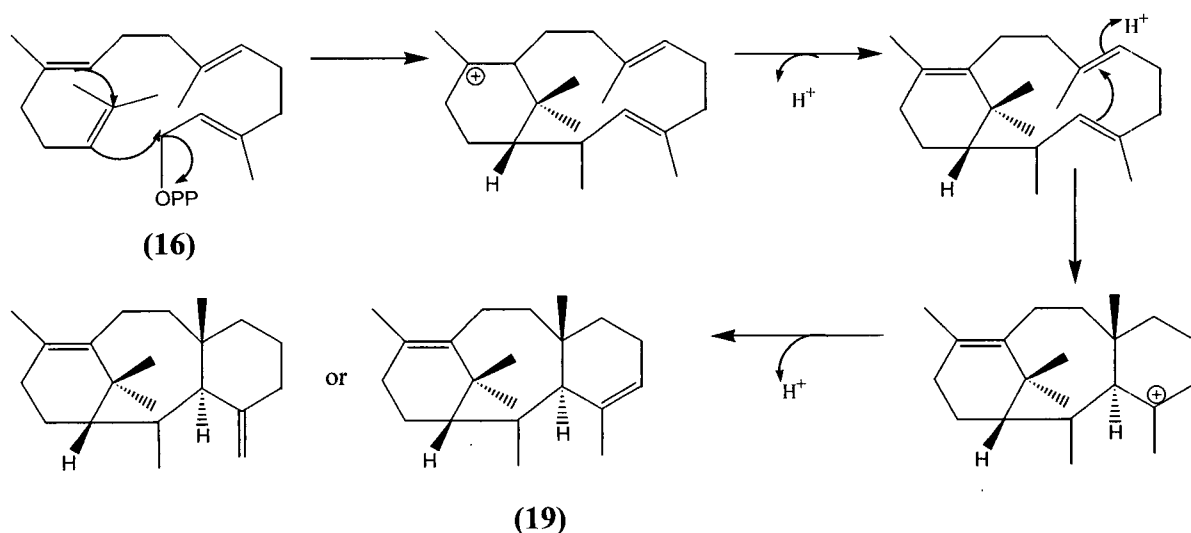
Initially it was believed that the first committed step in taxol biosynthesis was the cyclization of GGDP (**16**), via verticillene (**17**), to the hypothetical hydrocarbon precursor taxa-4(20),11(12)-diene (**18**). Many natural occurring taxanes contain the 4(20) and 11(12) double bonds and verticillene is a constituent of conifer wood. However, verticillene has the opposite configuration at C-1 and efforts to produce a taxane skeleton via Lewis acid treatment of verticillene failed (Floss 1995).

Fig. 24. Cyclization of GGDP (16) to Taxa-4(20), 11(12) -diene (18)



Labeling studies using $[1-^3\text{H}]$ GGDP were performed by Croteau which isolated and identified the hydrocarbon precursor Taxa-4(5), 11(12)-diene. The mechanism proposed involves GGDP cyclization followed by hydrogen transfer to 1S verticillene. The C ring formation creates a carbocation at C-4 which could eliminate to either the 4(5) or 4(20) diene (Croteau 1996).

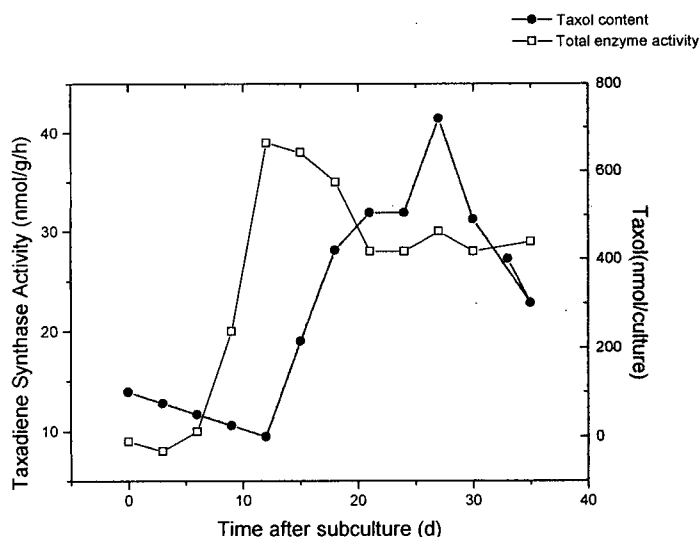
Fig. 25. Cyclization of GGDP (16) to Taxa-4(5), 11(12)-diene (19)



Croteau eventually isolated the cyclization enzyme responsible for formation of the taxadiene intermediate from the bark of *T. brevifolia*. The responsible enzyme requires only Mg^{2+} as a cofactor and was characterized as a 79-kDA monomeric protein. This enzyme closely resembled other gymnosperm terpenoid cyclases aside from its relatively low cyclization activity. In addition, it was shown that the identical enzyme was produced in cell culture of *T. canadensis*. It was initially proposed that the cyclization step was rate limiting in taxol biosynthesis due to the low amounts of the taxadiene intermediate (5-10 μ g /kg) isolated from *T. brevifolia* bark, coupled with the relatively low synthase activity ($1.37 \pm 0.009 \text{ nmol} \cdot \text{g}^{-1} \cdot \text{h}^{-1}$) (Croteau 1995).

A more detailed investigation into the enzyme activity over the course of taxol production was performed using suspension cell culture of *T. canadensis* which indicated that although slow, the cyclization step was not rate limiting. A plot of total taxadiene synthase activity indicated that activity preceded the onset of taxol accumulation by at least three days and that activity persisted into the stationary phase. As the ability to produce taxol was not dependent on taxadiene formation, later steps were deemed responsible for the bottleneck in the biosynthetic pathway (Hezari 1997).

Fig. 26. Taxol Content with Respect to Taxadiene Synthase Activity

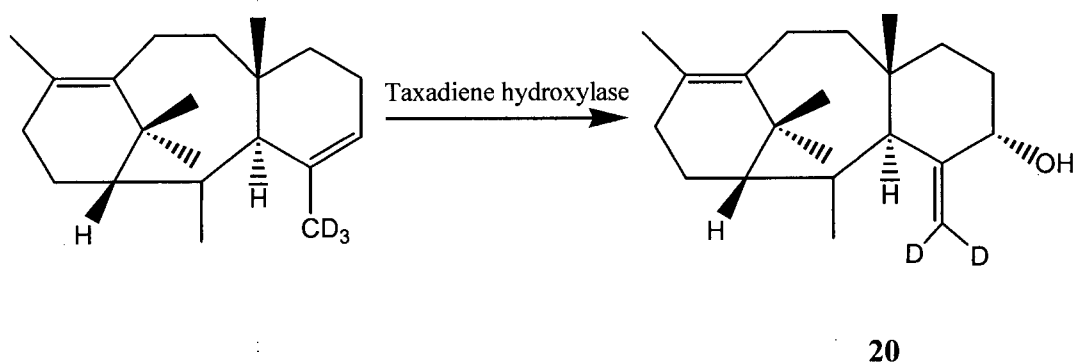


4.3 Oxygenation

Conversion of taxa-4(5), 11(12) diene to taxol requires eight oxidative steps, including the formation of an oxetane ring. The first and perhaps most important of the

oxygenation steps has been elucidated and the responsible enzyme isolated. No oxygenated taxoids having a 4(5) double bond have been isolated. However, many with the 4(20)-ene-5-oxy functional group are known. This suggests that hydroxylation at C-5 of the diene followed by double bond migration is a good candidate for the second step in the biosynthetic route. Microsomal cuttings from *Taxus* stem and cultured cells catalyzed conversion of [20-²H₃] taxadiene to taxa-4(20),11(12)-dien-5 α -ol (**20**) with loss of one deuterium atom which agreed with the proposed shift of the double bond to the 4(20) position. Furthermore, this labeled compound was shown to be a true biosynthetic intermediate by further conversion into baccatin III and taxol (Croteau 1997). The enzyme responsible is a membrane bound NADPH-dependant P450 oxygenase which uses molecular oxygen (Rohr 1997).

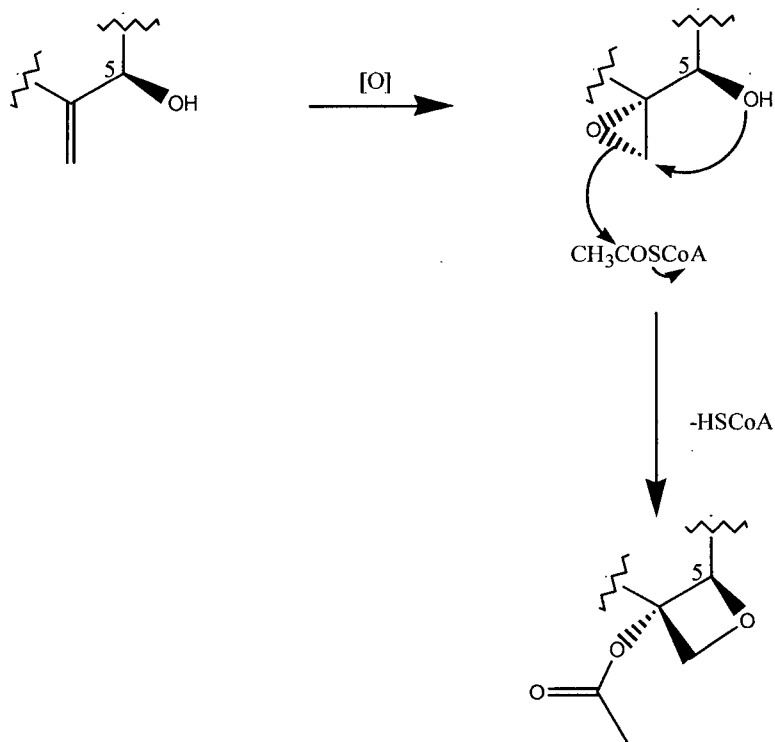
Fig. 27. Effect of Taxadiene Hydroxylase on Taxa-4(20), 11(12)-diene



4.4 Formation of the Oxirane Ring

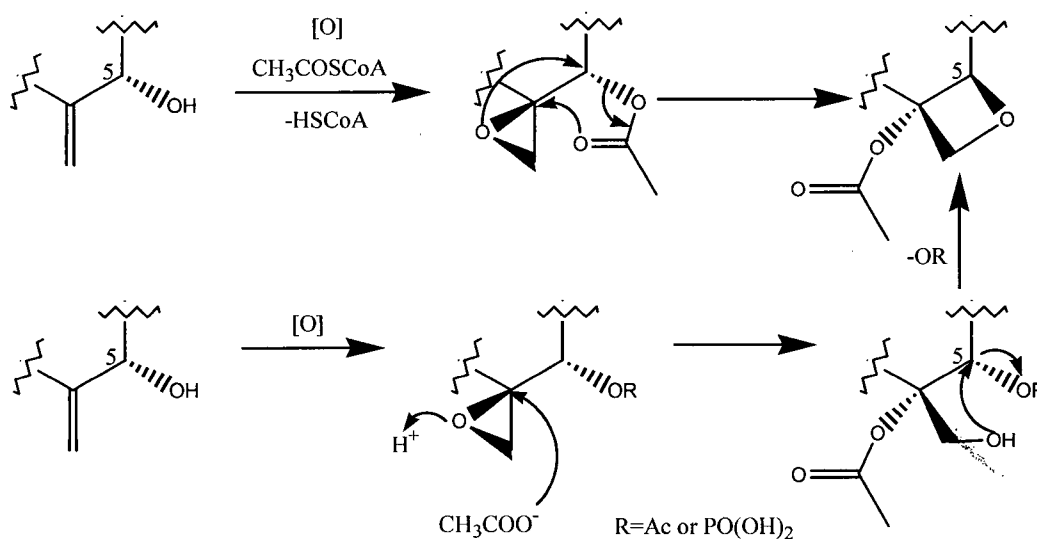
Assumption of the C-5 hydroxy-intermediate gives rise to some interesting mechanistic consequences in the formation of the oxetane ring and proposes that the third step may be acylation of the 5 α -ol. The first step in formation of the ring is hypothesized as epoxidation of the 4(20) double bond. However, the configuration at C-5 and the oxetane ring preclude direct attack of the epoxide by the hydroxyl group.

Fig. 28. Direct Intramolecular Mechanism of Oxetane Ring Formation



Two alternate mechanisms have been proposed which involve an acetate rearrangement with concomitant opening of the epoxide ring and a S_N2 reaction. However, it still remains unclear whether an inter or intramolecular reaction is responsible for final formation of the oxetane ring (Rohr 1997).

Fig. 29. Proposed Alternative Mechanisms of Oxetane Formation



4.5 Later Oxidative Steps

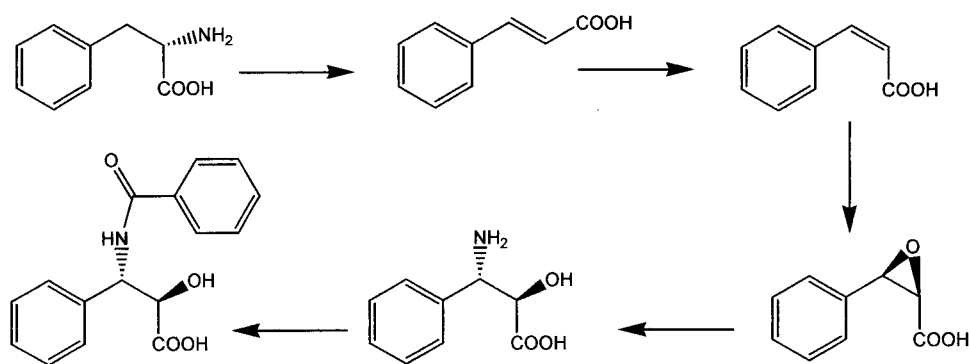
Little is known about the subsequent reactions which further oxygenate the taxane skeleton. Based on the relative abundance of taxoids bearing oxygenation on each position of the ring, it has been suggested the order of oxidation is C-10, followed by C-2

and C-9 then C-13 with oxygenation of C-1 and C-7 probably occurring last and possibly after formation of the oxetane functionality but before acylation of the C-13 side chain and oxidation of C-9 to a ketone. Attempts at feeding a labeled 5, 9,10 ,13 tetrol derived from taxusin to *T. brevifolia* bark did not result in synthesis of an enriched taxol (Croteau 1997; Floss 1995).

4.6 Formation of the N-benzoyl Phenylisoserine Side Chain

Feeding studies done by Floss determined that the phenylisoserine (**14**) side chain of taxol originated from phenylalanine via an aminomutase enzyme and not via a cinnamic acid pathway. The cinnamic acid pathway would require epoxidation of a *cis* acid with subsequent amination in order to achieve the proper stereochemistry.

Fig 30. Cinnamic Acid Pathway to Phenylisoserine Side Chain

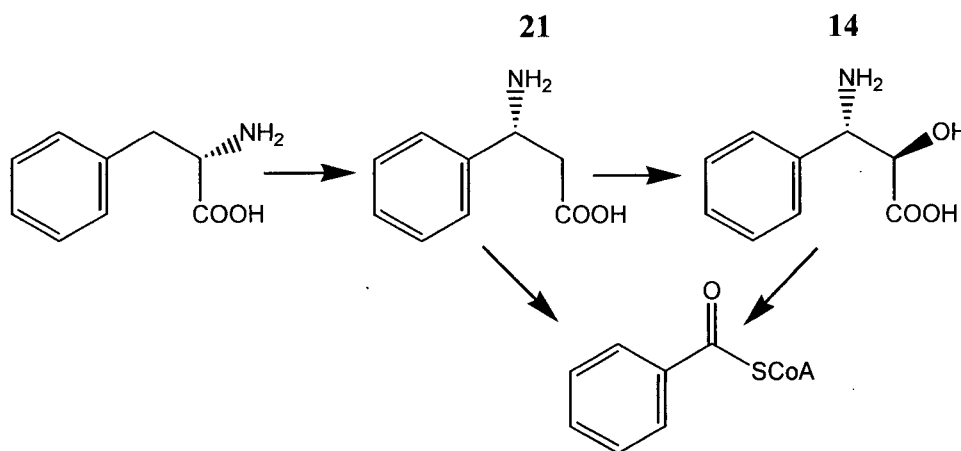


14

Neither [ring- $^2\text{H}_5$] cinnamic acid or its epoxide were incorporated into taxol or cephalomannine when incubated with pieces of bark or cambial tissue of *Taxus brevifolia*.

Interestingly and unexpectedly the mass spectra of the labeled taxanes showed M+10 fragment as well as a P+10 fragment for the side chain. This indicated that the deuterated β -phenylalanine (**21**) and phenylisoserine (**14**) must have been incorporated into the benzoyl group of the side chain as well. Coupled with the previous experiments, this indicates that the benzoyl moiety is also formed via β -phenylalanine or phenylisoserine instead of the cinnamic acid pathway which is used most commonly by plants (Floss 1993).

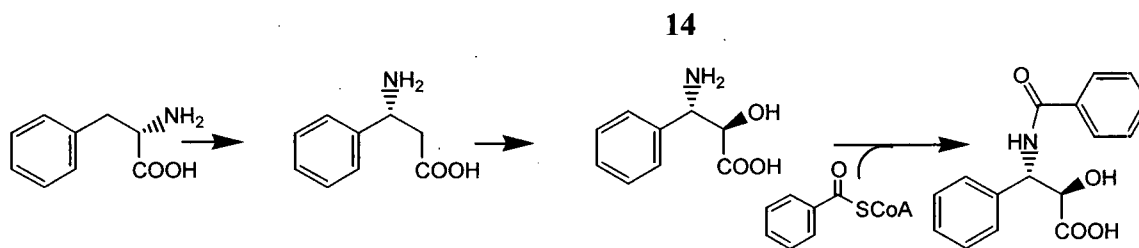
Fig. 31. Formation of Benzoyl Moiety



Similarly labeled L-Phenylalanine, slightly but notably, enriched taxol and cephalomannine. However, both [ring $^2\text{H}_5$] β -phenylalanine and phenylisoserine were

significantly incorporated into the two taxanes with all the isotope residing in the side chain. These results indicated that more likely pathway of biosynthesis was as follows:

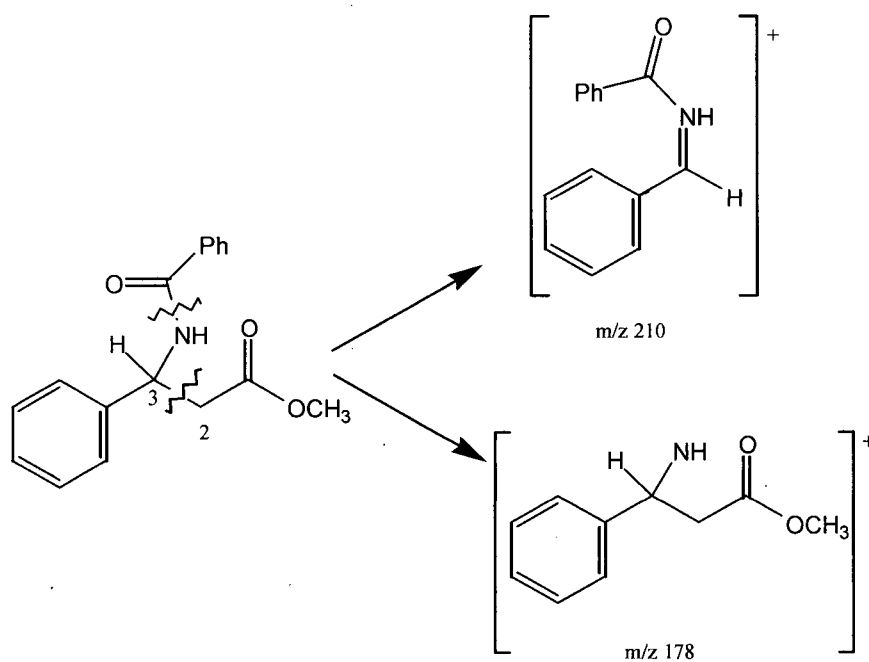
Fig. 32. Biosynthetic Pathway to Phenylisoserine (**14**)



Recently the aminomutase enzyme was isolated by Floss. This was a significant discovery because: a) it was the first example of an aminomutase from a higher plant and the first phenylalanine mutase from any source, and b) as the reaction proceeded with retention of stereochemistry, the mechanism is different from the known microbial aminomutases.

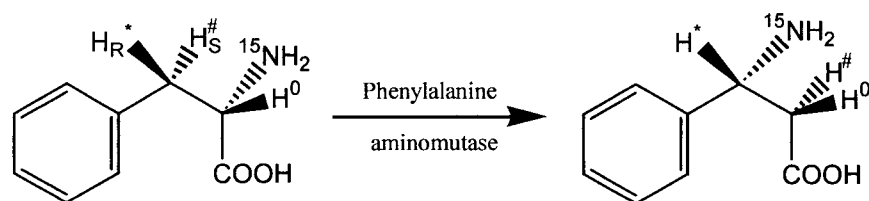
Incubation of (S)-[2- ^{15}N ring $^2\text{H}_5$] phenylalanine in cell free extracts of *T. brevifolia* gave a product which showed only side chain P+6 peaks in the mass spectra indicating that the nitrogen migrated quantitatively from the α to β carbon. Furthermore, incubation of (2S, 3R)- [ring, 3- $^2\text{H}_6$] phenylalanine gave a product which exhibited P+6 but not P+5 peaks, while (2S,3S)- [ring, 3- $^2\text{H}_6$] phenylalanine gave 59% P+5 and only 5% P+6.

Fig. 33. Mass Spectra Fragmentation of Side Chain



The spectra also revealed a complex labeling pattern at C-2 indicating that the pro-3S hydrogen of S phenylalanine migrates to C-2 of β - phenylalanine while the pro-3R proton remains at C-3 and that the reaction was at least partially intermolecular (Floss 1998).

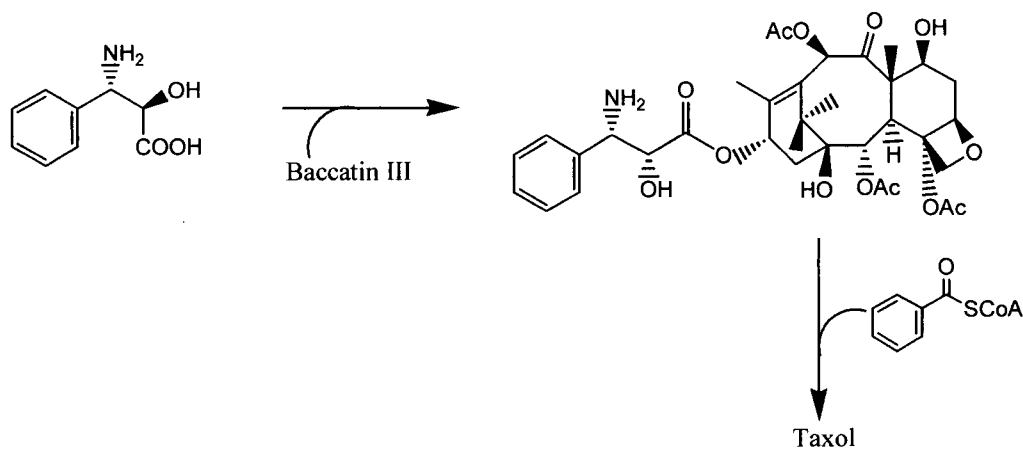
Fig. 34. Nitrogen Migration via Aminomutase Enzyme Isolated from *Taxus sp.*



4.7 Attachment of the Side Chain

Floss also discovered that the side chain is not synthesized and then attached to the diterpene moiety but attached as phenylisoserine, with tigoylation being the final step in the biosynthesis of taxol and cephalomannine.

Fig. 35. Sequence of Phenylisoserine Side Chain Attachment to Baccatin III



Feeding studies using [ring- $^2\text{H}_{10}$] -N-benzoylphenylisoserine and labeled side chains made it clear that the side chain was not attached as an intact unit. The taxol resulting from incorporation of the deuterated side chain was found to contain 1.7% [$^2\text{H}_5$] taxol with very little [$^2\text{H}_{10}$] taxol evident indicating that hydrolysis of the N-benzoyl group of the precursor was occurring. The extent of hydrolysis was determined to confirm that the rate of detachment of the N-benzoyl group was not occurring so rapidly that the *Taxus brevifolia* was not able to utilize intact [$^2\text{H}_{10}$] side chain. Approximately 92% of the radioactivity was found in the side chain after feeding the plant material N-benzoyl-7- ^{14}C with only 8% recovered as benzoate (Floss 1994).

Table 4. Major Fragments of Labeled Taxol from Various Feeding Studies

Molecule analyzed	M + MeNH ₃	M - side chain	M- side chain and 10 acetyl group	N-Acyl-phenylisoserine side chain
Taxol	885	569	509	286
Taxol from :				
[10 acetyl $^2\text{H}_3$, 13- $^2\text{H}_1$] Baccatin	885			
	889 (1.0%)	573	510	286
[ring- $^2\text{H}_{10}$]-N-benzoylphenylisoserine	885			
	890 (1.7%)	569	509	291
	895 (low)			

Table 4. cont.

Molecule analyzed	M + MeNH ₃	M - side chain	M- side chain and 10 acetyl group	N-Acyl-phenylisoserine side chain
[side-chain-ring ² H ₅ , 10 acetyl- ² H ₃] N-benzoyltaxol				
	885			
	888 (<1%)	569	509	286
	890 (<1%)	572	509	291
	893 (5.9%)	572	509	291

4.8 Conclusion

The exact biosynthetic pathway to taxol and other taxanes may never be completely determined, however in the past few years much progress has been made in discovering the building blocks and enzymes responsible for construction of this complicated molecule. While investigations were motivated initially by desire to understand biosynthesis as a means to increase yield in plant cell culture, a great deal of new knowledge has been collected due to the many ways in which the pathway to the taxanes has challenged accepted theories of plant biochemistry and physiology.

Results and Discussion

A plant cell culture system was developed in hopes of producing the anticancer agent taxol or other taxanes which could be converted to taxol.

5.0 Previous Work at UBC

Cell culture was established in 1994 from callus obtained from Dr. Shan Lin Gao. Propagation and maintenance in liquid media was carried on by Dr. Elena Polishchuk and David Chen in the Biological Services laboratories.

5.0A Initiation of Callus

Stems of *Taxus x media* were cut into 1 cm length segments and sterilized with 30 % commercial bleach solution for ten minutes then washed with sterilized water five times. Explants were placed on solidified nutrient media, (petri plates containing Gambourg B5 media supplemented with 2.5 - 3 % sucrose, double vitamins, 0.2% casein hydrolysate and 1 mg/ml of 2,4-D) and kept in darkness at 26 °C.

5.0B Media Composition

The modified Gambourg B5 medium was prepared as follows from stock solutions described in the following table.

Table 5. Modified Gambourg B5 Media

Stock solution / Component	Volume stock solution (ml/l)	Amount used (g/l)	Components	Concentration (g/l)
B5 Macronutrients	50.00		KNO ₃	50.00
			(NH ₄) ₂ SO ₄	2.680
			NaH ₂ PO ₄ . H ₂ O	3.000
			MgSO ₄ . 7 H ₂ O *	5.000
Calcium chloride	3.75		CaCl ₂ . 2 H ₂ O	40.00
Iron chelate	9.30		Na ₂ EDTA . 2 H ₂ O	4.010
			FeSO ₄ . 7 H ₂ O	2.990
B5 micronutrients	5.00		H ₃ BO ₃	0.600
			MnSO ₄ . H ₂ O	2.000
			ZnSO ₄ . 7 H ₂ O	0.600
B5 modified trace elements	1.00		KI	0.750
			Na ₂ MoO ₄ . 2 H ₂ O	0.250
			CoCl ₂ . 6 H ₂ O	0.250
			CuSO ₄ . 5 H ₂ O	0.250
B5 vitamins	20.00		Inositol	10.00
			Nicotinic acid	0.100
			Pyridoxine . HCl	0.100
			Thiamine . HCl	1.000
2,4-D	2.00		2,4-Dichlorophenoxyacetic acid**	0.500
Sucrose		25.00		
Casein hydrolysate		2.000		

* Dissolve MgSO₄ . 7 H₂O separately and then add to solution of the other components.

** Dissolve in 200 ml EtOH and make up the volume with water to 1000 ml.

Solid media is created by addition of 8 g/l of agar.

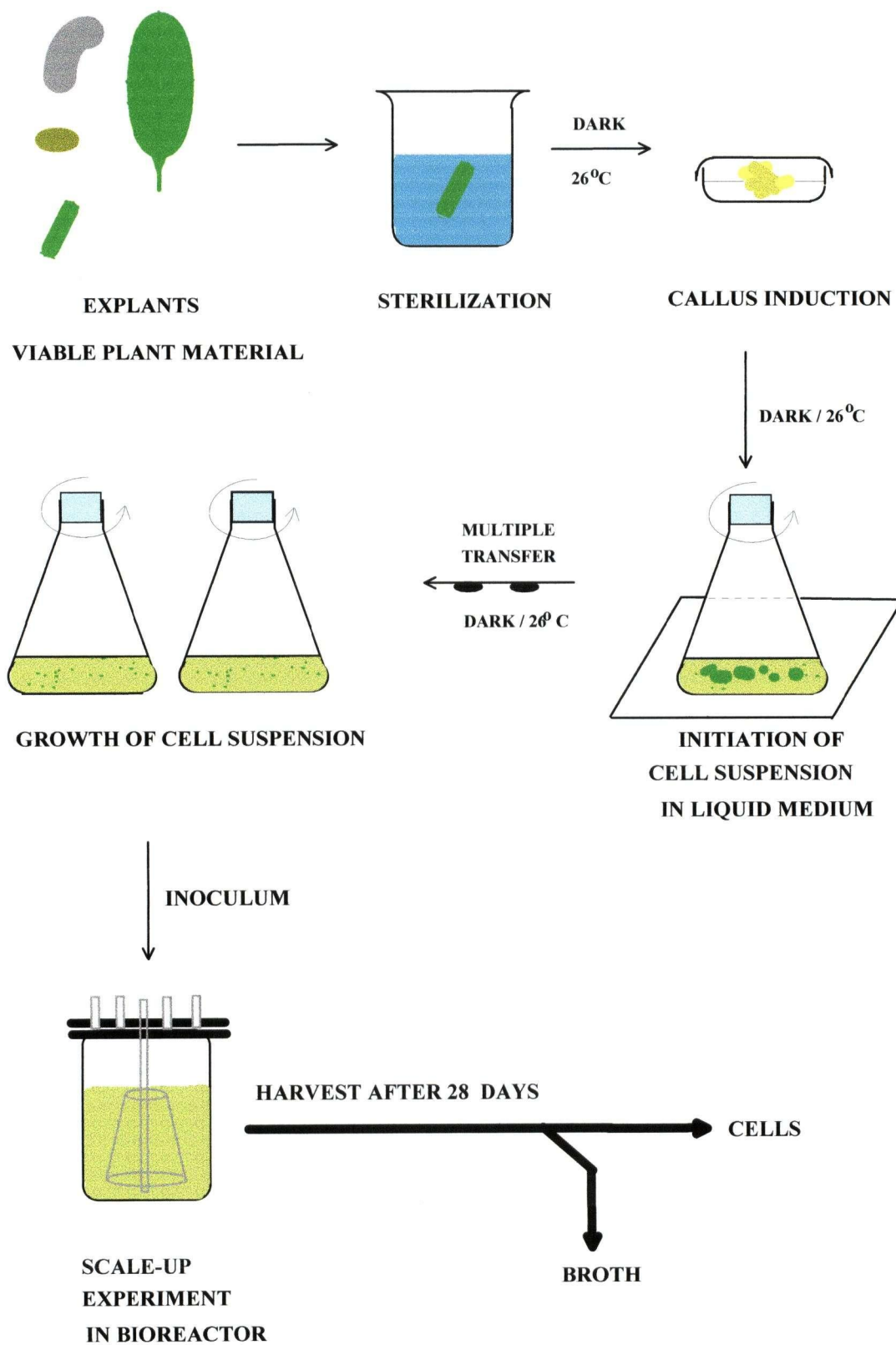
5.0C Maintenance of Callus

Callus was transferred to new solid media every two weeks and was maintained using conditions identical to those of initiation with one exception. Polyvinylpyrrolidone (PVP) was added to the media in order to suppress production of tannins or phenolic compounds. Oxidation products of phenolic compounds found in the cells lead to darkening or reddening of the culture and inhibited growth. It has been determined that PVP is most effective in uptake of these phenolic compounds in callus culture without itself being detrimental to growth (DiCosmo 1992).

5.0D Establishment of Suspension Cultures

Suspension cultures were established by transferring callus tissue into Erlenmeyer flasks containing Gambourg B5 liquid media. The cultures were kept in the dark at 26 °C on a rotatory shaker set at 135 rpm. Every 14 days the cell lines were propagated by transferring the culture into new media at a 1: 10 inoculum ratio. Fig. 36 briefly explains the method of creating suspension culture from explant material.

Fig. 36. Method of Creating Suspension Cell Culture



5.0E Screening of Cell Culture

A number cell lines originating from different callus culture were evaluated by high pressure liquid chromatography (HPLC) to determine the presence of eight different taxane standards under different growing condition in previous work. Fifty milliliter aliquots were lyophilized and then extracted with methanol (MeOH) for 24 hrs at 4°C. Solid residue was filtered off and ~1.2 ml of the filtrate was then passed through type HV Millipore filter. A Supelco LC-F column 150 x 4 mm was used in a Waters HPLC system (HPLC pump model 6000A, Auto sampler Model 712, Model 440 UV Absorbance Detector, and 730 Data module). The Ultraviolet (UV) absorbance at 254 nm was monitored in four separate solvent systems (B4, B6, D1 and D4) at a flow rate of 1 ml/min.

Table 6. HPLC Solvent Systems for Taxane Analysis

Solvent systems	Acetonitrile (CH ₃ CN)	Tetrahydrofuran (THF)	water (H ₂ O)
B4	20	20	60
B6	15	20	65
D1	20	-	80
D4	40	-	60

Calibration curves were prepared for each of the eight standards by correlating peak area with known amounts of the pure compounds in methanol. These curves were used to obtain the retention times and amount of the various taxanes in mg/l as well as

minimum detection limits. Sensitivity of the system was found to be 0.5 µg/ml for all the compounds except baccatin III which was 0.03 µg/ml and cephalomannine which was 0.9 µg/ml.

Forty - five samples originating from different cell lines, differing in number of times transferred, number of days fermented before harvest or grown in bioreactors as opposed to shake flasks were evaluated for presence of the eight available standards.

The results of these studies were inconclusive. Only one solvent system (D4) could be used to reliably evaluate the crude extract for presence of the baccatins since the solvent and polar constituents in the extract eluted at approximately the same retention times in the other systems.

Furthermore, in the forty-five tested samples for all but a few cases, retention times which matched the standards in one system failed to exhibit peaks corresponding to the same compound in any of the other solvent systems. As it is possible to have co-eluting compounds, unless the extract exhibits the appropriate peak in all solvent systems tested, it is unlikely that the compound is present in the extract. Only one of the forty-five samples tested showed presence of a standard compound in three solvent systems (cephalomannine and taxol in Fermentor 34). The remaining samples which showed presence of the baccatins in D4 or of the remaining taxanes in at least two solvent systems were evaluated for hypothetical titers. From these studies it was determined that if the compounds were indeed present, the amounts were estimated to be between 1 and 8 µg/ml.

The yield of biomass was also measured with respect to number of times subcultured and time fermented for these samples. The resulting data indicated that the

dynamics of cell growth of our culture did not follow the classical lag-curve.

Additionally, by comparing HPLC and thin layer chromatography (TLC) profiles of the extracts after each subculture, it was determined that the cell culture did not “stabilize” until after 60 subcultures (approximately 2 years of growth).

In order to gain insight into what types of compounds our cell line was producing a stabilized cell line was scaled up in bioreactors. Although the presence of our standards was not detected by HPLC in this line, it was possible that the culture contained other known or novel taxanes. Given that one bioreactor contained approximately 14 l of cell suspension and, if present it was likely the titers of taxanes could be as low as 1 µg/ml it was decided that the extract of many bioreactor experiments would be combined before separation. Dry weights of biomass obtained from our air lift bioreactors ranged between 30 and 150 g dry wt. / bioreactor. In the literature, reports of starting dry weight biomass between 120 g and 5 kg for isolation of taxanes from cell suspension culture are found (Cheng 1996; Ma 1994). Due to the length of each fermentation, and frequent problems with contamination, obtaining sufficient biomass for extraction and separation was a timely ordeal.

5.1 Partial Characterization of *Taxus x media* Cell line

Suspension cultures were grown 14 l airlift bioreactors in order to increase production of biomass. The methodology for initiation, propagation and scale up of the suspension culture is summarized in figure 36. Bioreactor experiments were harvested after 28 days of fermentation. The refractive index was checked prior to harvest in order to ensure all sugars had been consumed and therefore the cells had commenced secondary

metabolism. The refractory index (RI) at time of harvest was ~1.3333 for all processed bioreactors. The pH was also monitored, however the value ranged between 5-8 at the time of harvest for “healthy” bioreactors.

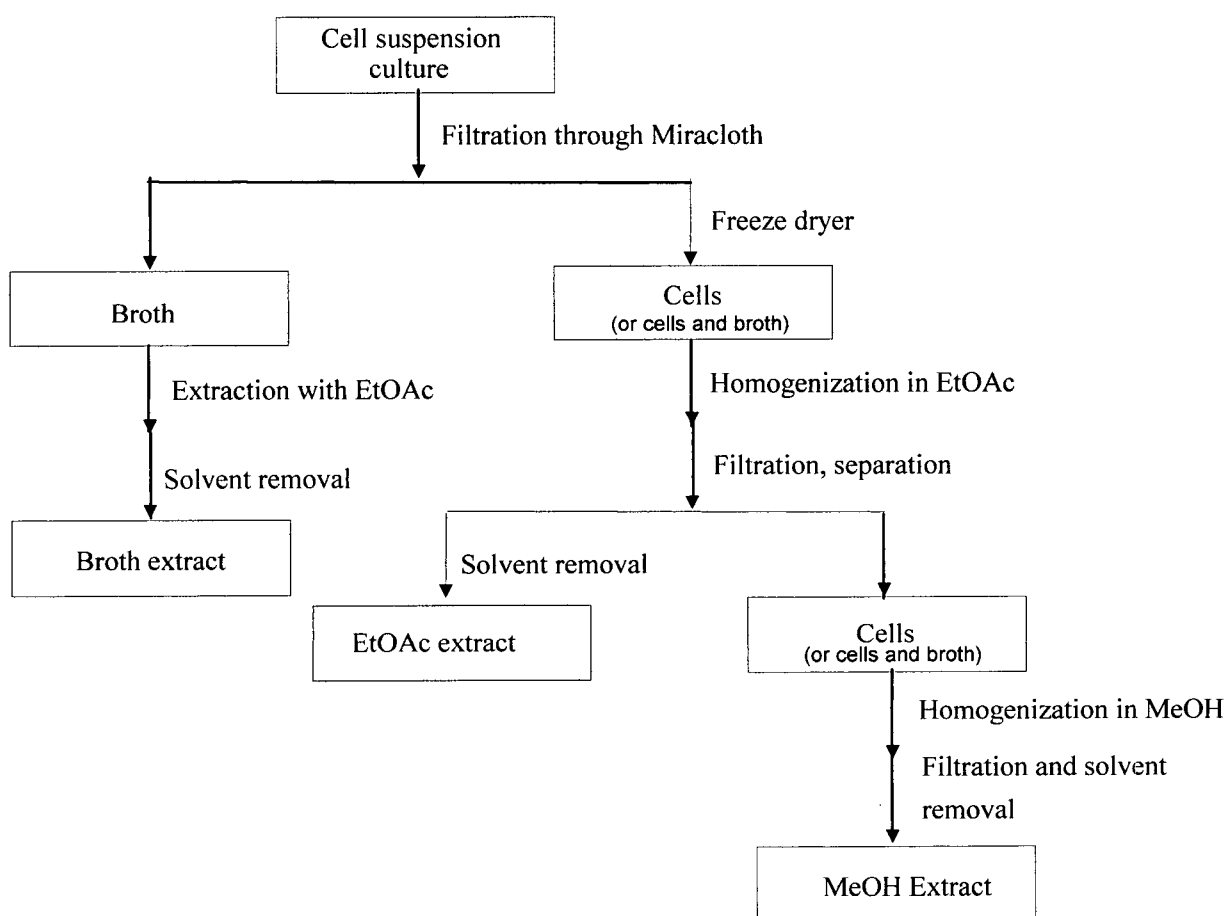
Cells and broth were separated if possible by filtration through three layers of Miracloth[®]. Cells were freeze dried while the broth was immediately extracted with ethyl acetate (EtOAc) and MeOH. In some cases cell growth was so good that essentially no broth was able to be filtered off. In such cases cells and broth were freeze dried together.

5.1A Extraction

Broth was extracted at the time of harvest using the following procedure. Typically 8-10 L of broth was obtained from fermentation in a 14-L bioreactor. One liter portions were extracted three times with of EtOAc in a 4 l separatory funnel. Large solvent volumes were required as problematic emulsions arose if less than a 1:2 solvent : broth ratio was used. The EtOAc and MeOH extracts were dried separately over sodium sulfate then filtered using #1 Whitman filter paper. Extracts were concentrated using rotoevaporators and dried on high vacuum.

Cells and dried broth were extracted in a similar manner. After weighing, the dried biomass was frozen using liquid nitrogen then pulverized using a mortar and pestle. Powdered cells (or broth) were transferred into plastic containers and extracted three times with EtOAc and once with MeOH. The extract was dried, filtered, concentrated and dried on high vacuum in the same manner as the broth extract.

Fig. 37. Method of Processing *Taxus x media* Cell Culture



Over the course of two years fifteen “successful” fermentations in Labroferm bioreactors were achieved. “Successful” being used in the context that no contamination was detected and the extracts produced a similar TLC chromatogram. Summarized below are the biomasses, and weights of extracts obtained from each experiment.

Table 7. Dried Biomass, EtOAc and MeOH Extract Masses from F66-107

Fermentor	Biomass (g)		EtOAc Extract (g)		MeOH Extract (g)	
	Cell	Broth	Cell	Broth	Cell	Broth
F66	45.24	*	0.2180	0.4031	not extracted	
F67	35.74	13.59	0.1628	0.1748	0.2931	1.670
F73	47.43	17.65	0.4096	0.1600	1.684	0.2823
F75	31.35	22.67	0.1526	0.2370	0.4300	
F77	82.81	30.23	1.202	0.4660	3.295	
F80	95.44	28.44	2.180	0.4583	7.303	
F81	130.5	F81-F85	3.585	F81 -F85	F81 -F85	
F84	111.4	combined	2.594	combined	combined	
F85	108.2	58.37	2.916	4.806	82.95	
F88	cell and broth combined 105.9		cell and broth combined 3.670		24.50	
F92	cell and broth combined 100.5		cell and broth combined 2.758		not extracted	
F94	cell and broth combined 104.4		cell and broth combined 3.893		not extracted	
F105	cell and broth combined 83.40		cell and broth combined 2.530		not extracted	
F106	cell and broth combined 99.97		cell and broth combined 1.984		not extracted	
F107	cell and broth combined 119.5		cell and broth combined 4.073		not extracted	

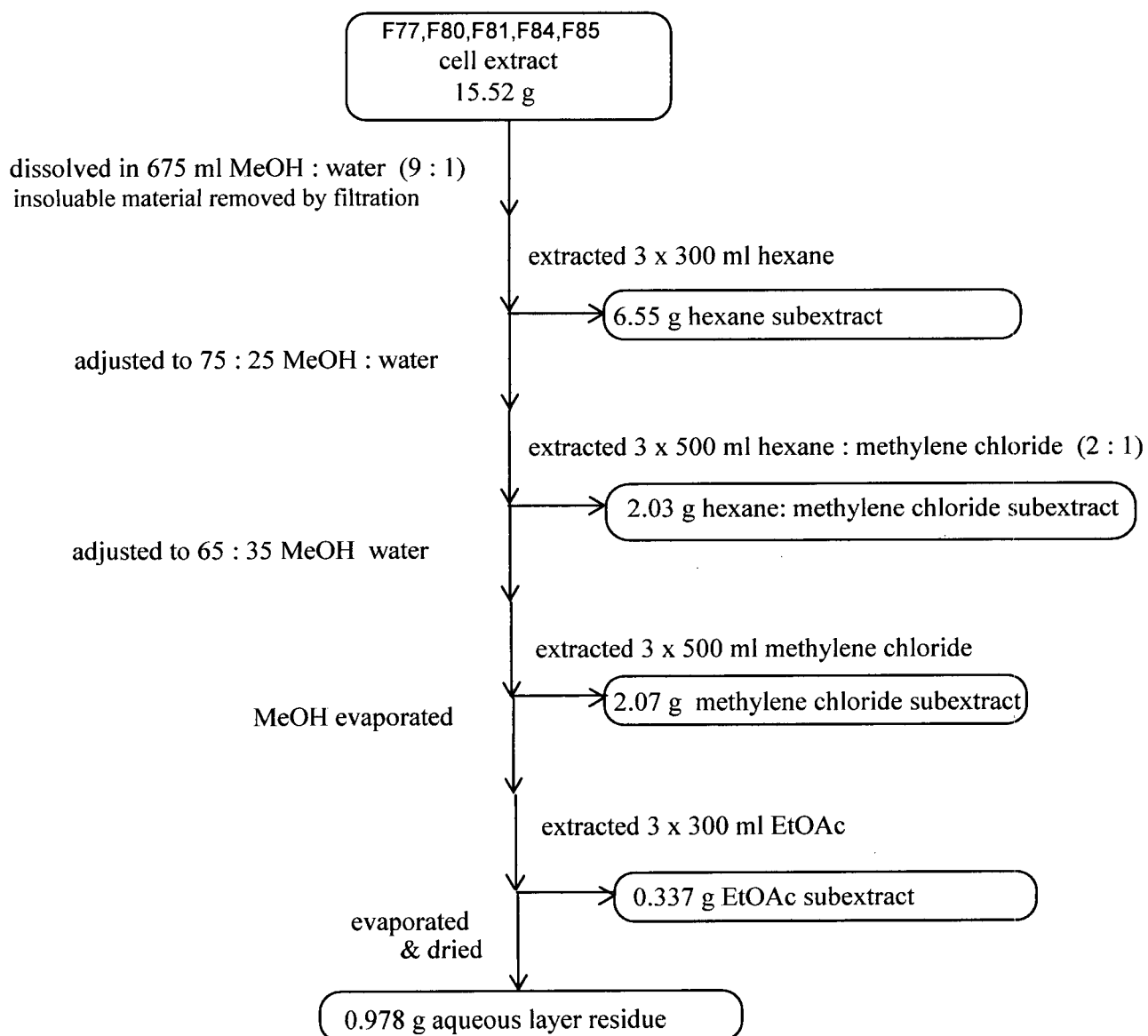
When it was believed that enough extract had been accumulated the fermentors were compared by TLC and combined.

5.1B Crude Separations: Solvent Washing and Partitioning

MeOH extracts were suspended in EtOAc and sonicated until it appeared all material that would dissolve was in solution. The EtOAc soluble portion was separated by filtration than combined with the original EtOAc extracts. Material which did not dissolve in EtOAc was checked by TLC and found to be polar material which did not move in the solvent systems which moved the most polar of our taxane standards, 10-DAB. A second rough separation was carried out by suspending the combined EtOAc extracts in MeOH followed by sonication and overnight refrigeration at 4 °C. Material that did not dissolve, or precipitated out after refrigeration was removed by filtration. This material was checked by TLC and contained mainly compounds with similar or higher in R_f than β -sitosterol. As, due to the great number of compounds present in the extract, it was difficult to compare the crude extract with our standards by TLC and this was postponed until after partitioning with solvents.

Extract was partitioned with solvents by a modified method based on that published by Cardellina (Cardellina 1991). The following scheme using data from F77 - F85 EtOAc cell extract as an example, was followed with the exception that volumes of solvent used in other experiments were proportional to the starting mass of the extract.

Fig. 38. Method of Solvent Partitioning



The following table represents the proportions of each subextract after partitioning.

Table 8. Subextract Masses after Partitioning with Solvents

Combined Extracts (g)	Hexanes Subextract (g) (% of extract)	Hexanes : CH ₂ Cl ₂ (g) (% of extract)	CH ₂ Cl ₂ (g) (% of extract)	EtOAc (g) (% of extract)	Water (g) (% of extract)
F67-75 Broth EtOAc (1.81g)	0.117 (9.78)	0.286 (15.8)	0.730 (40.3)	0.105 (5.80)	0.443 (24.5)
F77-85 Broth EtOAc (5.73g)	3.96 (69.1)	0.722 (12.6)	0.105 (1.83)	0.105 (1.83)	0.0620 (1.08)
F67-75 Cell EtOAc (1.23g)	0.512 (41.6)	0.263 (21.3)	0.238 (19.3)	0.070 (5.67)	0.0765 (6.21)
F77-85 Cell EtOAc (15.5g)	6.55 (42.3)	2.03 (13.1)	2.07 (13.4)	0.337 (2.17)	0.978 (6.31)
F88-F107 Cell EtOAc (43.4g)	13.67 (31.6)	4.05 (9.38)	8.32 (19.3)	5.68 (13.1)	7.98 (18.5)

From TLC and HPLC comparison with our standards it was decided that if taxanes were present it was likely that they would be found in the hexanes:CH₂Cl₂ or CH₂Cl₂ sub-extracts. HPLC samples of each of the subextracts were injected under the same conditions as described in section 5.0E to screen for the presence of our taxane standards. Injection volumes were optimized for each sample. Table 12 summarizes the HPLC data.

Table 9. HPLC Retention Times of Taxane Standards

Standards	Solvent System			
	B4	B6	D1	D4
Taxol	16.16	31.78	*	15.80
Cephalomanine	13.15	24.28	*	12.86
Baccatin III	*	*	33.48	*
10-DAB	*	*	13.36	*
14-hydroxybaccatin	*	*	13.63	*
14-hydroxy-10-desacetylbaccatin	*	*	13.63	*
7-methyltaxol	16.16	31.78	*	15.80
7-epitaxol	22.50	48.45	*	24.30

Retention times expressed in minutes

* Compound non-resolvable from solvent peak

Table 10 HPLC Retention Times of *Taxus x media* Cell Subextracts

Subextract	B4	B6	D1	D4
Hexanes F77-85	(80µl) 5.23,6.25, 14.53,17.50, 21.25,47.03,54.40	(80µl) 5.40, 5.50,8.76,10.62, 35.00	(80µl) 7.52	(80µl) 5.36, 5.76, 8.13, 12.53, 35.05
Hexanes F88-107	(20µl) 7.50, 11.90,12.50, 15.63, 21.53	(20µl) 21.17, 24.70	(10µl) 5.23, 6.20,7.36	(20µl) 5.06, 5.38,9.14,12.33, 13.96,17.26,19.38, 25.89,40.26

Subextract	B4	B6	D1	D4
Hex:CH ₂ Cl ₂ F77-85	(80μl) 5.13, 15.50,27.51,47.02, 54.51	(80μl) 5.51, 6.51,7.12,10.73, 38.75,41.10, 49.12	(80μl) 5.12, 7.52, 11.80, 13.10,	(80μl) 5.40, 12.07,12.52, 17.65,18.80,21.30 ,22.80,43.80,46.3
Hex:CH ₂ Cl ₂ F88-107	(3μl) 5.20, 5.96,7.00,11.70, 18.03,26.42,37.01 42.15, 52.65	(3μl) 5.46, 6.40,8.30,10.46, 21.13,22.30	(3μl) 5.40, 6.93,7.16,9.06, 11.40,13.00,13.80 ,15.20,16.53,17.2, 20.27,27.47,37.60	(3μl) 5.40, 6.93,7.16,9.06, 11.40,13.00,13.80 15.20,16.53,17.20 20.27,27.47,37.60
CH ₂ Cl ₂ F77-85	(80μl) 5.10, 13.05, 15.12	(80μl) 6.35, 10.53	(80μl) 6.27, 8.62, 11.30	(80μl) 5.67,7.80,8.80, 12.36,30.90
CH ₂ Cl ₂ F88-107	(3μl) 7.16, 8.12,11.70	(3μl) 10.43, 22.46	(3μl) 5.16, 6.06, 7.36, 8.59, 9.81,12.27,13.01	(3μl) 5.43, 7.13,8.20,11.36
H ₂ O F77-85	(80μl) 5.10, 13.04,15.53	(80μl) 5.63, 6.36,10.83	(80μl) 6.42, 10.70,12.63	(80μl) 5.58, 12.26
H ₂ O F88-107	(3μl) 5.35,5.76	(3μl) *	(3μl) 5.16, 5.90,7.31,7.95	(3μl) 5.53, 6.83,

* no peaks resolvable from solvent peaks

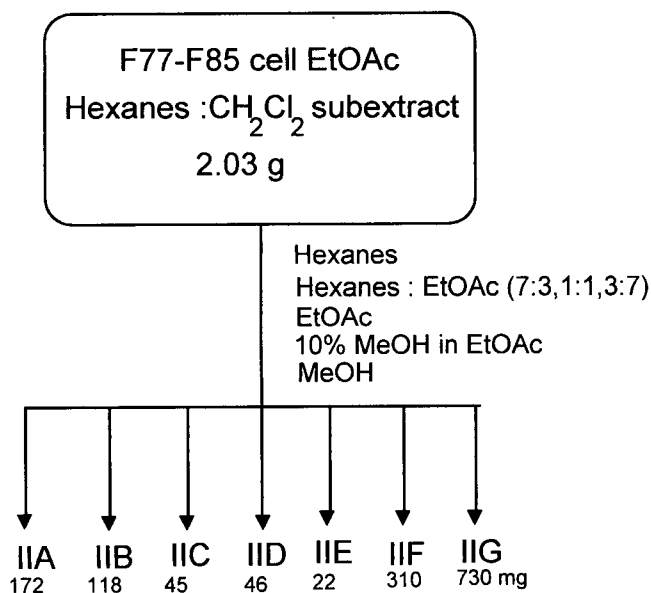
5.1C Separation and Purification

Attempts were made at chromatographing the CH₂Cl₂ subextract from F66-F75, and the hexanes :CH₂Cl₂ subextract from F77-F85 broth however further separation was not attempted after one column. Previous attempts by visiting scientists and post doctoral students to purify compounds from either the broth or cell extracts were unsuccessful due to the complexity of the mixture and insufficient amounts of starting material to chromatograph (unpublished reports Dr. Regina Naidu, Dr. Jaime Nino, Halldis Alxneit,

Catia Seri, Dr. Adrianna Casabuono). Given the masses and complexity of the fractions obtained, it was decided that further separation would be postponed until possible combination with like fractions from future experiments.

Separation was next attempted on the hexanes:CH₂Cl₂ subextract of the cell EtOAc extract from bioreactors F77-F85. Vacuum flash chromatography subextract gave seven fractions.

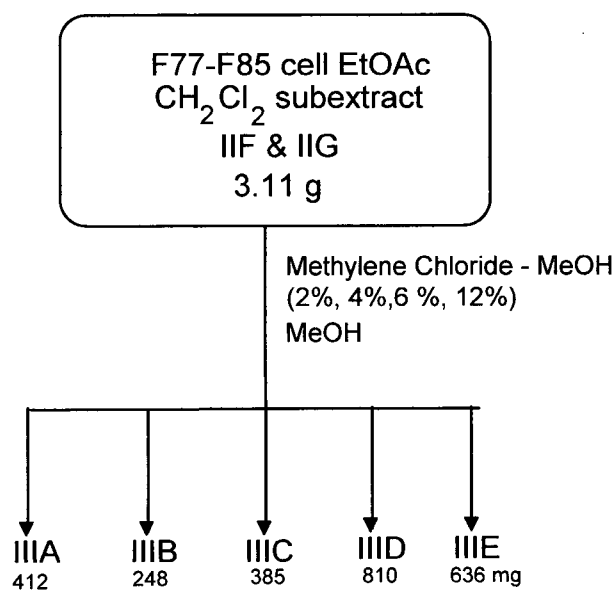
Fig. 39. Separation Scheme for Hexanes:CH₂Cl₂ Subextract



Fractions IIB-IIE were set aside for possible future combination with other like fractions. Fractions IIF and IIG were combined with the CH₂Cl₂ subextract which was

dissolved in CH_2Cl_2 , filtered using a fine sintered glass funnel, then subjected to vacuum column chromatography.

Fig. 40. Separation Scheme for CH_2Cl_2 Subextract



The largest fraction, IIID, showed two major compounds on TLC. These compounds were purified using multiple column chromatographies, crystallizations and preparative TLC described by the following schemes.

Fig. 41 Separation Scheme for Fraction IIID

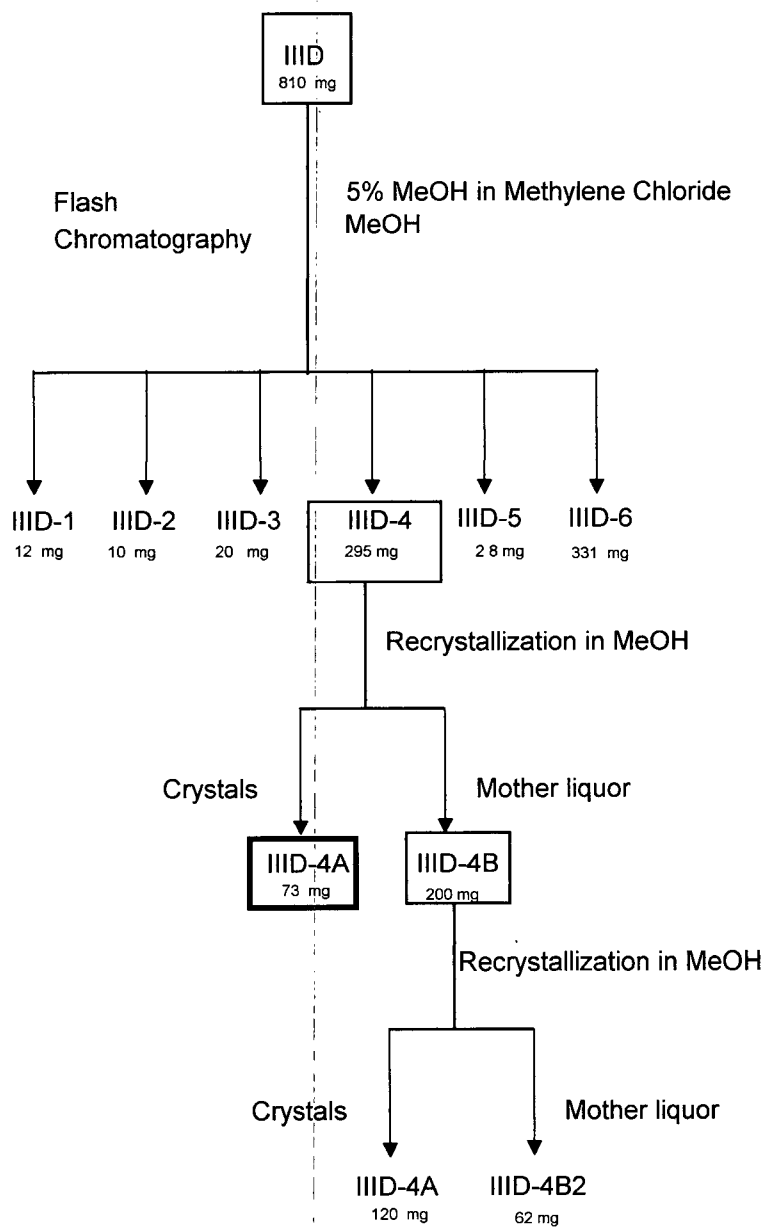
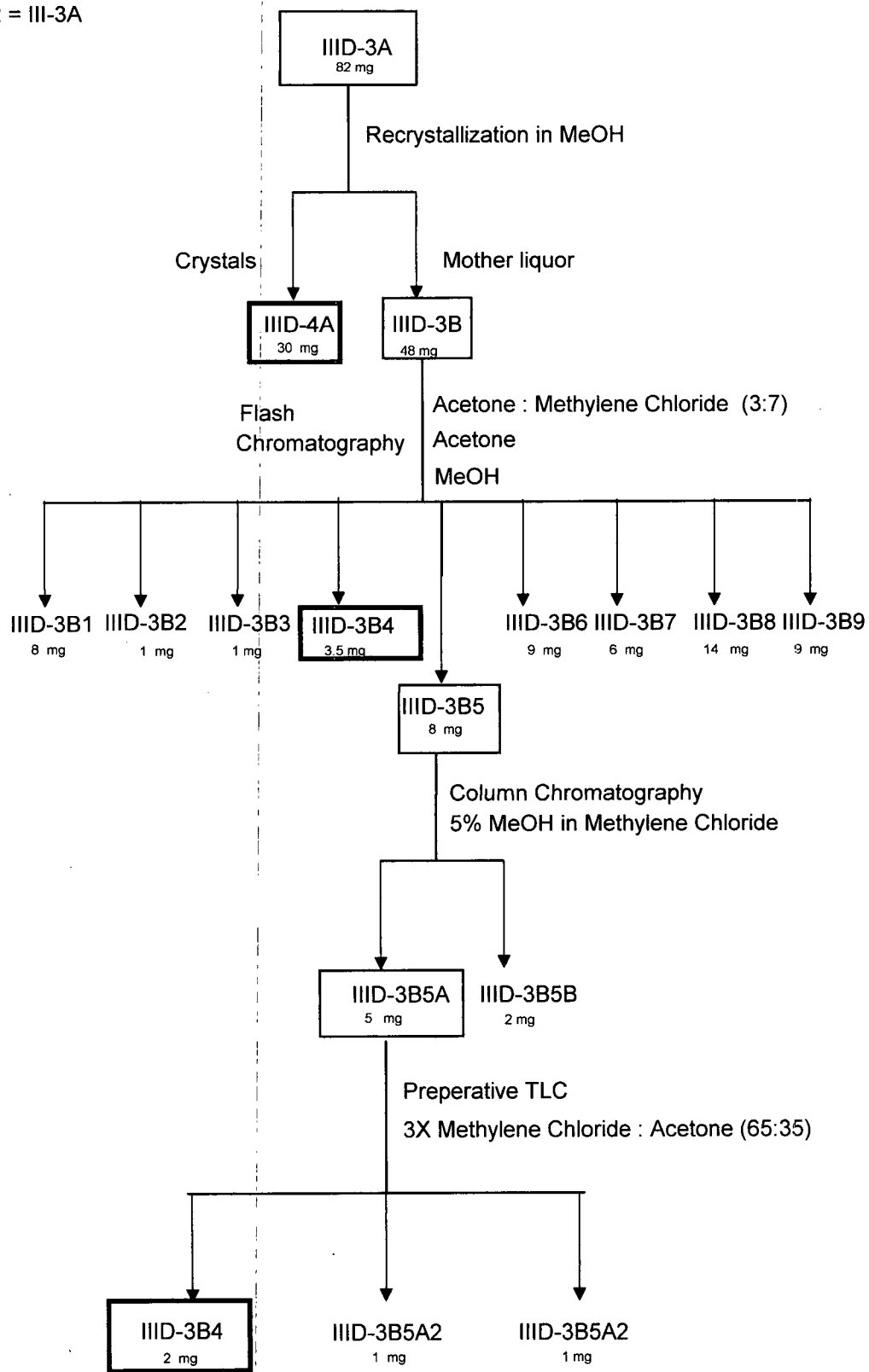


Fig. 41 cont.

IIID-3 + IIID-4B2 = III-3A



5.2 Isolates from Fraction IIID

5.2A IIID-4A

The first compound to be isolated, III D-4A, was identified using spectroscopic methods and by comparison with the literature. The results of ^1H , ^{13}C NMR and high resolution electron impact mass (EI) spectra are summarized in the table below.

Table 11. NMR and EI Mass Spec. Data for IIID-4A

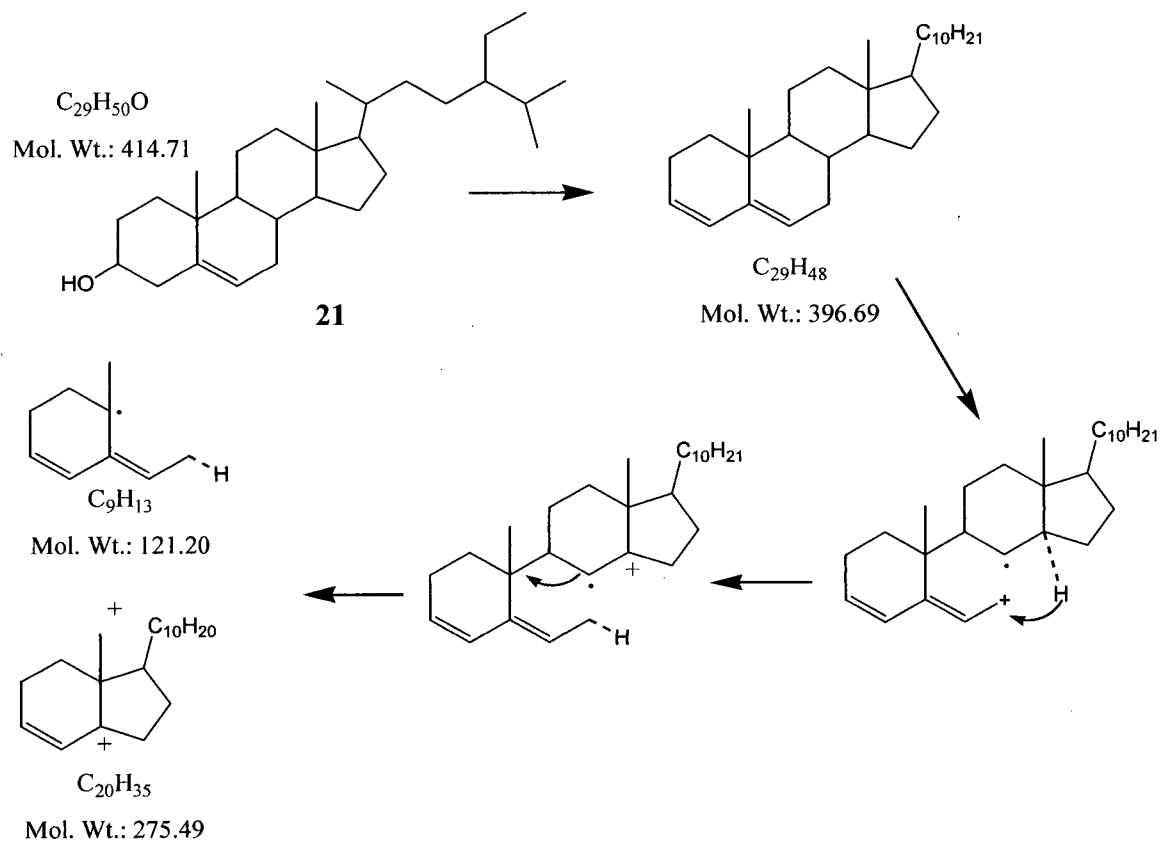
^1H (ppm) $\text{C}_5\text{D}_5\text{N}$	^{13}C (ppm) $\text{C}_5\text{D}_5\text{N}$	EI Mass Spec. (M/z)
0.65	11.98	576
s	12.16	415
0.85	19.02	396
d	19.21	382
0.89	19.43	329
d	20.00	330
0.93	21.28	275
s	23.38	255
0.99	24.52	229
d	26.36	213
1.1-2.0 multiplets	28.55	121
	29.44	
2.12 overlapping multiplets	30.26	
	32.05	
2.47	32.18	
t of d	34.19	
2.73	36.40	
d of q	36.92	
3.9-4.0 multiplet	37.48	
	39.33	
4.05	39.94	
t	42.47	

Table 11. cont

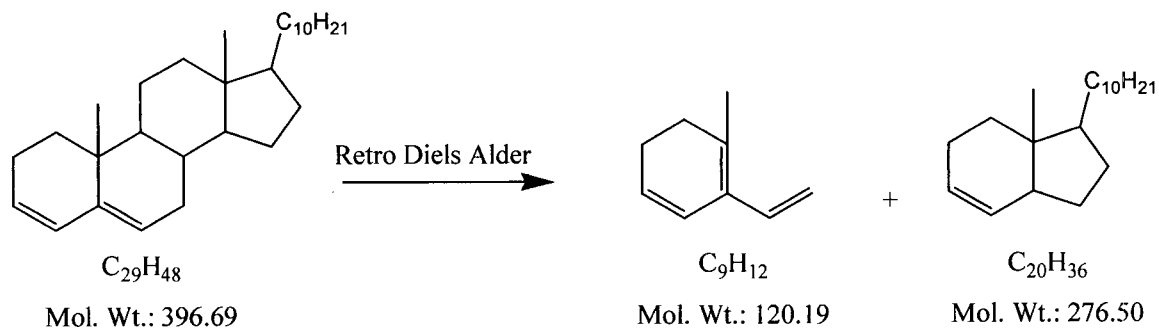
¹ H (ppm) C ₅ D ₅ N	¹³ C (ppm) C ₅ D ₅ N	EI Mass Spec. (M/z)
4.24-4.29 multiplet	46.03 50.33	
4.56 d of d	56.23 56.82	
4.8-5.0 broad s	62.81 71.66	
5.05 d	75.34 78.06	
5.34 d	78.51 78.61	
	102.6 121.9 140.9	

The high resolution EI mass spectrum gave a molecular formula of C₃₅H₆₀O₆. Due to the similarity of the mass spectrum with that of β-sitosterol it was correctly assumed that the isolated compound was a known compound, the glucoside of β-sitosterol (C₂₉H₅₀O). After loss of glucose, the compound followed the fragmentation pattern of β-sitosterol summarized below (Partridge1977).

Fig. 42. EI Mass Fragmentation Pattern of β -Sitosterol (**21**)



and/or:



A ^{13}C spectra of β -sitosterol in pyridine ($\text{C}_5\text{D}_5\text{N}$) was taken to aid in the assignment of the steroidal carbons of IIID-4A. Assignments of the ^{13}C signals of β -sitosterol obtained in pyridine were made comparing to the published spectrum taken in deuterated chloroform (CDCl_3) (Wright 1978).

Fig. 43. Structure and Numbering of β -Sitosterol (21)

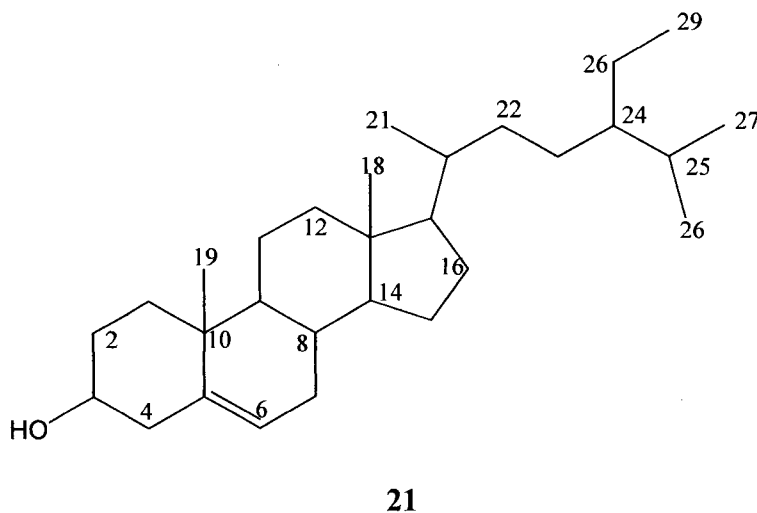


Table 12. Comparison of ^{13}C NMR Data between IIID-4A and β -Sitosterol in Pyridine

IIID4-A ^{13}C (ppm) $\text{C}_5\text{D}_5\text{N}$	β -sitosterol ^{13}C (ppm) $\text{C}_5\text{D}_5\text{N}$
11.98	12.06 C18
12.16	12.21 C29
19.02	19.08 C21
19.21	19.28 C26
19.43	19.66 C19
20.00	20.03 C27

IIID4-A ¹³ C (ppm) C ₅ D ₅ N	β-sitosterol ¹³ C (ppm) C ₅ D ₅ N
21.28	21.43 C11
23.38	23.44 C28
24.52	24.59 C15
26.36	26.46 C23
28.55	28.61 C16
29.44	29.52 C25
30.26	32.22 C2
32.05	32.27 C8
32.18	32.65 C7
34.19	34.27 C22
36.40	36.47 C20
36.92	36.94 C10
37.48	37.89 C1
39.33	40.09 C12
39.94	42.57 C4
42.47	43.53 C13
46.03	46.09 C24
50.33	50.54 C9
56.23	56.35 C17
56.82	56.98 C14
62.81	
71.66	
75.34	
78.06	
78.51	
78.61	71.29 C3
102.6	
121.9	121.2 C6
140.9	142.0 C5

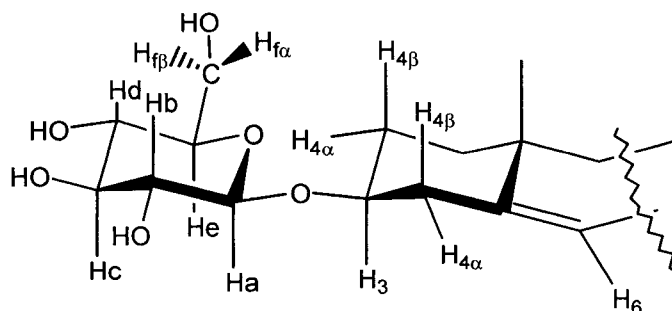
The six remaining signals were assumed to be the components of glucose and assigned using proton correlated (¹H COSY), heteronuclear multiple quantum coherence (HMQC) and attached proton test (¹³C APT) spectroscopy. The couplings relevant to assignment are summarized below.

Table 13. NMR Data of Glucoside Residue of IIID-4A

^1H ^1H coupling	$^1\text{H}, ^{13}\text{C}$ Coupling (C type, ^{13}C APT)
3.9-4.0 (m) with 2.73 (d of q) 2.47 (t of q) 2.12 (m) 1.75(m)	78.06 (CH) 78.50 (CH)
4.05 (t) with 5.05 (d)	75.34 (CH)
4.24-4.29 (m) with 3.9-4.0(m) 4.05 (t)	71.66 (CH) 78.61 (CH)
4.56 (d of d) with 3.9-4.0 (m) weak 4.56 (d of d) doublets strongly coupled	62.81 (CH_2)
5.05 (d) with 4.05 (t)	102.56 (CH)
5.34 (d) with 1.9-2.0 (m)	121.9 (CH)

To facilitate discussion of the assignments the following diagram is provided.

Fig. 44. Labeling of Glucoside portion of IIID-4A



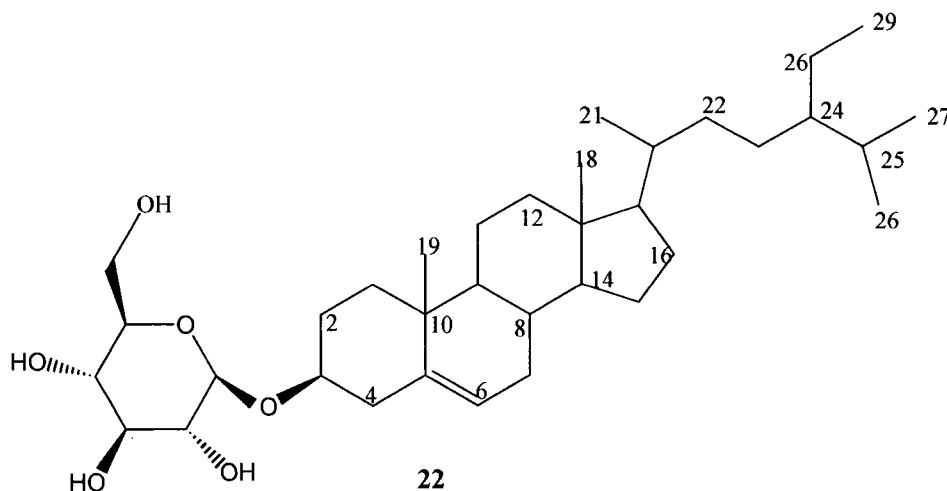
The signal at 5.05 ($J=7.7$ Hz) was assigned to the anomeric proton H_a, since it showed only one coupling to a downfield proton at 4.05, presumed to be H_b. The geometry being that of a β - glucoside is confirmed by the size of the H_a, H_b coupling constant. A smaller J would be observed for an α configuration (cf α -glucose $J=3.7$ Hz β -glucose $J=7.9$ Hz) (Friebolin 1993). The HMQC and APT experiments indicated that two methine protons were responsible for the multiplet at 4.2-4.3 which was in agreement with the integration of the ^1H spectra. Part of the multiplet was H_c, since a coupling was observed between the multiplet and the H_b triplet at 4.05 in the ^1H COSY. The HMQC, APT and ^1H integration indicated that the doublet of doublets at 4.56 were a single methylene group and thus had to be H_{f α} and H_{f β} . Besides a strong coupling between the doublets, a coupling to the multiplet at 3.9-4.0 was observed indicating that part of that multiplet was signal arising from H_e. The other part of the signal was attributed to H₃, since a) ^1H ^1H couplings from the multiplet were also observed to upfield protons attached to carbons in the steroid portion of the molecule and b) β -sitosterol contains a multiplet in its ^1H spectra assigned to H₃ in this vicinity. This left H_d to be assigned to the other portion of

the multiplet at 4.2-4.3. This assignment was confirmed by observation of a coupling to H_e in the 1H COSY. H_6 was assigned from the HMQC as it was the only upfield proton attached to a carbon with the chemical shift characteristic of an alkene. The final carbon assignments were made using the HMQC spectra after the protons had been assigned. The carbon assignments for the steroidal part of the structure remained as described in Table 12, the carbon assignments for the glucose attachment are as follows:

Table 14. IIID-4A Glucoside Residue ^{13}C NMR Assignments

^{13}C (ppm)	Assignment
62.81	C6'
71.66	C4'
75.34	C2'
78.06	C5'
78.61	C3'
102.6	C1'

Fig. 45. Structure and Numbering of 3- β -O[β -D-glucoside] β -sitosterol (22 IIID-4A)



The published spectra for 3- β -O[β -D-glucoside] β -sitosterol is in agreement with the assignments made for IIID-4A (Koizumi 1979).

Table 15. Published Spectra of 3- β -O[β -D-glucoside] β -sitosterol

IIID4-A ¹³ C (ppm) C ₅ D ₅ N	3- β -O[β -D- glucoside] β -sitosterol C ₅ D ₅ N
11.98	12.0 C18
12.16	12.2 C29
19.02	19.1 C21
19.21	19.2 C26
19.43	19.4 C19
20.00	20.0 C27
21.28	21.3 C11
23.38	23.4 C28
24.52	24.5 C15
26.36	26.5 C23
28.55	28.6 C16
29.44	29.5 C25
30.26	30.2 C2
32.05	32.1 C8
32.18	32.1 C7
34.19	34.3 C22
36.40	36.4 C20
36.92	36.9 C10
37.48	37.5 C1
39.33	39.3 C12
39.94	40.0 C4
42.47	42.5 C13
46.03	46.1 C24
50.33	50.3 C9
56.23	56.3 C17
56.82	56.9 C14
62.81	62.8 C6'
71.66	71.7 C4'
75.34	75.2 C2'
78.06	78.2 C3'

Table 15 cont.

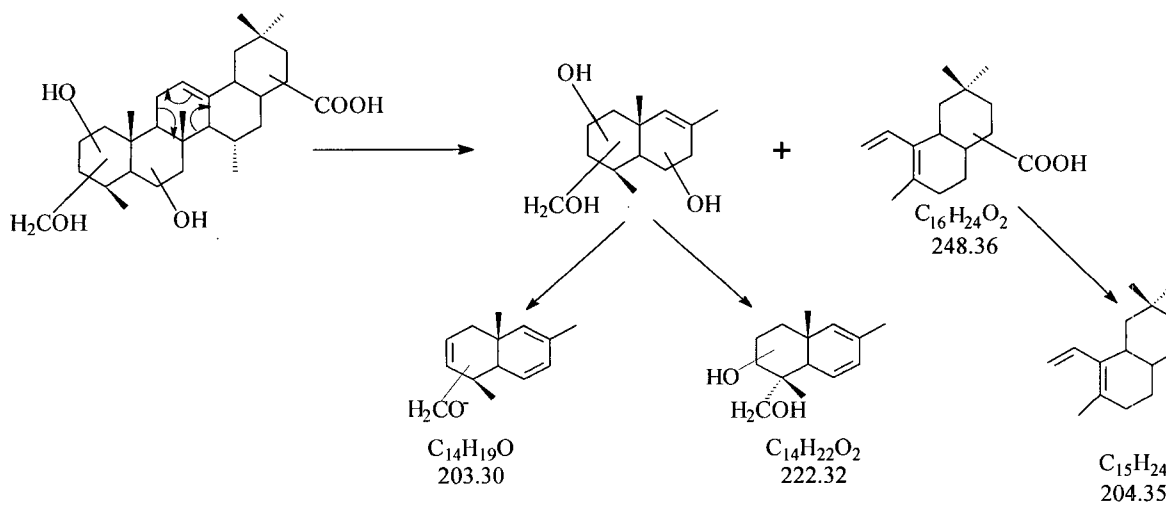
IIID4-A ¹³ C (ppm) C ₅ D ₅ N	3-β-O[β-D-glucoside]β-sitosterol C ₅ D ₅ N
78.51	78.3 C5'
78.61	78.5 C3
102.6	102.5 C1'
121.9	121.2 C6
140.9	142.0 C5

5.2B IIID-3B4

The second compound IIID-3B4 was isolated from fraction IIID in the manner described in fig 41. In order to get good spectral data, a joint effort was made between myself and Aleksandra Markovniv, whom had isolated approximately 15 mg of the same compound from Microferm type bioreactors.

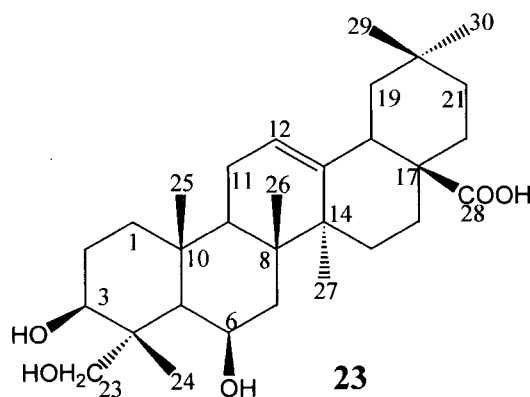
High resolution Mass spectra indicated C₃₀H₄₈O₅ as the chemical formula of the compound. Given that the compound had 30 carbons it was likely that it had a triterpene structure. Two of the main peaks in the structure 203, and 248 were characteristic of retro- Diels Alder fragmentation of oleananolic acid type pentacyclic triterpenes (Yamaguchi 1970). Additional peaks at 222 and 204 helped to place the approximate positions of the hydroxyl and carboxyl groups.

Fig. 46. Mass Spectrum Fragmentation Pattern of Trihydroxy Triterpene Acid



Comparison of our spectra with that of known pentacyclic triterpene compounds with formula $C_{30}H_{48}O_5$ led to the conclusion that 3 β ,6 β -23 trihydroxy olean-28-oic acid (**23**), numbered as follows, was the identity of the compound.

Fig. 47. Structure and Numbering of 3 β ,6 β -23 trihydroxy olean-28-oic acid (**23** IIID-3B4)



The following published NMR and Mass spectra are compared with those obtained for IID3-B4 (Mahato 1994).

Table 16. NMR and EI Mass Spec. Data of IID-3B4 Compared with Published Data

¹ H 300 MHz 3β,6β-23 trihydroxy olean-28-oic acid ppm, C ₅ D ₅ N	¹ H 400 MHz IID3-B4 ppm C ₅ D ₅ N	¹³ C 75 MHz 3β,6β-23 trihydroxy olean-28-oic acid ppm C ₅ D ₅ N	¹³ C 75 MHz IID3-B4 ppm C ₅ D ₅ N	EI MS (%) 3β,6β-23 trihydroxy olean-28-oic acid	EI MS IID3-B4
0.72 (H-30) s	0.92 s	14.7 C24 17.4 C25	14.78 17.51	484 (5) 470 (4)	488 (0.5) 470 (2)
0.80 (H-29) s	1.00 s	18.6 C26 23.7 C29 C11 23.9 C16	18.63 23.79 23.95	452 (8) 442 (15)	452 (1.5) 440 (1) 393 (1.5)
1.06 (H-27) s	1.26 s	26.2 C27 28.3 C2 C15 30.9 C20	26.29 28.08 28.35	288 (40) 248 (100)	288 (6) 248 (100) 222 (20)
1.42 (H-26) s	1.62 s	33.2 C30 34.2 C21	31.00 33.28	203 (60) 187(35)	203 (100) 189 (17)
1.47 (H-25) s	1.67 s	36.9 C10 39.2 C8	34.25 37.02		
1.51 (H-24) s	1.72 s	41.1 C1 C7 42.0 C18	39.29 41.14		
3.14 (H-18) d of d	3.34 d of d	42.7 C14 44.0 C4	42.11 42.73		
3.83 (H _α -23) d	4.04 d	46.4 C19 46.6 C17	44.08 46.51		
4.04 (H-3) d of d	4.26 d of d	48.7 C9 49.3 C5	46.71 48.75		
4.18 (H _β -23) d	4.39 d	67.1 C23 67.5 C6	49.37 67.15		
4.85 (H-6) m	5.04 br s	73.3 C3 122.9 C12	67.61 73.29		
5.44 (H-12) m	5.38 d	144.2 C13 180.2 C28	122.8 144.2		
	5.48 distorted t		180.2		

Additional ^1H COSY, ^{13}C APT and HMQC NMR spectral data confirmed that the compound was correctly identified. From the ^{13}C APT and HMQC correlations were observed between methyl carbon atoms at 14.78, 17.51, 18.64, 23.79, 26.29, and 33.28 ppm with protons at 1.72, 1.67, 1.62, 1.00, 1.26, and 0.92 ppm.

The doublet of doublets at 3.34 correlated to a methine type carbon at 42.11 ppm in the HMQC. This chemical shift of this signal is in good agreement with that published for C18. ^1H COSY correlations between this signal were observed only to upfield multiplets around 1.8 and 1.3 ppm which in turn both couple to a methylene type carbon at 46.51 ppm. The carbon resonance agrees with that in the literature for C-19 and the ^1H coupling pattern is as one would anticipate for coupling between a methine and diastereotopic methylene protons. Additionally, of the two ^1H couplings, the magnitude of the coupling to 1.8 ppm is larger indicating it represented the $\text{H}_{19\beta}$ proton.

In the HMQC, the two doublets at 4.04 and 4.39 ppm coupled to the same methylene carbon at 67.15 ppm. The chemical shifts were consistent with the published assignment of the hydroxyl methylene group at position 23. In the ^1H COSY the protons were observed to couple only to each which is consistent with this assignment.

The methine carbon at 73.29 ppm coupled to a doublet of doublets at 4.26 ppm in the HMQC. In the ^1H COSY, coupling was observed to a signal at 2.2 ppm with slightly weaker coupling to signal at 1.9 ppm. These upfield protons were coupled to a single methylene type carbon at 28.08 ppm. The published chemical shift of C-3 is identical to that recorded for our compound and the coupling pattern observed in the ^1H COSY is as expected for coupling H-C-3 with the diastereotopic protons of C-2. From the relative intensity of the two couplings $\text{H}_{2\beta}$ can be assigned as the upfield proton. In the published

75 MHz spectra, C-2 and C-15 are reported as having the same chemical shift at 28.3 ppm while in our 75 MHz spectra the signals are resolved into two at 28.08 and 28.35 ppm. Given the above information C2 is assigned at 28.08 ppm and C-15 at 28.35 ppm.

In the HMQC, the broad singlet at 5.04 ppm correlated to a methine carbon at 67.61 ppm while the distorted triplet at 5.48 ppm was coupled to a methine at 122.8 ppm and therefore were assigned as the H-6 and H-12 carbon respectively. The broad singlet at 5.38 ppm did not correlate to any carbon signals and therefore presumed to be due to the hydroxyl protons. A weak coupling was observed in the ^1H COSY between this signal and that assigned as H-6.

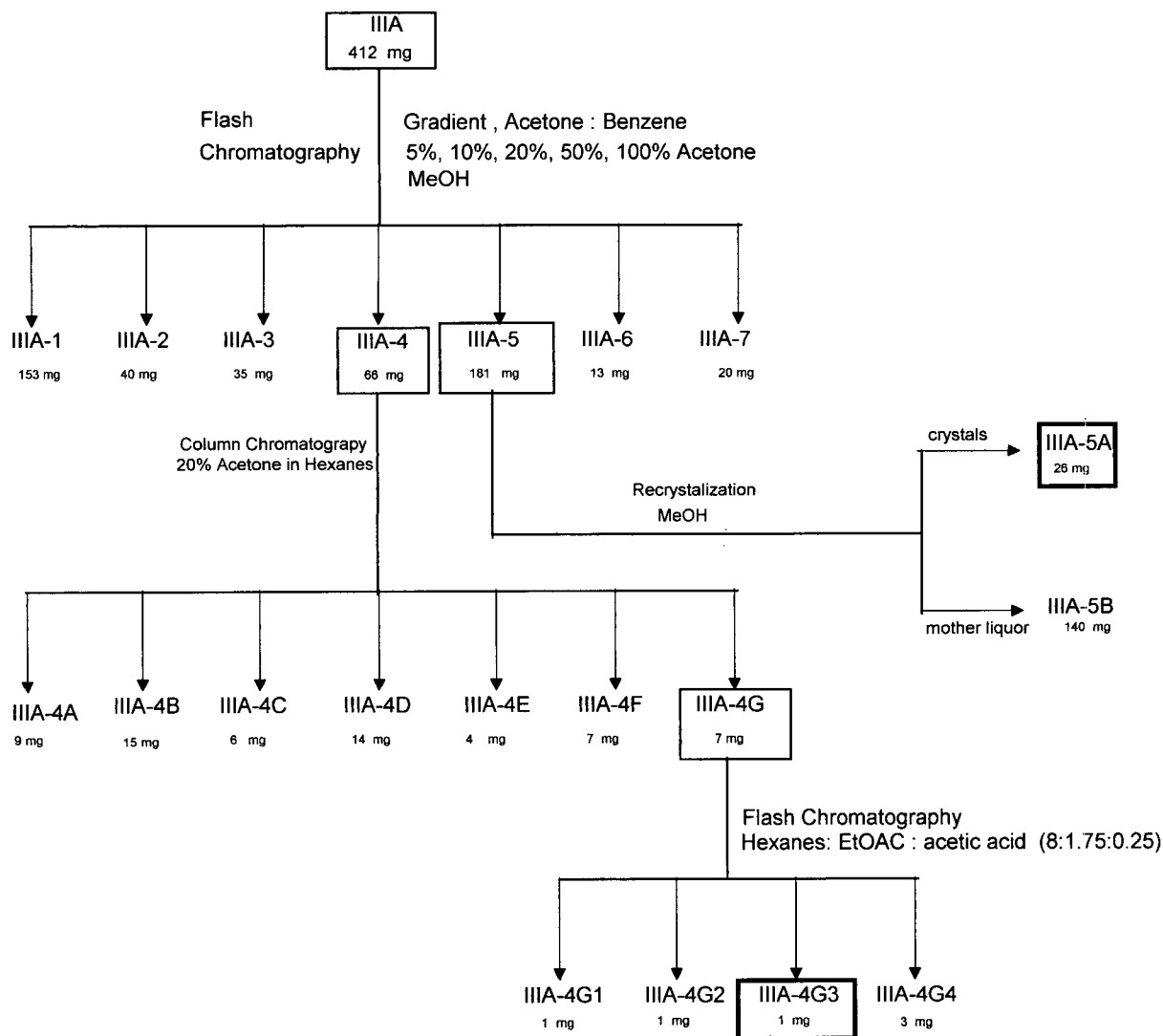
5.2C Remaining Material

Fractions IIID-5 and IIID-6 contained polar material and were not considered interesting. The remaining fractions resulting from purification of IIID-4A and IIID-3B4 were too small and complex to attempt purification and were set aside to combine with like material from later bioreactors.

5.3 Isolates from Fraction IIIA

The TLC plate of fraction A was treated with an anisaldehyde/acetic acid/ H_2SO_4 reagent that revealed different colored spots when developed. Our standard taxane compounds developed blue gray while phytosterols and triterpenes developed pink and purple. Although not identical in R_f (ratio to front) to any of our standards, fraction IIIA revealed a compound which developed the same gray hue as the taxanes. Separation was attempted using the following scheme:

Fig. 48. Separation Scheme of Fraction IIIA



5.3A IIIA5A

Recrystallization of fraction IIIA-5 from the above separation scheme yielded 26 mg of a compound (IIIA-5A) which melted at 174-176 °C but did not reveal in sulfuric acid (H₂SO₄)/MeOH, Ammonium Molybdate/H₂SO₄ or anisaldehyde/acetic acid/ H₂SO₄ TLC

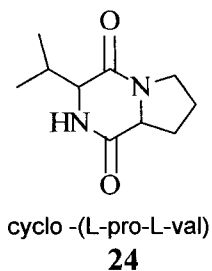
developing reagents. The following EI mass spectra, 200 MHz ^1H and ^{13}C NMR data were collected.

Table 17. NMR and EI Data for IIIA-5A

200 MHz ^1H (ppm)	^{13}C δ (ppm)	EI Mass Spectra (m/e)
0.95 d	39.4 42.5	196
1.1 d	45.9 52.0	167
1.8-2.2 m	52.1 68.6	154
2.2-2.4 m	82.4 84.0	138
2.5-2.7 m	188.5 193.9	125
3.4-3.8 m		98 97
6.6 b s		72 70

High resolution EI Mass Spectra indicated a chemical formula of $\text{C}_{10}\text{H}_{16}\text{O}_2\text{N}_2$. Search of the literature suggested that this compound may be a diketopiperazine of the following structure :

Fig. 49. Possible Structure of IIIA-5A (24)



The melting point determined for IIIA-5A was within the range of the three reported in the literature by Schmitz (169-172, 187-189, 191-193 °C). ¹H NMR and EI Mass Spectra data were reported for the compound which agreed with the data collected for IIIA-5A (Schmitz 1983).

Tabel 18. Published Spectra of Cyclo-(L-pro-L-val)

¹ H (100 MHz) NMR (ppm)	EI Mass Spectra (m/e)
0.92 d	196 169
1.10 d	167 154
1.2-2.8 m	140 138
3.6 m	125 98
3.96-4.1 m	97 72
	71 70

The compound was identified first in the literature as a sponge metabolite (Schmitz 1983). Later it was found that bacteria (*Micrococcus sp.*) which existed in a symbiotic relationship with the sponge actually were responsible for producing the isolated diketopiperazines (Cardellina II 1988).

5.3B IIIA-4G3

Fraction IIIA-4G3 appeared pure by TLC and developed the same gray hue as the taxane standards using the anisaldehyde developing reagent. Preliminary ^1H NMR and desorption chemical ionization (DCI) mass spectra indicated that the compound did not have a taxane structure. High resolution DCI MS gave a formula of $\text{C}_{29}\text{H}_{44}\text{O}_2$ with fragments at 203 and 248 m/e indicating the compound is possibly a pentacyclic triterpene which did not exhibit the M^+ ion. However, ^1H NMR spectra more closely resembled steroidal structure in the aliphatic region. Most likely the fraction is a mixture of the two and possibly the gray hue of the TLC spot is due to the combination of pink and purple that the steroidal and triterpene compounds develop in this reagent.

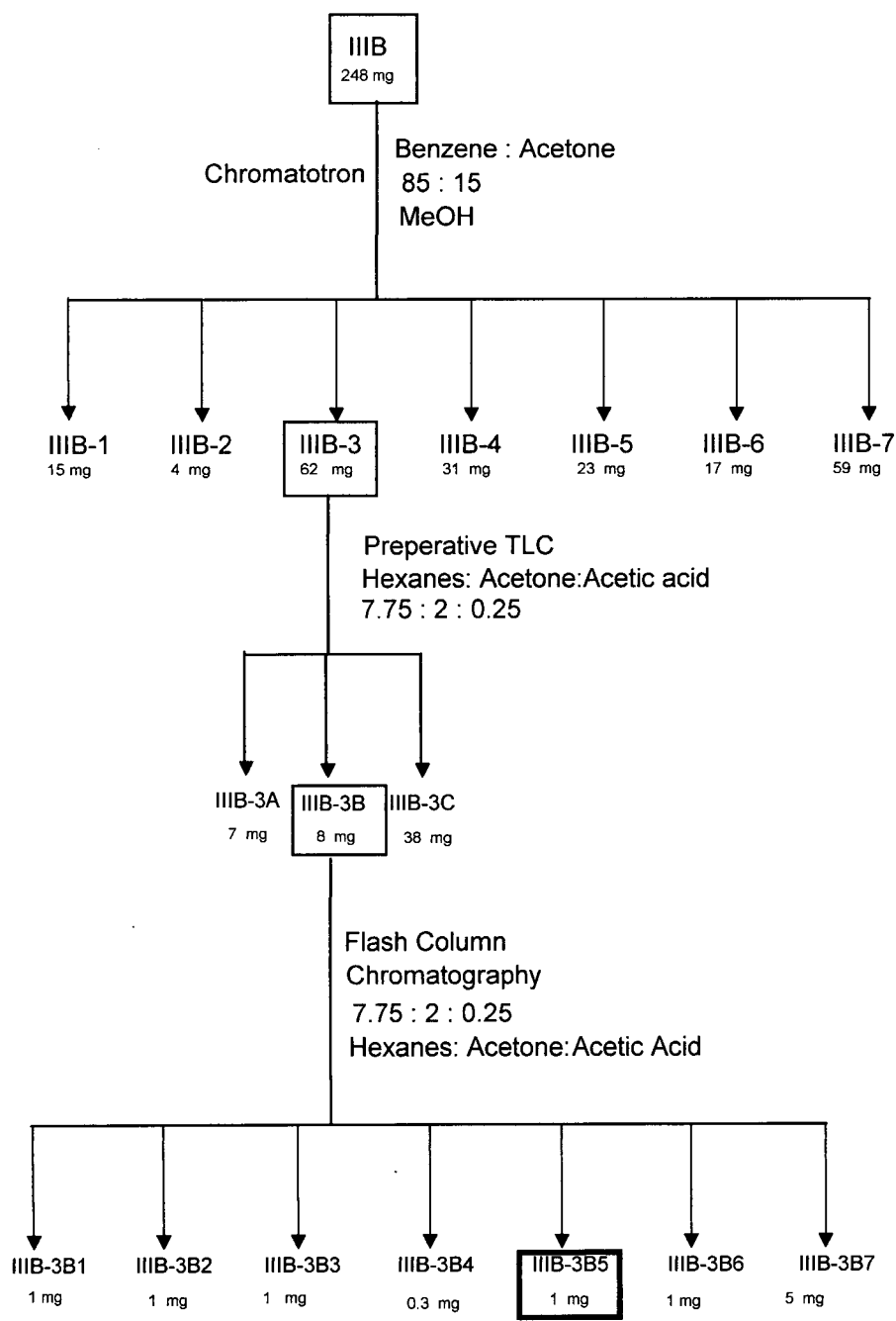
5.3C Remaining Fractions of IIIA

Fractions IIIA1 contained oily nonpolar material which had a higher R_f than the phytosterol standard and was considered uninteresting. IIIA2 and IIIA3 contained mainly material presumed to be phytosterols from TLC comparison of R_f values. The remaining fractions from IIIA were too complex for the amount available to attempt further separation.

5.4 Fraction IIIB

Separation of fraction IIIB was attempted using the following scheme:

Fig.50. Separation Scheme for Fraction IIIB



5.4A IIIB-3B5

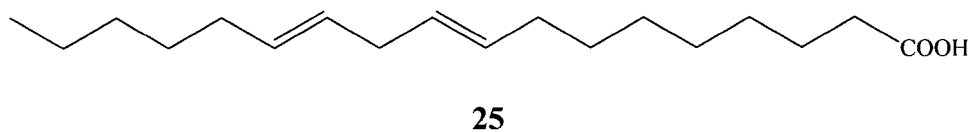
Fraction IIIB-3B5 was a clear oil which appeared pure by thin layer chromatography. High resolution EI mass spectrometry gave a chemical formula of $C_{18}H_{32}O_4$.

Table 19. NMR and EI Mass Spec. Data of IIIB-35B

1H (ppm) $CDCl_3$	^{13}C (ppm) $CDCl_3$	EI Mass Spec. (m/e)
0.87	14.0	312
t	22.5	294
1.23- 1.41	24.6	278
overlapping m	26.7	237
1.41-1.61	28.1	223
m	28.4	187
1.61-1.70	28.8	169
m	29.0	155
2.08	29.1	140
overlapping	29.2	125
symmetric m	31.5	109
2.33	33.9	
distorted t	58.2	
2.98	60.3	
t?	66.3	
3.00	126.7	
m	135.1	
4.27		
t		
5.47		
t		
5.62		
d of t		

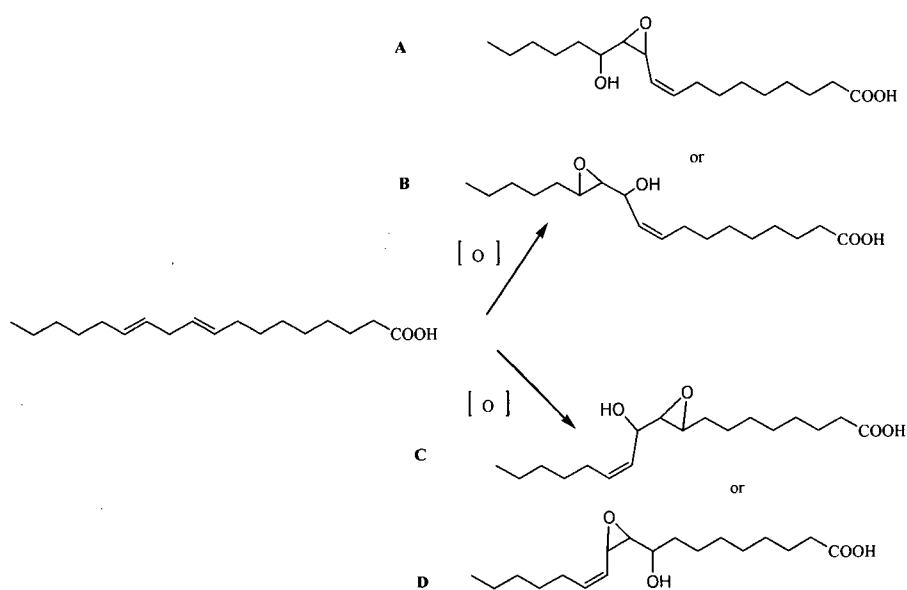
By comparison with compounds found in the literature which had been isolated from plants it was concluded that IIIB-3B5 is a linoleic acid derivative. Linoleic acid is a common plant metabolite with the following structure:

Fig. 51. Structure of Linoleic Acid (**25**)



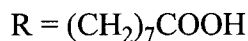
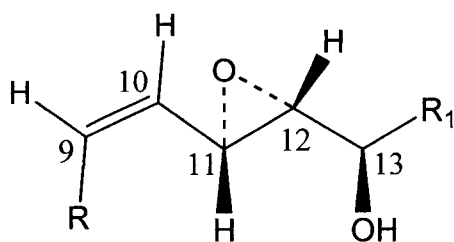
Enzymatic oxidation could result in the following compounds. The *cis* isomers are shown as the coupling constant between the olefinic protons at 5.47 and 5.42 ($J = \sim 10$) indicated a *cis* rather than *trans* ($J = 11-15$ Hz) double bond (Friebolin 1993).

Fig. 52. Possible Products from Oxidation of Linoleic Acid



The structures in which the epoxy group is located next to the olefin (Fig. 52, A and D) were eliminated based on comparison of ^1H and ^{13}C NMR data with that of methyl 11(R), 12(R)-epoxy-13(S)-hydroxy-(9Z)-octadecenoate (**26**). A 0.6 ppm difference between the chemical shifts of the two epoxide protons is observed while in IIIB3-B5 they resonate at nearly the same frequency (2.98 and 3.00 ppm). Likewise, the ^{13}C spectrum of IIIB-3B5 shows resonances of 58 and 60 ppm for the oxirane carbons while in **26** the difference is 10 ppm (Piazza 1997).

Fig. 53. Structure and Numbering of Methyl 11(R), 12(R)-epoxy-13(S)-hydroxy-(9Z)-octadecenoate (**26**)



26

Table 20. Comparison of NMR Data Between IIIB-3B5 and **26**

¹³ C (ppm)				¹ H (ppm)			
IIIB-3B5		26		IIIB-3B5		26	
(CDCl ₃)		(C ₆ D ₆)*		(CDCl ₃)		(C ₆ D ₆)	
CH _L	135	C9	138	H _L	5.62	C ₉ H	5.80
CH _K	127	C10	129	H _K	5.47	C ₁₀ H	5.39
CH _J	66	C11	64	H _J	4.26	C ₁₁ H	3.88
CH _H	58	C12	54	H _H	2.98	C ₁₂ H	2.97
CH _I	60	C13	72	H _I	3.00	C ₁₃ H	3.60

*Chemical shifts in d₆-benzene except C9 and C10 which were obtained in *p*-dioxane-d₈

Comparison of the ^{13}C and ^1H NMR data of IIIB3-B5 with that of methyl esters of (9Z,15Z-12S, 13S) 11 -hydroxy-12,13-epoxyoctadeca-9-15-dienoic acid (11S = **27**, 11R = **28**) gave further indications of the structure (Kato 1986).

Fig. 54. Structure and Numbering of **27** and **28**

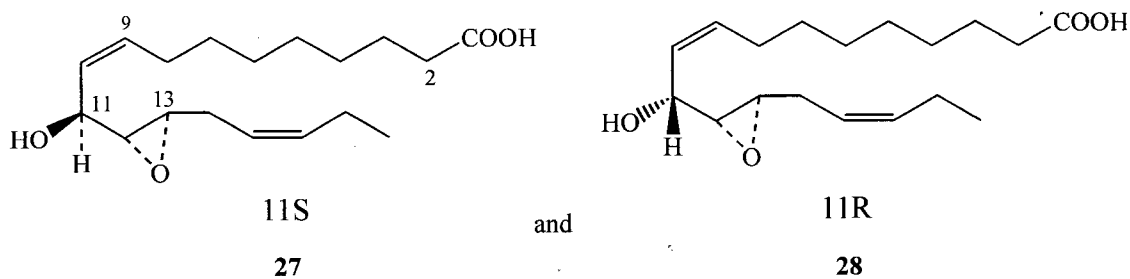


Table 21. Comparison of NMR Data of IIIB-3B5 with **27** and **28**

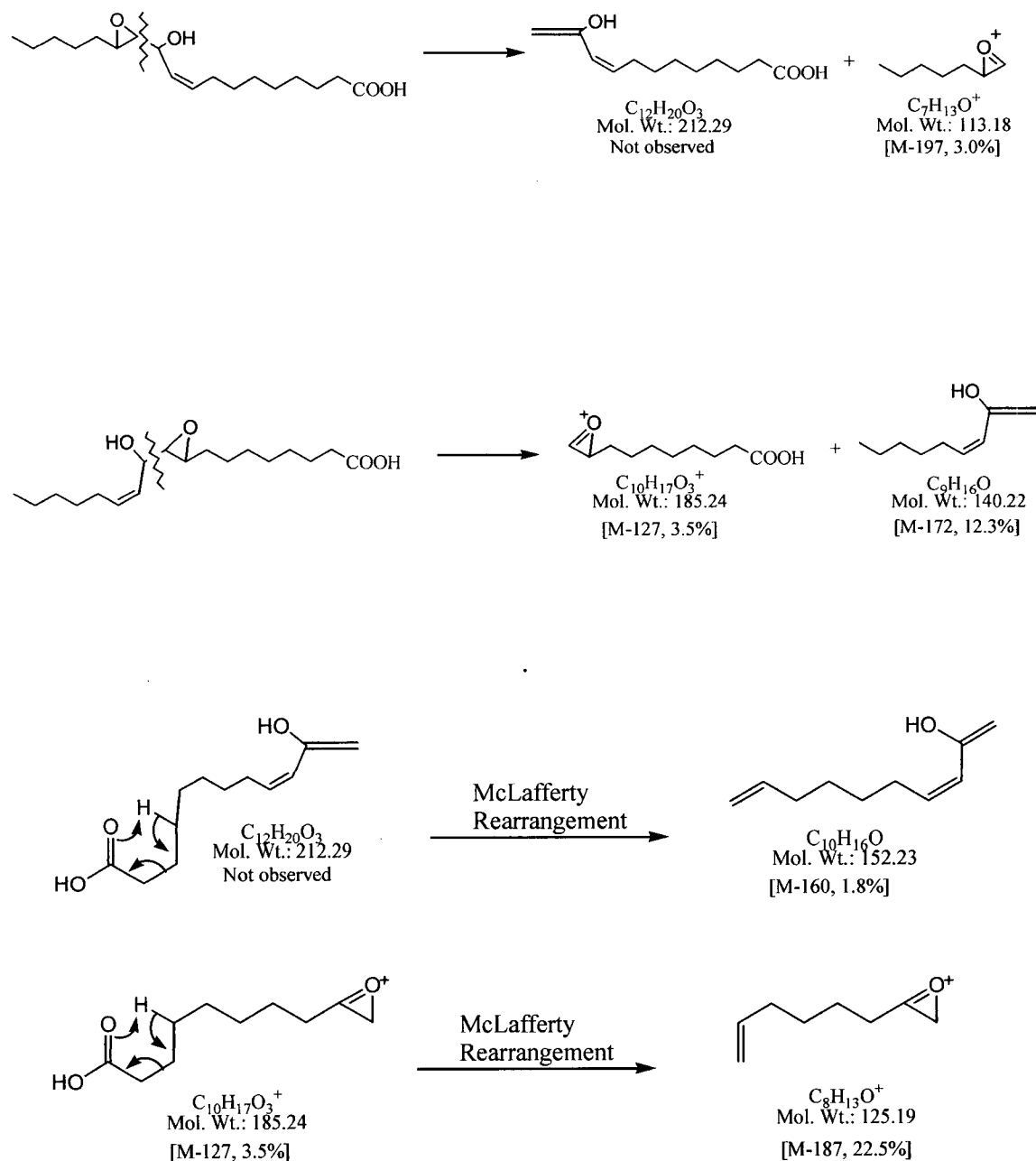
IIIB-3B5		11-S epimer (27)		11-R epimer (28)	
¹³ C (ppm)	¹ H (ppm)	¹³ C (ppm)	¹ H (ppm)	¹³ C (ppm)	¹ H (ppm)
CH _J 66.3	4.26	C11 64.9	4.66	C11 67.7	4.29
CH _I 60.3	3.00	C12 59.8	2.84	C12 61.0	2.97
CH _H 58.2	2.98	C13 54.1	3.05	C13 56.2	2.83

From comparison of the chemical shifts, IIIB-3B5 more closely resembles the 11 R (**27**) epimer, however, examination of the coupling constants between H_I and H_H, and H_I and H_J could not confirm the *trans* epoxide geometry. Generally the coupling constant between the protons of a *trans* epoxide are 2.1-2.4 Hz while those with *cis* conformation are 4.3 Hz (Piazza 1996). Due to the overlapping peaks of H_I and H_H it was difficult to distinguish the coupling constants. Again due to indeterminable coupling constants it could not be concluded whether a *threo* or *erythro* relationship existed between the epoxy and neighboring protons. Generally a smaller ($J = \sim 3$ Hz) coupling is observed for *erythro* configurations while larger ($J = 5$ Hz) are observed for *threo* structures (Piazza 1997). The coupling constant between H_J and H_H could not be evaluated due to peak overlap between H_H and H_I. Additionally as H_J appeared as a distorted triplet, peaks due to coupling to H_K probably overlap with those due to coupling to H_H thus again making the coupling constants unable to be evaluated. However, given the similarities in the NMR data between IIIB-3B5 and the 11 R epimer I feel this type of structure is more likely.

Comparison of the mass spectral data of compounds with that of IIIB-3B5 indicated that structure C (fig. 52) was more consistent with the data than structure D. If

following a similar fragmentation pattern to Kato's compounds, one would expect to find fragments of the following molecular weights for structures B and C.

Fig. 55. Mass Spectrum Fragmentation of Hydroxy, Epoxy Linoleic Acid



Assuming structure C (fig. 52), the ^1H COSY and HMBC was checked for inconsistencies. Assignments of ^1H chemical shifts were made by comparison with compounds and by comparison of the ^{13}C data of known linoleic acid derivatives using the HMQC to identify the proton in question (Kato 1986 ; Gustone 1994)

Fig. 56. Proposed Structure and Assignment of IIIB-3B5 (29)

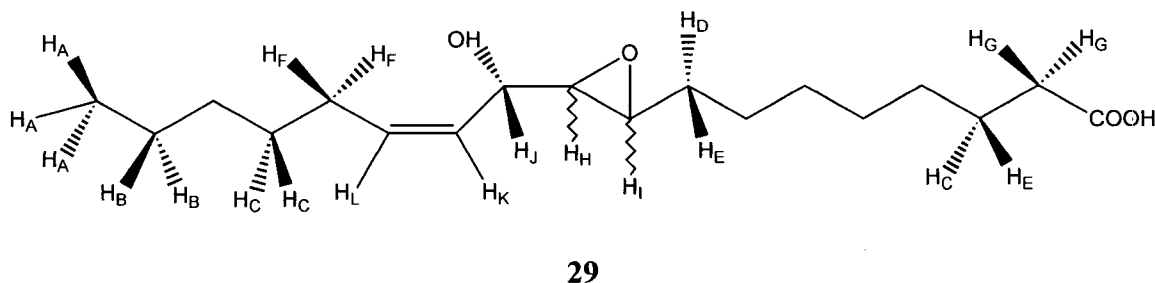


Table 22. Results of 2D NMR Experiments of IIIB-3B5

^{13}C (type)	Correlated to ^1H	^1H COSY
14.0 (CH ₃)	0.87 H _A	H _A \propto H _B
22.5 (CH ₂)	1.28 H _B	
24.6 (CH ₂)	1.32 H _C , 1.61 H _E ,	H _D \propto H _H or H _I
26.7 (CH ₂)	1.55 H _D , 1.61 H _E	
28.1 (CH ₂)	H _C or H _D	H _E \propto H _G , H _C
28.4 (CH ₂)	H _C or H _D	
28.8 (CH ₂)	H _C	H _F \propto H _C , H _L
29.0 (CH ₂)	1.98-2.13 H _F	H _F \propto H _K (weak)
29.1 (CH ₂)	H _C	H _G \propto H _C H _I \propto H _E
29.2 (CH ₂)	H _C	
31.5 (CH ₂)	H _C	
33.9 (CH ₂)	2.32 H _G	H _H \propto H _J
58.2 (CH)	2.98 H _H	
60.3 (CH)	3.00 H _I	H _J \propto H _K
66.3 (CH)	4.26 H _J	
126.7 (CH)	5.47 H _K	H _L \propto H _K
135.1 (CH)	5.62 H _L	

Structure **29** was not found in the literature. As the NMR and mass spectra data are in agreement with this assignment, and the remaining unassigned carbon signals were consistent with linoleic acid derivatives with similar substructures, it is concluded that IIIB-3B5 is most likely 9, 10-epoxy- 11 (R)-hydroxy-12(Z)-octadecenoic acid (**29**) (Gunstone 1994; Sterner 1993; Jan 1976).

5.4B Remaining Fractions of IIIB and Fraction IIIC

The remaining fractions of IIIB were too small and complex to attempt further separation and were set aside for possible combination with future fractions. Fraction IIIC was subjected to multiple chromatographies however no compounds were sufficiently purified to attempt identification.

5.5 Bioreactors F88-107

Bioreactors F88-107 were extracted in the same manner as described for F77-85 with the exception that the methanol extraction was omitted. After partitioning by solvents as described in section, the subextracts were evaluated by TLC and HPLC. Neither method suggested the presence of our standards. The hexanes:CH₂Cl₂ was focused on for further separation as it contained compounds in the R_f range of our standards, and the CH₂Cl₂ subextract appeared by TLC to contain the same compounds identified in F77-85.

Fig. 57. Separation Scheme of Hexanes:Methylene Chloride Subextract

Labroferms F88, F92, F94, F105, F106, F107

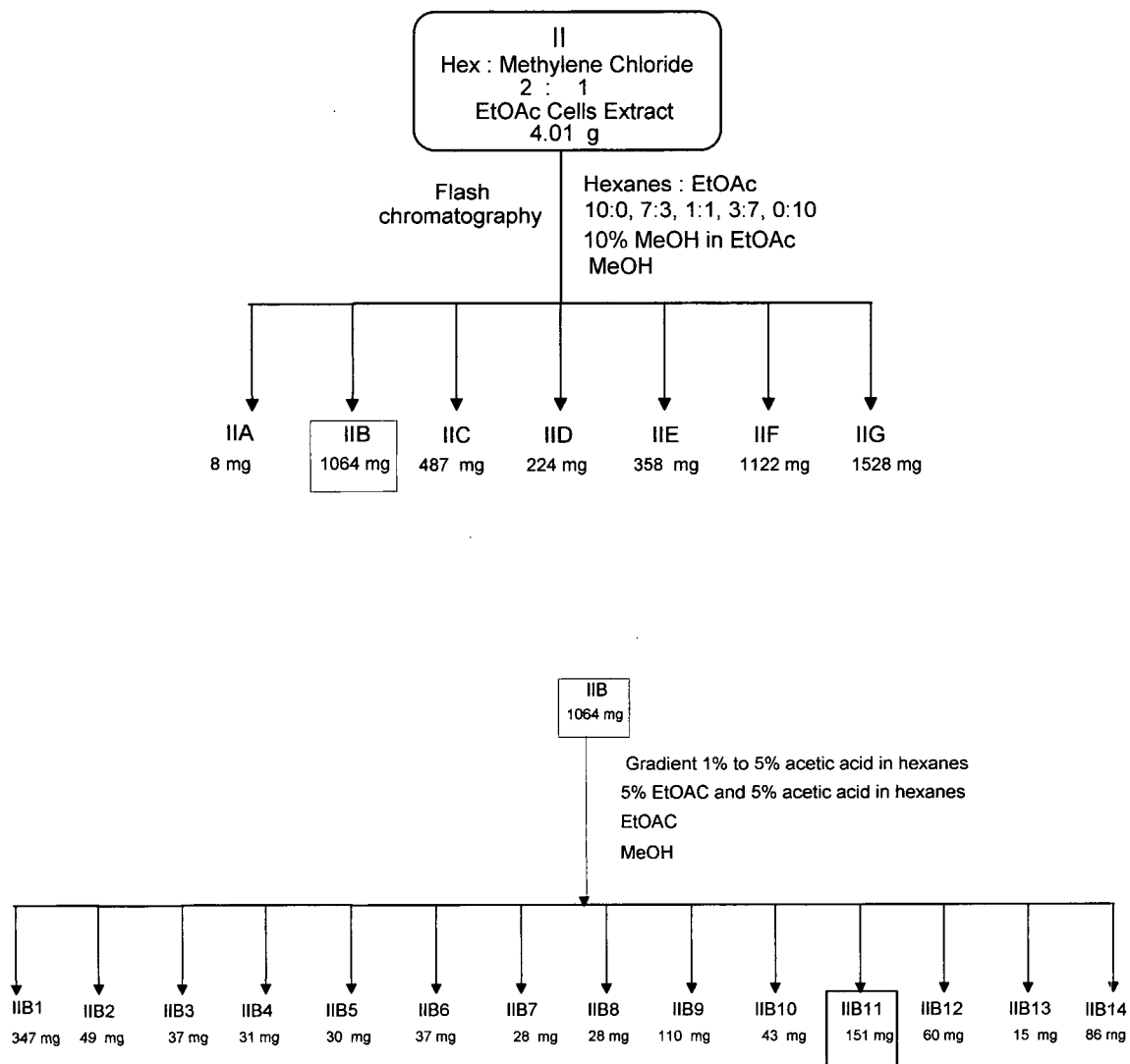
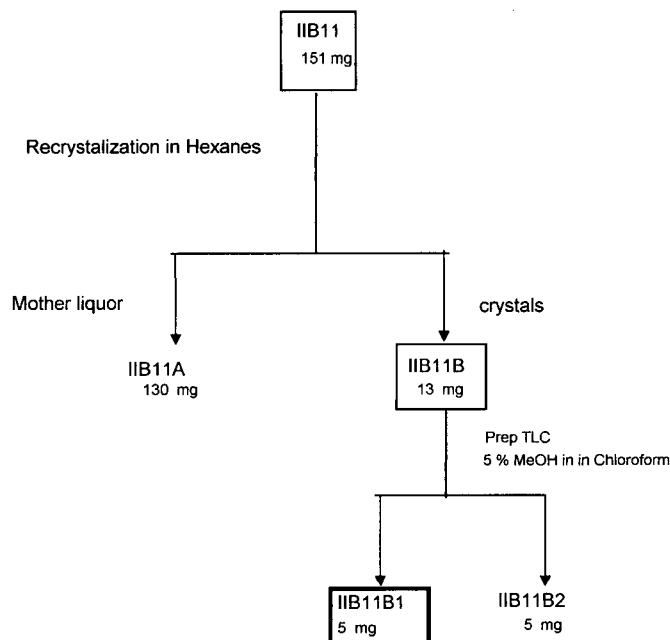


Fig. 57 cont.



5.5A IIB11B1

Fraction IIB11B1 appeared pure by thin layer and gas chromatography and melted between 248 and 250 °C. The compound fluoresced light blue under UV radiation but did not develop using either H₂SO₄ or molybdate developing reagents.

UV spectroscopy in MeOH revealed four maxima located at 256, 289, 300, and 343 nm. Additionally spectra was recorded in the presence of shift reagents with the following results: sodium methoxide (NaOMe) 265 and 368 nm, aluminum chloride (AlCl₃) 260, 310 and 370 nm, AlCl₃/hydrochloric acid (HCl) no change from AlCl₃, sodium acetate (NaOAc) 260 and 356 nm. The results of these experiments implied that : 1) ionizable hydroxy groups were present (NaOMe induced shift), and 2) a hydroxy group was present at either position 3 or 6 (see fig. 59 for xanthone numbering system) as a shift

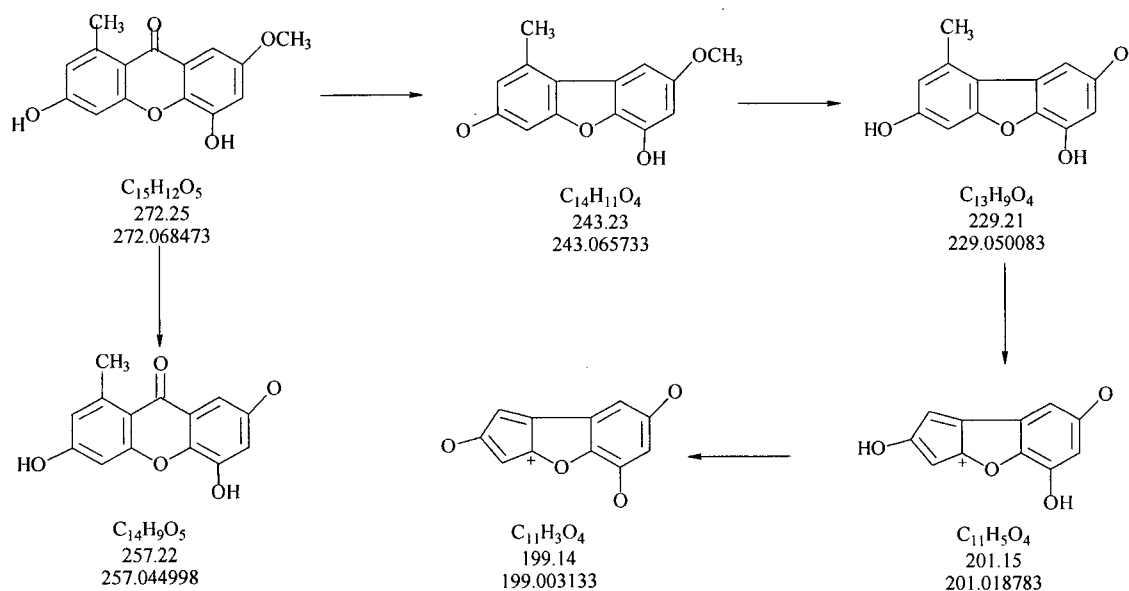
was also observed with NaOAc (Sultanbawa 1975). The shifts induced by AlCl_3 but unchanged by addition of HCl implied that: 1) a hydroxy group was in position 1 and 2) the hydroxy groups were not in a ortho relationship to one another. The Uv shift reagent experiments are in agreement with the structure determined by NMR, with the exception that formation of the hydroxy - keto AlCl_3 complex can not be explained.

^1H and ^{13}C NMR in indicated presence of a methyl and methoxy group, two aromatic meta coupled spin systems. Deuterated water (D_2O) exchange confirmed the presence of two labile protons. Infrared spectroscopy (IR) revealed strong absorbencies at 3440 and 1665 cm^{-1} indicating alcohol and carbonyl functional groups. High resolution EI and DCI mass spectrometry gave a formula of $\text{C}_{15}\text{H}_{12}\text{O}_5$ with a fragmentation pattern characteristic of a xanthone.

Table. 23. NMR and EI Mass Spectrum Data of IIB11B1

^1H (ppm) d_6 -acetone	^{13}C 125 MHz (ppm) d_6 -acetone	EI Mass Spec. (m/e)
2.80	25.6	272
m	56.2	257
4.00	99.9	243
s	102.7	229
6.60	104.5	201
d	109.7	199
6.70	118.4	
d	139.6	
6.82	154.1	
d of d	159.4	
7.30	165.9	
d	166.1	
9.61	167.6	
bs		
12.0		
bs		

Fig. 58. Mass Spectrum Fragmentation Pattern of Xanthenes



1H COSY, ^{13}C APT, HMQC and HMBC, experiments gave the following information:

Table 24. Results of 2D NMR Experiments with IIB11B1

^{13}C (type)	Correlated to 1H	1H COSY	HMBC
25.6 (CH ₃)	2.80 H _A	H _A \propto H _E , H _F	H _E
56.2 (CH ₃)	4.00 H _B	H _B \propto H _C , H _F weak	H _B
99.9 (CH)	6.60 H _C	H _C \propto H _F	H _F
102.7 (CH)	6.70 H _D	H _D \propto H _E	H _E
104.5 (CH)	7.30 H _F		H _C
104.5 (C)			H _F
109.7 (C)			H _A , H _F , H _D

Tabel 24. cont.

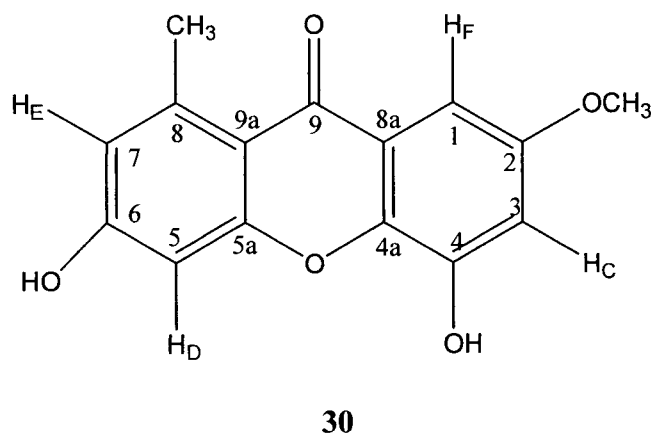
¹³ C (type)	Correlated to ¹ H	¹ H COSY	HMBC
118.4 (C)	6.82 H _E		H _A ,H _D
139.6 (C)			H _A
154.1 (C)			H _A ,H _D
159.4 (C)			H _D ,H _E
165.9 (C)			*H _C *H _F
166.1 (C)			*H _C *H _F
167.6 (C)			H _B , H _C , H _F
	9.61 [∇]		
	12.0 [∇]		

* Carbon signals may be exchanged

∇ Exchanged with D₂O

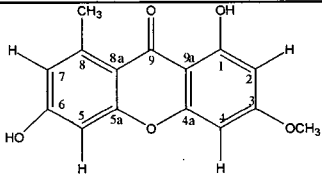
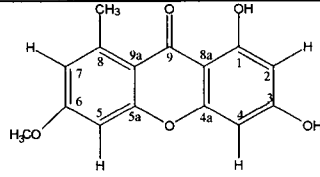
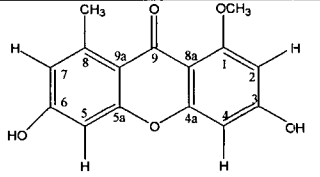
Based on the results of these experiments and by comparing with like compounds in the literature IIB11B1 appears to be a previously undescribed compound with the following structure.

Fig. 59. Proposed Numbered Structure of IIB11B1 (**30**)

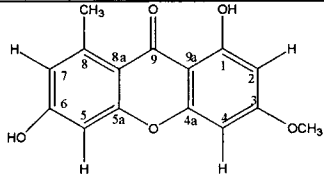
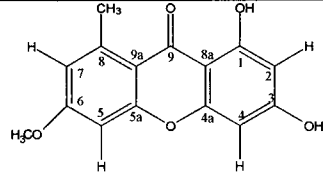
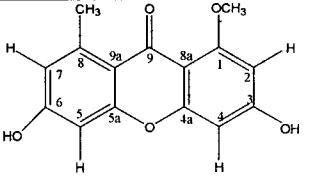


^1H COSY confirmed that the two aromatic spin systems were H_C and H_F , and H_E and H_D . Since the coupling constants were ~ 2.3 Hz it was assumed that the protons meta as opposed to ortho ($J \sim 10$ Hz) or para ($J \sim 1$ Hz) coupled. Three xanthenes with similar formulae, functional groups and a meta relationship between the groups were found in the literature, however NMR data was not in agreement with that collected for IIB11B1 (Sundholm 1978 ; Sairenji, JP8012666 1996).

Table 25. Published NMR Data of Meta Coupled $\text{C}_{15}\text{H}_{12}\text{O}_5$ Xanthenes

 <p>1,6-dihydroxy,3-methoxy,8-methyl-xanthone (m.p 253-255 $^\circ\text{C}$)</p>	 <p>1,3-dihydroxy,6-methoxy,8-methyl-xanthone (m.p 263-265 $^\circ\text{C}$)</p>	 <p>3,6-dihydroxy,1-methoxy,8-methyl-xanthone[†] (m.p not reported)</p>
^{13}C (DMSO) ^1H (d_6 -acetone)	^{13}C (DMSO) ^1H (d_6 -acetone)	^{13}C (d_4 -MeOH) ^1H (d_4 -MeOH)
1 162.6 13.42	1 163.0 13.36	1 166.6* (s)
2 96.3 6.27 (d)	2 97.6 6.20 (d)	2 98.9 (d) 6.25 (brs)
3 165.2 *	3 164.2 9.61	3 165.0* (s)
4 91.5 6.43 (d)	4 92.8 6.32 (d)	4 92.3 (d) 6.40 (brs)
4a 156.1	4a 156.1	4a 159.1** (s)
5a 158.6	5a 158.1	5a 160.9** (s)
5 100.2 6.72 (m)	5 98.3 6.80 (m)	5 102.7 (d) 6.62 (brs)
6 162.6	6 162.7	6 164.9* (s)
7 116. 6.70 (m)	7 114.3 6.73 (m)	7 117.6 (d) 6.62 (brs)
8 142.5	8 141.9	8 144.6 (s)
8a 110.6	8a 111.7	8a 112.6 (s)

Tabel 25. cont.

 <p>1,6-dihydroxy,3-methoxy,8-methyl-xanthone (m.p 253-255 C°)</p>	 <p>1,3-dihydroxy,6-methoxy,8-methyl-xanthone (m.p 263-265 C°)</p>	 <p>3,6-dihydroxy,1-methoxy,8-methyl-xanthone^φ (m.p not reported)</p>
9a 102.8	9a 102.2	9a 105.4 (s)
Me 22.5 2.79 (m)	Me 21.6 2.79 (m)	Me 23.6 (q) 2.78 (s)
OMe 55.5 3.92	OMe 55.0 3.94	OMe 57.1 (q) 3.86 (s)
CO 181.1	CO 181.1	CO 183.4 (s)

φ resonances reported but not assigned, my assignments based on comparison with like compounds in the literature.

* assignments may be reversed

** assignments may be reversed

Location of the functional groups on the two rings was accomplished by a combination of comparison with like compounds, and NMR data. Upon examining many xanthenes with various substitution patterns, trends were observed in the proton and carbon chemical shifts. When a xanthone is 1,3,6,8, substituted protons at 2 and 4 fall within 0.2 ppm of each other and protons 5 and 7 within 0.1 ppm, with an approximate separation being 0.5 ppm between the two spin systems. IIB11B1 did not exhibit this pattern, having instead three protons in close proximity (6.60, 6.70 and 6.82 ppm) and one shifted 0.5 ppm down field (7.30 ppm).

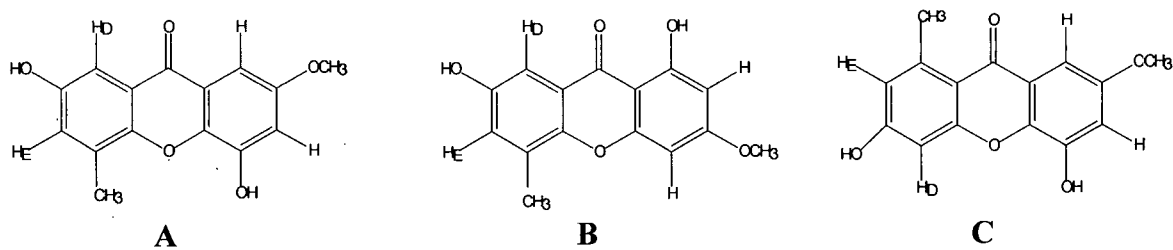
In the ¹H COSY a weak interaction was observed between methyl protons and H_E which could be explained by W coupling. HMBC data confirmed the proximity of H_E to

the methyl group. Long range couplings were observed between CH₃ protons at 2.80 ppm with the carbon attached to H_E at 118.7 ppm. H_D did not exhibit coupling either in the ¹H COSY or HMBC to the methyl protons or the carbon at 118.7 ppm indicating that it must be in a para relationship to the methyl group.

Likewise HMBC data indicated that the methoxy group was located on the same ring as H_F and H_C. A strong correlation between methoxy protons at 4.00 ppm and a quaternary carbon at 167.7 ppm indicated a two bond coupling. Coupling of methyl protons through oxygen to the directly attached carbon in the methoxy group of xanthenes has been documented previously in the literature (Chang 1995). The protons at 6.60 and 7.30 ppm both couple to the carbon at 167.7 indicating that the methoxy group must be located between them.

Given these constraints and eliminating the known compound which does not match the data the three possible structures which remain are:

Fig. 60 Possible Structures of IIB11B1



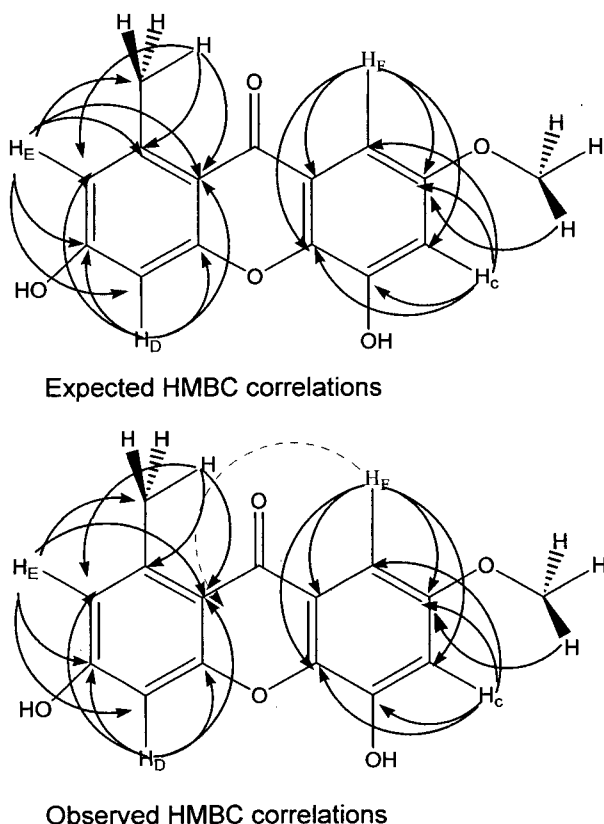
In order to determine the correct structure, assignment of carbons 4a, 5a, 8a and 9a were required. As expected, in other xanthenes, carbons 8a and 9a are reported at lower frequencies than 4a and 5a. Typical values for 8a and 9a ranged between 100 and

123 ppm while those for 4a and 5a between 145 and 160 ppm depending on the substituents and substitution pattern of the rings. After HMQC assignment and elimination of the carbons at 139.4 and 167.7 ppm which were unambiguously assigned through the HMBC, the remaining unassigned carbons were at 104.5, 109.7, 154.9, 159.4, 165.9 and 166.1 ppm. The first two resonances were reasonable for 8a and 9a. Examination of the HMBC revealed correlation between the methyl protons and a carbon at ~110 ppm. No correlations were observed between the methyl protons and any carbon atoms above 140 ppm. This would eliminate structures **A** and **B** (fig. 60) as possibilities as correlations between the methyl protons and C_{5a} not C_{9a} would be expected in the HMBC spectra. Utilizing this information, the peak at 109.7 ppm could be assigned to C_{9a} and that at 104.5 ppm to C_{8a}.

The remaining four resonances were assigned in the following manner. H_D and H_E correlated with equal intensity to a carbon at 159.4 ppm thus assigning it to C₆. H_D additionally coupled to a carbon at 154.1 ppm which showed no couplings to any other protons in the HMBC, indicating it must be at position 5a. It was not possible to distinguish between C_{4a} and C₄ since the resonances (165.9 and 166.1 ppm) were so close together. In the HMBC spectra H_F exhibited a weak correlation with a carbon at ~166 ppm, while H_C exhibited a strong coupling. Since H_C couples both these carbons, observance of a stronger signal is expected for H_C than H_F at this frequency.

Given these assignments the HMBC correlations were investigated for discrepancies. The following diagram represents the expected vs. observed correlations:

Fig. 61. Expected vs. Observed HMBC Correlations



One correlation is observed in HMBC which is not expected (H_F to C_{9a}) and one which is expected is not observed (H_E to C_8). Although long range ($^{3+n}J(C,H)$) couplings are not usually observed, exceptions have been noted for conjugated π bond systems possibly explaining the extra correlation between H_F and C_{9a} (Friebolin 1993). Absence of the two bond coupling between H_E and C_8 may be explained by the fact that $J^2(C,H)$ couplings are generally *smaller* than $J^3(C,H)$ in benzene derivatives (Friebolin 1993). Given the small sample size it is possible that this correlation would not be observed.

5.5B Remaining Fractions

The remaining fractions from bioreactors F88 - 107 were set aside for future work. As IIE-G seemed to contain large amounts of 3- β -O[β -D-glucoside] β -sitosterol by comparison of R_f and color when developed with the anisaldehyde mixture, it is recommended that prospective separation begin with fraction IIC.

Conclusion

Although our cell culture was not found to produce taxanes at levels measurable by our techniques, as the biotechnology industry is currently among the fastest growing, any information gained as to how biological systems behave *in vitro* is of great interest. Furthermore, some of the compounds isolated have shown biological activity and if in the future developed as pharmaceuticals, need of a non synthetic, environmentally friendly production method may arise.

Xanthones have shown great diversity in their biological activity. Isolates from *Gentian* species have been shown to have antipsychotic activity and inhibition of monoamine oxidase in rats. Xanthones from *Psorospermum febifugum* have been found to have cytotoxic and antitumor activity, while those from *Swertia japonica* have mutagenic activity. *Garcinia mangostana* L. and *Callophyllum inophyllum* L. have produced xanthones with antibacterial, antifungal and anti-inflammatory action (Hostettmann 1989).

Triterpenes with an oleanene skeleton have shown antitumor and anticancer activity. Arjunolic acid (2 α , 3 β ,23-trihydroxy-olean-12-en-28-oic acid) isolated from the rhizome of *Cochlospermum tinctorium* had *in vitro* inhibitory effects on skin cancer tumor promoter greater than those of all previously studied natural products. Other oleanenes such as the dihemiphthalate derivative of 18 β -olean-12-en-3 β ,30-diol and 11-oxo-olean-12-en-30oic acid 3 β succinate have shown anti-inflammatory and cholesterol

lowering effects respectfully. Oleanolic acid has shown to be effective in the prevention of experimentally induced (by CCl₄ injection) liver injury in rats (Mahato 1992).

Beta sitosterol and its glucoside have been well studied for numerous medical applications. Currently a mixture of the two is used to treat benign prostate hypertrophy, however it is likely that it will be used to treat other conditions in the future (Bouic 1996). These compounds are the major components and antihyperglycemic principle of *Centaurea seridis* L. var. *maritima*, a plant used as a folk remedy for diabetes mellitus in Spain. It is believed that the mechanism of action of these compounds may be related to insulin releasing effects on pancreatic cells (Ivorra 1990). Also pertaining to treatment of diabetes, both compounds were found to enhance absorption of nasally applied insulin in rabbits without histological changes to nasal tissue (Maitani 1998). Other biological effects such as anti-inflammatory, anti-pyretic, anti-ulcer, and inhibition of spermatogenesis have also been noted (Bouic 1996). However, perhaps the most exciting effects seen to date, are the apparent ability of these compounds to stimulate T-cell production at picogram and femtogram/ ml levels *in vitro*. There is a great need for immunostimulents not only for the treatment of HIV related illness, but also to increase the success rate of organ transplants and recovery from infectious disease (Bouic 1996).

As much of the screening of plant extracts for potential pharmaceutical development has been fueled by folkloric medicine, fully characterizing the extracts and testing not only single compounds but mixtures of compounds for biological activity, could be of great interest since synergistic relationships between components of the extracts may be responsible for medicinal properties. Additionally, as the non taxane

compounds isolated have shown biological activity, it is possible that *Taxus sp.* cell culture may be an effective way to simultaneously produce a number of different pharmaceuticals.

Experimental

Cell culture was established in 1994 from callus obtained from Dr. Shan Lin Gao. Propagation and maintenance in liquid media was carried on by Dr. Elena Polishchuk and David Chen in the Biological Services laboratories. Stems of *Taxus x media* were cut into 1 cm length segments and sterilized with 30 % commercial bleach solution for ten minutes then washed with sterilized water five times. Explants were placed on solidified nutrient media, (petri plates containing Gambourg B5 media supplemented with 2.5 - 3 % sucrose, double vitamins, 0.2% casein hydrolysate and 1 mg/ml of 2,4-D) and kept in darkness at 26 °C. Suspension cultures were established by transferring callus tissue into Erlenmeyer flasks containing Gambourg B5 liquid media. The cultures were kept in the dark at 26 °C on a rotatory shaker set at 135 rpm. Every 14 days the cell lines were propagated by transferring the culture into new media at a 1: 10 inoculum ratio.

Stabilized cell culture was transferred from shake flasks to 10 L airlift bioreactors (Labroferm , New Brunswick Scientific Model FS-314) and fermented for 28 days. Growth of the cell cultures was monitored by refractive index (Galileo refractometer, 25 °C), while pH and microscopic purity were determined at the end of the growth cycle. After harvest, cells and broth were separated if possible. The broth was either extracted fresh or lyophilized before extraction.. The cells were lyophilized before extraction.

Harvested bioreactors were extracted either by myself, Mark Ross, or Carmel Ng. Dried cells and broth were frozen using liquid nitrogen then pulverized using a mortar and pestle. Powdered cells (or broth) were transferred into plastic containers and

extracted three times with EtOAc and once with MeOH using approximately 1.5 l per extraction. Broth extracted fresh was filtered using Whitman #1 filter paper then transferred into a 4 l separatory funnel and extracted 3 X with EtOAc. A 2:1 solvent : broth ratio was used due to problems with emulsions. Raw extracts were dried over Na_2SO_4 and filtered using Whitman #1 filter paper before the solvent was removed using a rotoevaporator.

In brief, the experiments F77-F85 from which four pure compounds were obtained and characterized proceeded in the following manner. Bioreactors F77-F85 were extracted separately as described above. In total, 528.3 g of cell biomass gave 12.47 g of EtOAc extract and 93.54 g of MeOH extract. The MeOH extract was washed with EtOAc to add ~ 4 g to the EtOAc extract weight. The EtOAc extract was next suspended in roughly 750 ml of MeOH and refrigerated (4 °C) overnight. Material that precipitated out was filtered off using a sintered glass funnel.

After addition of the EtOAc soluble portion of the MeOH extract and removing the MeOH insoluble material 15.52 g of extract was subjected to partitioning by solvents. The extract mostly dissolved in 675 ml of 9:1 MeOH : H_2O . Small amounts of insoluble material were filtered off and the filtrate was placed in a 4 l separatory funnel. The filtrate was extracted 3 X 300 ml with hexanes to give 6.55 g of subextract. The aqueous layer was adjusted to 75:25 MeOH : H_2O and extracted 3 X 500 ml with hexanes : CH_2Cl_2 (2:1) to give 2.03 g of subextract. The aqueous layer was the adjusted to 65:35 MeOH : H_2O and extracted 3 X 500 ml with CH_2Cl_2 to give 2.07 g of subextract. The MeOH was evaporated from the aqueous layer using a rotoevaporator. Next a 3 X 300 ml

extraction with EtOAc was performed which gave 0.337 g of subextract. After extraction with EtOAc the aqueous layer was evaporated to leave 0.978 g of material.

The hexanes : CH_2Cl_2 subextract was processed first using vacuum flash chromatography. Approximately 100 g of Sigma 10-40 μ type H silica gel was packed into a 70 ϕ mm sintered glass funnel. The sample was loaded "dry" by dissolving the subextract in CH_2Cl_2 , adding ~ 2g of silica gel then removing the solvent by evaporation. The solvents hexanes, hexanes:EtOAc (7:3, 1:1, 3:7, 0:10), MeOH : EtOAc (2:8, 10:0), were washed over the column and seven fractions (IIA-IIG) were collected. The last two fractions (IIF&G ~1.0 g in total) were combined with the CH_2Cl_2 subextract.

The CH_2Cl_2 subextract was chromatographed on an identical column. A MeOH/ CH_2Cl_2 solvent gradient (2:98, 4:96, 6:94, 12:88, 100:0) was used to collect five fractions (IIIA-E). The largest fraction (IIID, 0.810 g) was chromatographed using 95:5 CH_2Cl_2 : MeOH on a 2.5 ϕ cm x 18 cm glass column packed with BDH 70 - 230 mesh silica gel. Argon was used to maintain a satisfactory flow rate. Seventy fractions were collected and combined into six (IIID-1-6), the fourth of which (IIID-4, 295 mg) was recrystallized in MeOH to yield 73 mg of crystals(**IIID-4A**) which were pure by TLC. The mother liquor (200 mg) was recrystallized again with MeOH to produce another 120 mg of crystals (**IIID-4A**) and 62 mg of mother liquor which contained a component similar by TLC to one found in fraction (IIID-3). The two, mother liquor and IIID-3, were combined to give 82 mg which was recrystallized in MeOH one more time to removed traces of IIID-4A. The mother liquor (62 mg) was chromatographed using 3:7 acetone: CH_2Cl_2 on a 1 cm ϕ x 18 cm column packed with BDH 10 - 40 μ type H silica

gel. Seventy five fractions were collected and combined into nine, the fourth of which (3.5 mg IIID-3B4), appeared pure by TLC. More of the compound was obtained by chromatographing IIID - 3B5 using 95 : 5 CH_2Cl_2 on a 0.75 ϕ cm x 13 cm column packed with 10 -40 μ type H silica gel. Argon was used to maintain a satisfactory flow rate. Fifty fractions were collected and combined into two. The first fraction (5 mg IIID-3B5A) was purified using preparative TLC (0.25 mm plate, 3X development with 65:35 CH_2Cl_2 : acetone) to give 2 mg more of IIID-3B4.

Fraction IIIA (412 mg) from the CH_2Cl_2 subextract was processed to yield two pure compounds. IIIA was vacuum flash chromatographed using acetone: benzene (5:95, 10:90, 20:80,50:50, 100:0), MeOH on a 70 ϕ mm sintered glass funnel packed with Sigma 10-40 μ type H silica gel to yield seven fractions (IIIA-1-7). IIIA-5 was recrystallized using MeOH yielding crystals (26 mg **IIIA-5A**) which did not develop using any of our TLC developing systems. These crystals were submitted for MS and NMR analysis. Fraction IIIA-4 (65 mg) was chromatographed using 20 : 80 : acetone : hexanes on a 2.5 ϕ cm x 17 cm glass column packed with BDH 70 - 230 mesh silica gel. Thirty- six fractions were combined into seven (IIIA-4A-G), the last of which (7 mg, IIIA-4G) was purified using 77.5: 20: 2.5 : hexanes : EtOAc : Acetic acid on a 0.75 ϕ cm x 17 cm glass column packed with Sigma 10 -40 μ type H silica gel. Twenty-two fractions were combined into four, the third of which (1 mg, IIIA-4G3) appeared pure by TLC.

Fraction IIIB (248 mg) from the CH_2Cl_2 subextract was chromatographed on the Chromatotron[®] using 85:15 : benzene : acetone on a 2 mm plate. Seven fractions were

collected, the third (62 mg IIIB-3) was further purified using preparative TLC (1 mm plate, 2 X 77.5:20:2.5: hexanes:acetone:acetic acid). The compound collected was further purified using the same solvent system on a 0.75 ϕ cm x 12 cm column packed with Sigma 10 - 40 μ type H silica gel. Argon was used to maintain a satisfactory flow rate. Fifty -seven fractions were collected and combined into seven, the fifth of which (1 mg **IIIB-3B5**) appeared pure by TLC.

Bioreactors F88-F92 were extracted separately from each other, however in each experiment as no broth could be filtered off from the biomass, the cells and broth were freeze dried then extracted together. The method of extraction was the same as described above with the exception that excluding F88, a MeOH extraction was not performed. In total 613.7 g of biomass gave 18.9 g of EtOAc extract. The MeOH extract from F88 (24.50 g) was similar to the combined EtOAc extracts by TLC and therefore was added to the combined EtOAc extract for partitioning by solvents. The combined extract (43.4 g) was dissolved in 1350 ml of 9:1 MeOH : H₂O and extracted 3x 800 ml hexanes to give 13.67 g subextract. The aqueous layer was adjusted to 75:25 : MeOH : H₂O and extracted 3 X 1000 ml with hexanes : CH₂Cl₂ (2:1) to give 13.67 g subextract. The aqueous layer was then adjusted to 65:35 : MeOH : H₂O and extracted 3 X 1000 ml with CH₂Cl₂ to give 8.32 g of subextract. The MeOH was evaporated from the aqueous layer using a rotoevaporator before a 3 X 800 ml extraction with EtOAc was performed which gave 5.68 g of subextract. After extraction with EtOAc the aqueous layer was evaporated to leave 7.98 g of material

Column chromatography of the hexanes:CH₂Cl₂ subextract started with vacuum flash chromatography using hexanes, hexanes:EtOAc (7:3, 1:1, 3:7, 0:10), MeOH : EtOAc (2:8, 10:0). A 70 ϕ mm sintered glass funnel packed with approximately 100 g of Sigma 10-40 μ type H silica gel was washed with the solvent gradient to yield seven fractions (IIA-G). The second fraction (1.06 g, IIB) was chromatographed via the same method except the following solvent gradient was used : 1:99 , 2.5:97.5, 5:95 : acetic acid : hexanes, 5:85:10 acetic acid : hexanes: EtOAc, EtOAc, 1:9 MeOH EtOAc, MeOH. Fourteen fractions were collected, the eleventh of which (151 mg, IIB11) was recrystallized in hexanes to give 13 mg of crystals. The crystals were purified by preparative TLC (0.5 mm plate, 2 X 95:5:CHCl₃: MeOH) to give 5 mg of a compound which was pure by TLC, **IIB11B1**.

HPLC samples were made by dissolving approximately 1 mg of solvent partitioned extract in 1 ml of HPLC grade methanol purchased from Aldrich. Subsequent filtration of the samples was performed using type HV Millipore filters. A Supleco LC-F column (particle size 5mm, pore size 120 A, 25 x 4.6 cm) with a smaller but identical precolumn was used in a waters HPLC system (pump model 6000A, Auto sampler model 712, model 440 UV Absorbance detector). The flow rate was adjusted to 1 ml/min and the absorbance monitored at 254 nm.

Analytical and preparative thin layer chromatography was performed on precoated silica gel 60 PF₂₅₄ plates. Preparative chromatography performed on Chromatotron[®] (Model 7924T, Harrison research, Palo Alto, CA, USA) used silica gel 60 PF₂₅₄ (7794-2 EM Science/Merck) supported on glass disks. Raw extracts were developed using three

solvent systems (5% MeOH in CH_2Cl_3 , 8:2 CH_2Cl_2 :EtOAc, 1:1 hexanes:acetone) when compared with standards. Visualization using a UV lamp was performed before using one or more of the following developing reagents: 5% solution of ammonium molybdate in 10% H_2SO_4 , 1% p-anisaldehyde and 2% H_2SO_4 in concentrated acetic acid or 10% H_2SO_4 in MeOH. TLC plates were dipped in a beaker containing one of the above solutions, drained of excess reagent then dried in an $\sim 125^\circ$ oven to reveal blue spots in the case of the molybdate reagent, or multi-colored spots for the other two reagents.

The UV absorbance was determined using a Perkin Elmer UV/VIS Lambda 2 spectrometer. A samples was made up at $\sim 10^{-7}$ M in HPLC grade MeOH. Shift reagents were prepared by the method of Markham for flavanoid analysis (Markham 1982).

IR spectra was obtained by preparing a thin film in DMSO on NaCl plates and recorded using a Perkin Elmer 1710 FT IR

DCI spectra was performed in the positive mode using a Delsi-Nermaga R10-IOC with ammonia used as the carrier gas for low resolution and an ammonia/methane mixture for high resolution. Low resolution EI mass spectra was obtained on Kratos MS 50 and MS 80 spectrometers. High resolution EI mass spectra were recorded on the Kratos MS 50. NMR spectra were run in various deuterated solvents with signals recorded in ppm relative to TMS (0.00 ppm). ^{13}C decoupled and APT spectra were performed at 75 MHz on a Varian XL- 300. ^1H , and ^1H ^1H COSY were collected at 400 MHz and run on a Bruker WH 400 instrument. ^1H , ^{13}C HMQC, HMBC, ^1H at 500 MHz and ^{13}C at 125 MHz were recorded on a on an AMX 500 spectrometer. All samples were

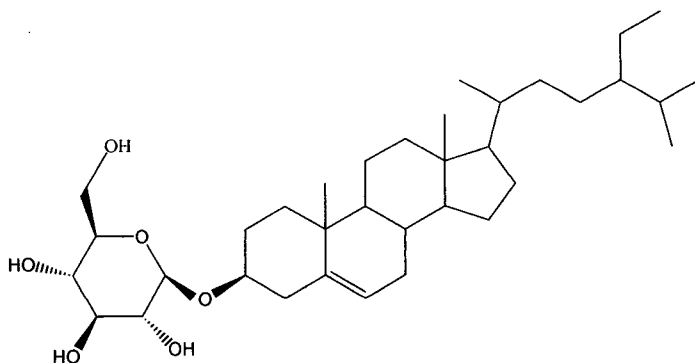
run under standard conditions with the exception of the HMBC of IIB11B1 in which the delay between pulsing and acquisition was increased from 1 to 1.7 sec in order to better observe the couplings between protons and quaternary carbons.

Melting points were uncorrected and recorded on a Reichert melting point apparatus.

The physical data for the compounds isolated from *Taxus x media* cell culture are as follows:

3- β -O[β -D-glucoside] β -sitosterol

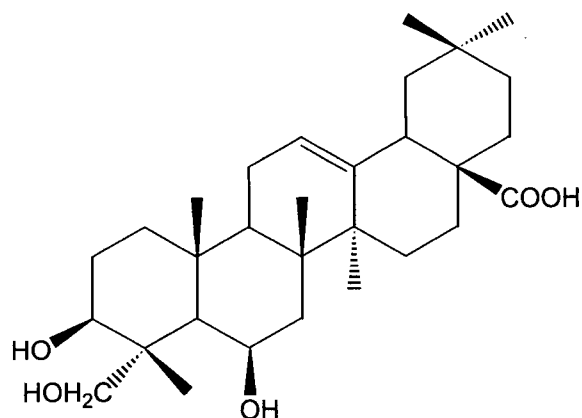
IIID-4A



White powder. Mp = 240-242 °C decomposed. 3300 (OH) and 1620 (C=C) cm^{-1} . EI mass spectrum, m/e, (% abundance) 576 [M^+] (1.39), 415(9.68), 396 (100), 382 (23.8), 275 (11.3), 255 (22.7), 229 (8.0), 213 (20.7), 121 (26.5) 400 MHz ^1H NMR (ppm, pyridine) 0.65 (s, 3H), 0.85 (d, J = 7, 3H), 0.89 (d, J = 8.6, 3H), 0.93 (s, 3H) 0.99 (d, J = 6.5, 3H) 1.1 - 2.0 (overlapping m), 2.12 (overlapping multiplets), 2.47 (t of d, J = 13.6,

~2), 2.73 (d of q, $J = 12$, ~2), 3.9 - 4.0 (m, 2H), 4.05 (t, $J = 8.4$, 1H), 4.24-4.29 (m, 2H), 4.56 (d of d, 5.6, 2.3, 2H), 4.8- 5.0 (br s), 5.05 (d, $J = 7.8$, 1H), 5.34 (d, $J = 5.0$, 1H). 75 MHz ^{13}C NMR (ppm, pyridine) 11.98, 12.16, 19.02, 19.21, 19.43, 20.00, 21.28, 23.38, 24.52, 26.36, 28.55, 29.44, 30.26, 32.05, 32.18, 34.19, 36.40, 36.92, 37.48, 39.33, 39.94, 42.47, 46.03, 50.33, 56.23, 56.82, 62.81, 71.66, 75.34, 78.06, 78.51, 78.61, 102.6, 121.9, 140.9.

3 β ,6 β -23 trihydroxy olean-28-oic acid



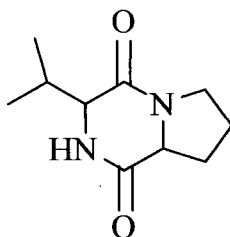
IIID-3B4

White powder. Mp 182-184 decomposed. 3238 (OH) 2970 (OH acid) 1664 (C=O) cm^{-1} .

El mass spectrum, m/e , (% abundance) 488 [M^+] (0.5%), 470 (2%), 452 (1.5%), 440 (1%), 288 (6%), 248 (100%), 222 (20%), 203 (100%), 189 (17%). 400 MHz ^1H NMR (ppm, pyridine) 0.92 (s, 3H), 1.00 (s, 3H), 1.26 (s, 3H), 1.62 (s, 3H), 1.67 (s, 3H), 1.72 (s, 3H),

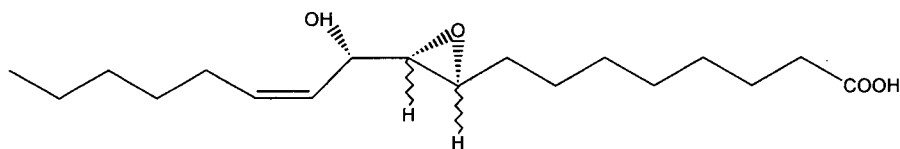
3.34 (d of d, J = 3.9, 6.8, 1 H), 4.04 (d, J = 8.3, 1H), 4.26 (d of d, J= 4.3, 11.6 Hz, 1H),
 4.39 (d, J = 10.3, 1H), 5.04 (br s, 1H), 5.38 (d, J = 3.6, 1H) 5.48 (distorted t, J=3.3, 1H).
 75 MHz ^{13}C NMR (ppm, pyridine) 14.78, 17.51, 18.63, 23.79, 23.95, 26.29, 28.08, 28.35,
 31.00, 33.28, 34.25, 37.02, 39.29, 41.14, 42.11, 42.73, 44.08, 46.51, 46.71, 48.75, 49.37,
 67.15, 67.61, 73.29, 122.8, 144.2, 180.2.

III A-5A



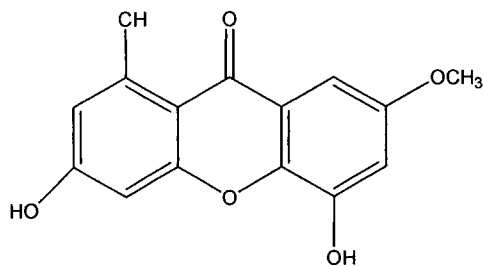
White solid. Mp. 174-176 °C. IR 3411 (NH) and 1651 (C=O) cm^{-1} EI mass spectrum,
 m/e, (% abundance) 196 [M^+], (3.83%), 169(0.85%), 167(0.92%), 154
 (100%), 140(1.57%), 138(2.50%), 125(20.46%), 98(2.31%), 96(2.04%), 72(55.53%),
 71(6.10%), 70 (91.54%). 200 MHz ^1H NMR (ppm, CDCl_3) 0.95 (d, 3H), 1.1 (d, 3H), 1.8-
 2.2 (m, 4H), 2.2-2.4 (m, 1H), 2.5-2.7 (m, 1H), 3.4-3.8(m, 2H), 4.1-4.2 (m, 1H). 75 MHz
 ^{13}C NMR (ppm, CDCl_3) 39.4, 42.5, 45.9, 52.0, 52.1, 68.6, 82.4, 84.0, 188.5, 193.9.

9, 10-epoxy- 11 (R)-hydroxy-12(Z)-octadecenoic acid



Clear oil. EI mass spectrum, m/e, (% abundance) 312 [M^+] (1.23%), 294(0.77%), 278(5.29%), 237(2.06%), 223 (2.66%), 187(4.23%), 169(13.53%), 155(10.42%), 140 (12.33%), 125(25.53%), 67(100%). 400 MHz ^1H NMR (ppm, CDCl_3) 0.87(t, $J=7$, 3H), 1.23-1.41 (overlapping multiplets, 16H), 1.41-1.61 (m, 2H), 1.61-1.70(m, 2H), 2.08 (overlapping symmetric multiplets, $J=16, 7$, 2H), 2.33 (distorted t, $J=6$ Hz, 2H). 2.98 - 3.00 (overlapping multiplets, 2H), 4.27(m, 1H), 5.47 (t, $J=10$, 1H), 5.62 (d of t, $J=10$, 3.5). 75 MHz ^{13}C NMR (ppm, CDCl_3) 14.0, 22.5, 24.6, 26.7, 28.1, 28.4, 28.8, 29.0, 29.1, 29.2, 31.5, 33.9, 58.2, 60.3, 126.7, 135.1.

4,6-dihydroxy,2-methoxy,8-methyl-xanthone



Light yellow needles. Mp. 248 - 250°C. IR 3440 (OH) and 1665 (C=O) cm^{-1} . UV-Vis absorbance maxima in nm ($\log \epsilon$). λ_{MeOH} 256 (4.72) ,289(4.07), 300(4.05), and 343(4.08).

λ_{NaOMe} 265 (4.63) and 368 (4.25). λ_{NaOAc} 260 (4.58) and 356 (4.13). λ_{AlCl_3} 260 (4.75),
 310 (4.02) and 370(4.14). $\lambda_{\text{AlCl}_3 + \text{HCl}}$ no change from AlCl_3 . DCI ($\text{NH}_3 + \text{CH}_4$) mass
 spectrum, m/e, (% abundance) 272 [M^+] (100), 257 (0.67), 229(4.13), 243 (9.75), 201
 (2.15), 199(3.04), 171(1.88). 400 MHz ^1H NMR (ppm, d_6 -acetone) 2.80 (m, $J = \sim 0.75$),
 4.00 (s), 6.60(d, $J = 3.3$) 6.70 (d, $J = 2.6$), 6.82 (d of d , $J = 1.89, 0.70$), 7.30 (d, $J = 2.1$),
 9.61 (br s), 12.0 (br s). 125 MHz ^{13}C NMR (ppm, d_6 -acetone) 25.6, 56.2, 99.9, 102.7,
 104.5 (x2), 109.7, 118.4, 139.6, 154.1, 159.4, 165.9, 166.1 and 167.6.

Bibliography

Aapro, Matti and Goldhirsch, Aron. Seminars in Oncology. 25(6) *Suppl.* 13. 1-3. 1998.

Arbuck, Susan and Blaylock, Barbara. Taxol Science and Applications. (Suffness, M. ed).CRC Press. Bocan Rouge, FL. 379-416. 1995.

Bouic, P.J.D. *et. al.* International Journal of Immunopharmacology.18(12). 693-700. 1996.

Bringi, V. Kadkade. Enhanced Production of Taxanes by Cell Cultures of *Taxus* Species. International Patent WO/97/44476. 1997.

Bus, Jan, Sies, Izaak *et al.* Chemistry and Physics of Lipids. 17. 501-518. 1976.

Campbell, S.J. and Whitney, S.A. Taxane Anticancer Agents: Basic Science and Current Status (Georg, Gund, Chen, Thomas T. *et. al.* eds). 59. American Chemical Society. Washington DC. 1994.

Cardellina II, J.H. Stierle, A.C. and Singleton, F.L Experienta. 44. 1021. 1988.

Cardellina II, J.H. Stierle. Journal of Liquid Chromatography. 14(4). 659-665. 1991.

Cheng, K.D, Li J.X. *et al.* Phytochemistry. 42(1). 73-75. 1996.

Chang, Cheng-Hsiung. Lin, Chun-Ching *et al.* Phytochemistry. 40(3). 945-7. 1995.

Christen, A.A., Gibsom, D.M. and Bland, J. Production of Taxol or Taxol -like Compounds in Cell Culture. US Patent 5,019,504. 1991.

Croom, Edward. Taxol Science and Applications. (Suffness, M. ed).CRC Press. Bocan Rouge, FL. 37-70. 1995.

Croteau, Rodney. Hezari, Mehri. *et al.* Phytochemicals and Health (Flores, HE and Gustin, DL eds.) American Society of Plant Physiologists. **1995.**

Croteau, Rodney. Koepp, Alfred E. *et al.* Journal Of Biological Chemistry . 270(15). 8686-90. **1995.**

Croteau, Rodney, Hezari, Mehri. *et al.* Archives of Biochemistry and Biophysics. 337(2). 185-90. **1997.**

Croteau, Rodney. and Hezari, Mehri. Planta Medica. 63. 291-5. **1997.**

DiCosmo, Frank, Fett-Neto, Arthur G. *et al.* Bio/Technology 10. 1572-75. **1992.**

DiCosmo, Frank, Fett-Neto, Arthur G. *et al.* Bio/Technology 11. 731-3. **1993.**

DiCosmo, Frank, Fett-Neto, Arthur G. *et al.* Biotech.Bioeng 44. 967-71. **1994.**

DiCosmo, Frank, Fett-Neto, Arthur G. and Zhang Wen Yi. Biotech.Bioeng 44. 205-10. **1994.**

Dicosmo, Frank, Fett-Neto, Arthur G. *et al.* J.Plant Physiol. 146. 584-90. **1995.**

Eisenriech, Wolfgang. Zenk, Meinhard H. *et al.* Proc. Natl. Acad. Sci. USA. 93. 6431-36. **1996.**

Floss, Heinz G. Fleming, Paul E. *et al.* J.Am.Chem.Soc. 115. **1993.**

Floss, Heinz G. Fleming, Paul E. *et al.* J.Am.Chem.Soc. 116. **1994.**

Floss, Heinz G. and Mocek, Ursula. Taxol Science and Applications. (Suffness, M. ed).CRC Press. Boca Rouge, FL. 3-26. **1995.**

Floss, Heinz G. and Walker, Kevin D. J.Am.Chem.Soc. 120. **1998.**

Freibolin, Horst. Basic One- and Two-Dimensional NMR Spectroscopy 2nd ed. 95-98. Verlagsgesellschaft. Weinheim, FDR. **1993**.

Gibson, Donna M., Ketchum, R.E.B, Hirasuna, T.J and Shuler, M.L. Taxol Science and Applications. (Suffness, M. ed).CRC Press. Boca Rouge, FL. 71-96. **1995**.

Gustone, F.D. Developments in the Analysis of Lipids. (Tyman, J.H.P. and Gordon M.H. eds). Royal Society of Chemistry. Cambridge, England . 109-122. **1994**.

Hall, J.L., Flowers, T.J. and Roberts, R.M. Plant Cell Structure and Metabolism. 245-7. Longman Group Limited. London. **1974**.

Hartzell, Harold. Taxol Science and Applications. (Suffness, M.ed).CRC Press. Boca Rouge, FL. 27-36. **1995**.

Hasslam, Edwin. Shikimic acid, Metabolism and Metabolites.pp. 159 and 185 John Wiley & Sons Ltd. West Sussex, England. **1993**.

Hayashi, Takaaki. and Yamagishi, Takashi. Phytochemistry. 27(11). 3696-99. **1988**.

Holton, Robert A. *et al.* Taxol Science and Applications. (Suffness, M ed).CRC Press. Boca Rouge, FL. 97-122. **1995**.

Hortobagyi, Gabriel. Seminars in Oncology. 25(5) *Suppl. 12*. 1-2. 1998.

Hostettmann, K., and Hostettmann, M., Methods in Plant Biochemistry Vol. I. 493- 506. Academic Press Ltd. **1989**.

Hostettmann, Kurt. Gupta, Mahabir P. *et al.* Phytochemistry. 40(6). 1791-5. **1995**. (uv ms nmr xanth)

Ivorra. M.D. *et al.* Die Pharmazie. 45(4). 271-3. **1990**.

- Jacobs, Madeline (ed.) Chemical&Engineering News. 76(24). 37. **1998**.
- Jazri, Mondher. Zhiri, Abdesslam. *et al.* Plant Cell Tissue and Organ Culture. 46. 59-75. **1996**.
- Kapoor, V.K. and Mahindoo, Neeraj. Indian Journal of Chemistry. 36B. 639-652. **1997**.
- Kato, Tadaihiro *et al.* Journal of the Chemical Society, Chemical Communications. 743-4. **1986**.
- Ketchum, R.E.B and Gibson, D.M *et. al.* Plant Cell Reports.12. 479-82. **1993**.
- Ketchum, R.E.B and Gibson, D.M. Plant Cell, Tiss. Org. Cult. 46. 9-16.**1996**.
- Kim, Dong-Il. Byun, Sang Yo *et al.* Biotech. Letts. 17(1).101-6. **1995**.
- Kobayashi, Jun'ichi and Shigemori, Hideyuki. Heterocycles. 47(2). **1998**.
- Koizumi, Naoyuki. Fujimoto, Yoshinori. *et.al* Chem. Pharm. Bull. 27. 38-42. **1979**.
- Kuwajima, Isao *et al.* Journal of the American Chemical Society. 120. 12980-12981. **1998**.
- Lambie, A.J. Secondary Products from Plant Tissue Culture. (Charlwood, B. and Rhodes, M.J.C. eds). Clarendon Press. Oxford. 265-278. **1990**.
- Linden James C. and Mirjalili Noushin. Biotech.Bioeng 48. 123-32. **1995**.
- Ma, Wenwen. Park, Gary L. *et. al.* Journal of Natural Products. 57(1) 116-122. **1994**.
- Maitani, Yoshi *et al.* Biol. Pharm Bull. 21. 862-5. **1998**.
- Mahato, Shashi , Nandy, Ashoke K. and Roy Gita. Phytochemistry. 31(7). 2199-2249. **1992**.

- Mahato, Shashi and Kundu, Asish. Phytochemistry. 37.1517-75. 1994.
- Markham, K.R. Techniques of Flavanoid Identification. 36-51. Academic Press Inc. New York, NY. 1982.
- McGuire, William and Ozols, Robert F. Seminars in Oncology. 25(3). 340-8. 1998.
- Mukaiyama, Teruaki. *et. al.* Chemistry Letters. 1-4. 1998.
- National Cancer Institute. Clinical Brochure : Taxol. NSC 125973. Bethesda MD. 1983.
- Nicolaou, Costa Kyriacos *et al.* Angew. Chem. Int. Ed. Engl. 33.15-44. 1994.
- Partridge, L.G and Djerassi, Carl. Journal of Organic Chemistry. 42(17). 2799 -2821. 1977.
- Phillips, Andrew J. and Abdell, Andrew D. Chem.N.Z. . 61(4). 1997.
- Piazza, G.L. *et al.* JAACS. 74(11). 1385-1390. 1997.
- Pierk, R.L.M. In Vitro Culture of Higher Plants. Kluwer Academic Publishers. Dordrecht, Netherlands. 1997.
- Pinto, M.M. *et al.* Magnetic Resonance in Chemistry. 36. 305-9. 1998.
- Pomilo, Alicia B. and Tettamanzi, Maria C. Magnetic Resonance in Chemistry. 34. 165-71. 1998.
- Rhone-Poulenc Rorer. Product Monograph : Taxotere. St.Laurent, Quebec. 1995.
- Rohmers, Micheal. Schwender, Jorg. *et. al.* Biochem. J. 316. 73-80. 1996.

Rohr, Jurgen. Angew.Chem. Int. Ed. Engl. 36(20).1997.

Rose, William. Taxol Science and Applications. (Suffness, M. ed).CRC Press. Boca Rouge, FL. 209-236. 1995.

Rowinsky, Eric K. Seminars in Oncology. 24(6).S12-19. 1997.

Sairenji, Yomiko *et al.* Newly Invented Antibiotic F483A. Japanese Patent JP8012666. 1996

Saito, Koji. Ohashi, Hiroaki *et. al* Process for Producing Taxol by Cell Culture of Taxus Species. US Patent 5312,740. 1994. (Nippon)

Schmitz F.J *et al.* Journal of Organic Chemistry. 48(22). 3941-3945. 1983

Schulz, Georg E. and Wendt, K Ulrich. Structure. 6(2). 127-33. 1998.

Shuler, Micheal L. Srinivasan, Venkatesh. *et al.* Biotech.Bioeng 47. 666-76. 1995.

Shuler, M.L. Srinivasan,V. *et al.* Biotechnol. Prog. 12(4). 457-65. 1996.

Shuler, M.L. Hirasuna, Thomas. *et al.* Plant Cell, Tissue and Organ culture. 44. 95-102. 1996.

Shuler, Micheal L. and Roberts, Susan C. Current Opinion in Biotechnology. 8 . 154-9. 1997.

Simpkins, H., and Parekh, H., Gen. Pharmac. 29. 167-72. 1997.

Singh, Gurmett and Curtis, Wayne R. Biotechnological Applications of Plant Cell Cultures. (Shargool, Peter D. and Ngo, That T. eds) CRC Press. Boca Raton, FL. 1994.

Straubinger, Robert M. Taxol Science and Applications. (Suffness, M.ed).CRC Press. Bocan Rouge, FL. 237-258. **1995**.

Suffness, M. Taxane Anticancer Agents: Basic Science and Current Status (Georg, Gund, Chen, Thomas T. *et. al.* eds) p.7. American Chemical Society. Washington DC. **1994**.

Suffness, M. and Wall, M.E. Taxol Science and Applications. (Suffness, M.ed).CRC Press. Bocan Rouge, FL. 3-26. **1995**.

Sultanbawa, Uvais S. Gunasekera, Sarah.*et al* Journal of the American Chemical Society : Perkins Transactions I. 2447 - 2450.**1975**.

Sundholm, L. Goran. Acta Chemica Scandanavia B.32. 177-181. **1978**.

Sundholm, L. Goran. Tetrahedron.34. 577-86.**1978**.

van der Sluis, W.G. and LaBadie , R.P. Phytochemistry. 24(11). 2601-5. **1985**.

Wall, M.E, and Wani, M.C. Alkaloids: Chemical and Biological Perspectives (S.W Pelletier ed.). 9. 1-22. Elseviser. New York. **1995**.

Wall, M.E, and Wani, M.C. TheAlkaloids vol. 50. Academic Press.London. 521- 36. **1998**.

Wickremesinhe, Enaksha R.M. and Arteca, Richard N. J. Liq. Chrom. 16(15).3263-74. **1993**.

Wickremesinhe, Enaksha R.M. and Arteca, Richard N. Plant Cell, Tiss. Org. Cult. 35. 181-93. **1993**.

Wickremesinhe, Enaksha R.M. and Arteca, Richard N. J. Plant Physiol. 144..183-8. **1994**.

Wickremesinhe, Enaksha R.M. and Arteca, Richard N. Biotechnology in Agriculture and Forestry. (Bajaj, Y.P.S ed) Medicinal and Aromatic Plants Vol. 41. Springer-Verlag. Berlin. **1998**.

Wink, Michael. Secondary Products from Plant Tissue Culture. (Charlwood, B. and Rhodes, M.J.C. eds). Clarendon Press. Oxford. 23. **1990**.

Willaims, Robert M. and Rubenstein, Steven M. J.Org.Chem. **60**. 7215-23. **1995**.

Yamaguchi, K. Spectral Data of Natural Products. Vol. I. Elsevier Publishing Co. New York. **1970**.

Yeoman, M.M. *et al.* Secondary Products from Plant Tissue Culture. (Charlwood, B. and Rhodes, M.J.C. eds). Clarendon Press. Oxford. 143. **1990**.

Young, Robert C. and Pecorelli, Sergio. Seminars in Oncology. **25**(3). 335-9. **1998**.

Yukimune, Yukihiro, *et al.* Nature Biotechnology. **14**. 1129-32. **1996**.

Yukimune, Yukihiro. Hara, Yashuhiro *et al.* Method of Producing a Taxane-Type Diterpene and a Method of Obtaining Cultured Cells which Produce the Taxane -Type Diterpene at a High Rate. US Patent 5,637,484. **1997**.

Zamir, Lolita. Nedeia, Maria E. *et al.* Tetrahedron Letters. **33**(36). 5235-36. **1992**.

Zenk, Meinhard H. *et al.* Proc. Natl. Acad. Sci. USA. **89**. 2389-93. **1992**.

Zhong, Jian-Jiang. Plant Tissue Culture and Biotechnology. **1**(2). 75-80. **1995**.